SAPIENZA
UNIVERSITÀ DI ROMA

Dipartimento di
Ingegneria Astronautica, Elettrica ed Energetica

PhD Thesis

Improving the quality of PV plant performance analysis by increasing data integrity and reliability: a data-driven approach using Machine Learning techniques

submitted by

Guillermo Oviedo Hernández

Matriculation Nr.: 1805629

DOTTORATO DI RICERCA IN
ENERGIA E AMBIENTE
33° CICLO
Anno Accademico 2017/2018

Academic Supervisors: Prof. Franco Rispoli, Sapienza Università di Roma
Prof. Alessandro Corsini, Sapienza Università di Roma
Industrial supervisor: Paolo V. Chiantore, BayWa r.e. Operation Services S.r.l.

Improving the quality of PV plant performance analysis by increasing data integrity and reliability: a data-driven approach using Machine Learning techniques

Guillermo Oviedo Hernández

This thesis work was developed within the framework of the SOLAR-TRAIN project “PV module lifetime forecast and evaluation”, a Marie Sklodowska Curie-Action (MSCA) funded by the European Union's Horizon 2020 programme (GA No. 721452, solar-train.eu). The programme’s aim was to qualify 14 selected early-stage researchers in the field of Photovoltaic durability as part of a highly innovative, multi-disciplinary project meeting industry requirements.

During the whole development of this work the author was hosted as a full-time employee at BayWa r.e. Operation Services S.r.l. (baywa-re.it), an industrial partner of the project, represented by Paolo V. Chiantore.

The academic supervision was in charge of the Sapienza University of Rome, under the PhD Programme Energy and Environment (uniroma1.it).

Rome, September 2021

Acknowledgements

I would like to dedicate this work to my beloved family, for their unconditional support throughout my entire life. Their sacrifice and guidance helped me to forge my own independent and autonomous way and to understand and appreciate the great significance of being loved despite great distances.

I am very grateful to BayWa r.e. Operation Services S.r.l., especially to Paolo V. Chiantore, Tommaso Simoni and Elena Bernardi, who paved my life in Italy and who's support was key for my development in the company's professional world.

My special thanks to the European Union's H2020 programme, whose financial support through the Marie Sklodowska scholarship made this research work possible.

Finally, I would like to thank my friends and all the people who make my daily life a continuous wonderful journey.

“Our dependence on fossil fuels amounts to global pyromania, and the only fire extinguisher we have at our disposal is renewable energy.”

Hermann Scheer (1944-2010)

Table of contents

List of abbreviations

AI	Artificial Intelligence
ANN	Artificial Neural Network
AV	Availability
BAG	Bagging Regressor
BEPI	Baseline energy performance index
BOS	Balance of System
BPPI	Baseline power performance index
CF	Capacity Factor
COD	Commercial Operation Date
COP	Conference of Parties
CPN	Cost Priority Number
CPV	Concentrated Photovoltaic(s)
DBN	Deep Belief Network
DHI	Diffuse Horizontal Irradiance/Irradiation
DNI	Direct Normal Irradiance/Irradiation
DQC	Data Quality Check
ECMWF	European Centre for Medium-Range Weather Forecasts
ECT	Equivalent Cell Temperature
EL	Electroluminescence
EPC	Engineering, Procurement and Construction
EPI	Energy Performance Index
EVA	Ethylene-Vinyl Acetate
FAC	Final Acceptance Certificate
FFNN	Feed Forward Neural Network
GBR	Gradient Boosting Regressor
GHGs	Greenhouse Gases
GHI	Global Horizontal Irradiance/Irradiation
IEC	International Electrotechnical Commission
IR	Infrared
ISO	International Organization for Standardization
I-V	Current-Voltage
JB	Junction Box
KNN	K-Nearest Neighbours
KPI	Key Performance Indicator
LR	Linear Regression
MAE	Mean Absolute Error
MBE	Mean Bias Error
MIT	Minimum Irradiance Threshold
ML	Machine Learning
NMOT	Nominal Module Operating Temperature
NOCT	Nominal Operating Cell Temperature
nRMSE	Normalized Root Mean Square Error
NWP	Numerical Weather Prediction
O&M	Operation and Maintenance
PAC	Partial Acceptance Certificate

PID	Potential Induced Degradation
PL	Photoluminescence
PLR	Polynomial Regression
POA	Plane of Array
PPI	Power performance index
PR	Performance Ratio
PV	Photovoltaic(s)
R&D	Research and Development
RFR	Random Forest Regression
RH	Relative Humidity
RMSE	Root Mean Square Error
RT	Regression Trees
SCADA	Supervisory Control And Data Acquisition
SGD	Stochastic Gradient Descent Regressor
SL	Soiling Losses
SP	Smart Persistence
SR	Soiling Ratio
STC	Standard Test Conditions
SVR	Support Vector Machine Regression
TRC	Target Reference Conditions
UAS	Unmanned Aircraft System
UAV	Unmanned Aerial Vehicle
WS	Wind Speed

1 Introduction

On 4th November 2016 the Paris Agreement went into force, acknowledging the necessity to limit the increase in global average temperature below 2°C and pursuing efforts to keep it as close as possible to 1.5°C to foster the global response towards climate change [1]. And to no surprise, the energy sector is the great responsible for worldwide greenhouse gas (GHG) emissions.

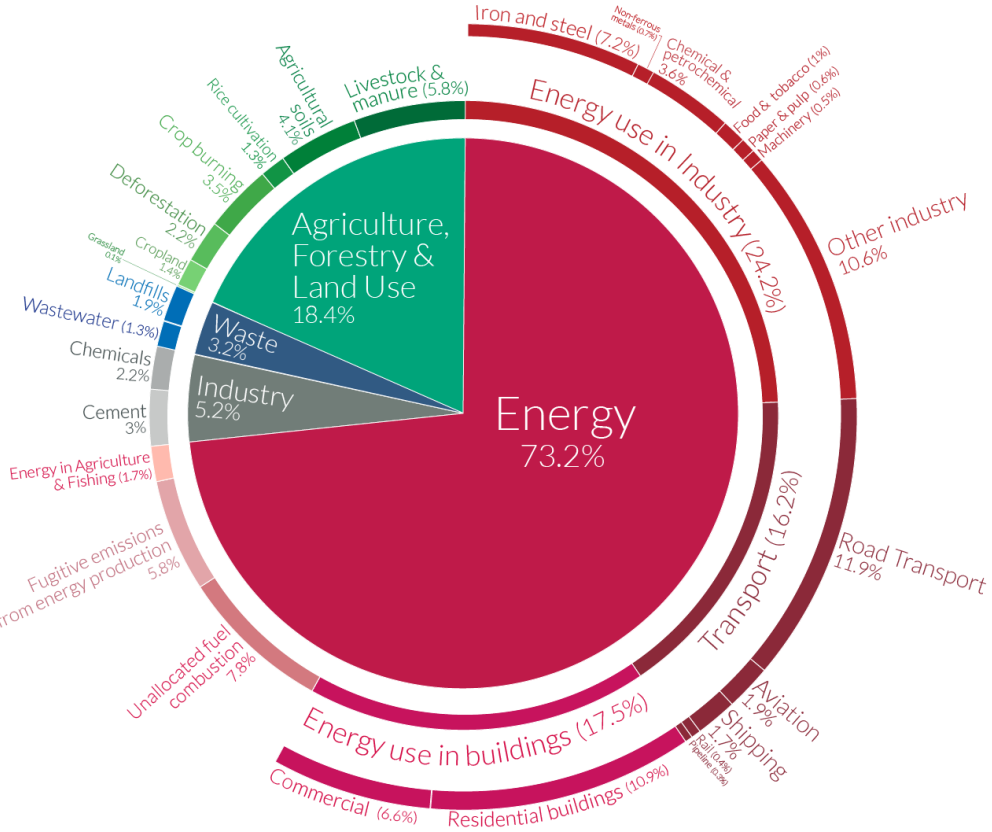

Figure 1. **Global greenhouse gas emissions by sector**, shown for the year 2016, where GHG emissions were 49.4 billion tons CO_2 eq. Source: OurWorldinData.org by the author Hannah Ritchie (2020)

Despite the fact that the burning of fossil fuels for energy purposes still accounts for 68% of the world's GHGs [2], emissions from the power sector are estimated to drop by more than 40% by 2030 [3] (*see Figure 2*). Furthermore, as a strong response to tackle the enormous electricity demand by the ever-growing human population[1] and towards the decarbonisation of the global energy system, more and bigger renewable energy power plants are being built worldwide.

[1] World population reached 7,794,799 in 2020 (https://population.un.org

Figure 2. **Historical CO_2 emissions and projected emissions from operating energy infrastructure** as it was used historically, 1900-2100. Source: IEA, last updated 12 May 2021

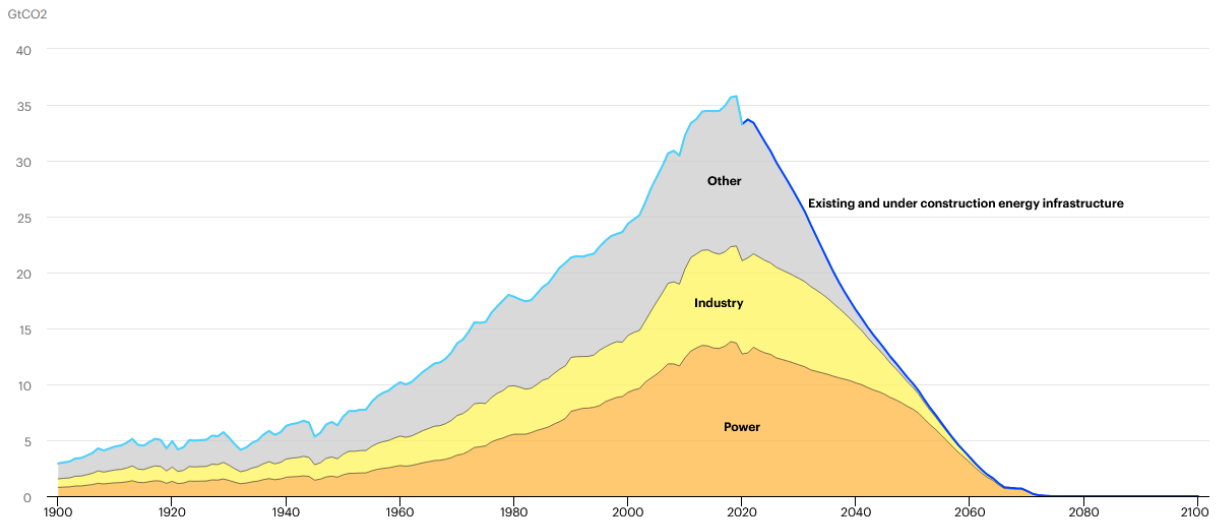

As the world economy and in particular energy markets are going through difficult times due to the COVID19 crisis and the strong wave of global restrictions, Photovoltaics (PV) is becoming more competitive, more versatile and more robust, emerging as a key technology of the ongoing energy transition. *"Solar is the new king of the electricity markets"* was one of the first key statements of the International Energy Agency (IEA) when launching the most recent *World Energy Outlook* in October 2020, acknowledging that PV electricity is becoming the cheapest source of new electricity in many countries around the world and will therefore continue to grow strongly over the decades to come [4].

PV is a mature technology and has proven to be competitive even without any kind of financial support, i.e., where grid parity has been reached[1]. Leading the way are utility-scale applications (see Figure 3), which are more cost-effective that fossil fuels in all unsubsidised investment cases [5]. However, large-scale solutions come with large-scale challenges, one of these being their long-term reliability and performance assurance.

The ten largest solar power plants in the world

1. Tengger Desert Solar Park, China – 1,547MW
2. Sweihan Photovoltaic Independent Power Project, UAE – 1,177MW
3. Yanchi Ningxia Solar Park, China – 1,000MW
4. Datong Solar Power Top Runner Base, China – 1,070MW
5. Kurnool Ultra Mega Solar Park, India – 1,000MW
6. Longyangxia Dam Solar Park, China – 850MW
7. Enel Villanueva PV Plant, Mexico – 828MW
8. Kamuthi Solar Power Station, India – 648MW
9. Solar Star Projects, US – 579MW
10. Topaz Solar Farm / Desert Sunlight Solar Farm, US – 550MW

Figure 3.**Top 10 PV plants in the world**. Source:/www.power-technology.com

[1] "Grid parity" means that solar electricity is as cheap as other grid connected sources of power (coal-fired and gas-fired power plants, for example).

1.1 Abstract, motivation and goal

Abstract

PV modules are engineered to produce electricity for 30+ years and are being deployed worldwide in ever more and ever bigger PV plants. Continuous quality assurance and performance analysis are the cornerstone for long-term reliability to maximize financial and energy returns. In today's highly competitive Operation and Maintenance (O&M) market, employing and maintaining extensive networks of on-site sensors for remote monitoring purposes, proves challenging. Within this framework, data-driven solutions play a leading role to turn raw data from the field into reliable actionable insights. PV plant's data from SCADA and monitoring systems is constantly subject to quality issues and the uncertainty related to it is directly reflected on the quality and reliability of the performance metrics used. In this work, the impact of the quality of the most relevant input parameters (i.e., output energy and irradiation) for the calculation key performance indicators (KPIs) is evaluated and different data cleaning and imputation techniques are benchmarked.

The main objective of this work is to improve the quality of PV performance analysis by minimizing the negative effects of using incomplete and/or corrupted time-series as input for the calculation of PV plant KPIs (such as Performance Ratio and Availability). This objective is achieved through the assessment of different data sources with different intrinsic quality. In chapter 2, the methodology and data used are explained. Then, in chapter 3, as a pre-liminary data analysis, raw data from on-site sensors was compared with satellite-derived data to define and validate its uncertainty values. Special emphasis is given to irradiance sensors (pyranometers and reference cells), being the plane of array (POA) irradiance one of the variables with the greatest impact on performance evaluation. Later, in chapter 4, a consistent data quality analysis is proposed to assess the sensors' health status to proceed with the corresponding cleaning procedure. At this stage, the concept of '*virtual sensor'* is introduced, that solves the problem of having incomplete raw data by generating time-series with no missing data that efficiently combine on-site measurements with satellite data. Finally, in chapter 5, the advantage of performing data imputation using Machine Learning (ML) techniques is demonstrated by applying three good-performing algorithms (*Random Forest*, *Bagging and Gradient Boosting Regressor*) to replace missing data with highly accurate predicted values.

Motivation

The data-driven solutions explored in this work take a step back from the mainstream application areas of big data analysis, AI and Machine Learning (power forecast and failure analysis) and take a closer look at the quality of the raw data which is later on used for performance analysis of

utility-scale PV plants. Using as starting point the concept of *garbage-in*, *garbage out*, that states that the quality of the output is determined by the quality of the input, the results of this work will not only improve the quality of the data used on a daily basis by O&M contractors and Asset managers but also, and most importantly, will allow the consistent and comparable use of KPIs to assess PV plants performance at portfolio level. In this way, it will facilitate decision makers prioritise maintenance activities and identify potential revamping/repowering interventions. Furthermore, the 'enhanced KPIs' output of this work could be integrated into the CPN methodology for the assessment of the economic impact of failures [6-8].

Goal

This work aims at improving the quality of the most relevant PV plant KPIs in the industry by increasing the integrity and reliability of the monitoring data available to the O&M contractors and Asset Managers.

1.2 PV market outlook

The success of solar is due to many factors. A primary one is its cost leadership, which continues to improve without an end in sight. Another is its versatility: solar covers an unmatched spectrum of power applications from very small residential systems to very large utility-scale plants, individual installations to building-integrated solutions in carports, apartment houses or agricultural green houses. There are also mobile applications and off-grid systems for rural electrification. Finally, no other power plant can be planned and built as rapidly as solar PV, while at the same time involving the highest job intensity [4].

Despite the severe impact of the COVID-19 crisis across the world in 2020, the year still saw 138.2 GW of solar installed, representing an 18% growth compared to 2019, yet another global annual installation record for the solar PV sector. This brings the global cumulative solar capacity to 773.2 GW, a 22% increase, and marks a new milestone for the solar sector by exceeding three quarters of a terawatt. Even though solar's total power generation share increased by 0.5 percentage points to around 3.1%, nearly 70% still comes from fossil fuel and nuclear, highlighting the need to rapidly accelerate solar deployments [5].

Figure 4. **Global Total Solar PV installed capacity 2000-2020**. Source: SolarPower Europe 2021

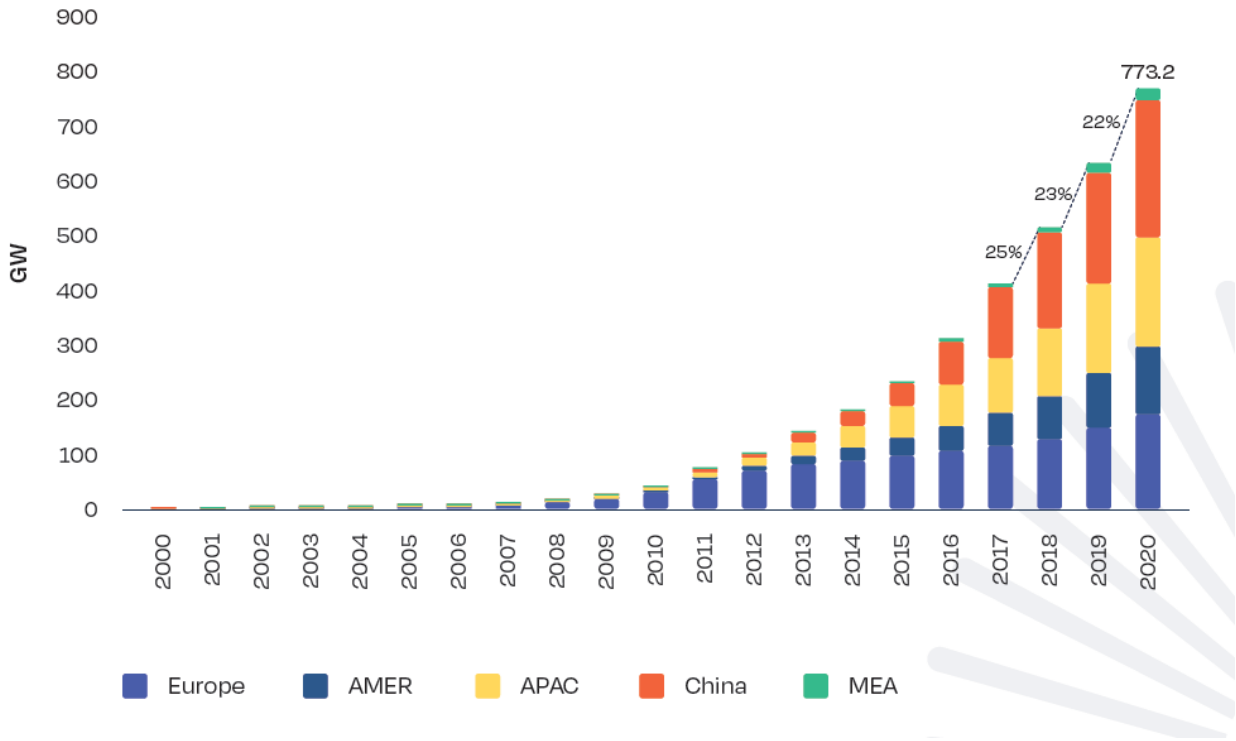

Figure 5. **Global Total Solar PV Market Scenarios 2021-2025**. Source: SolarPower Europe 2021

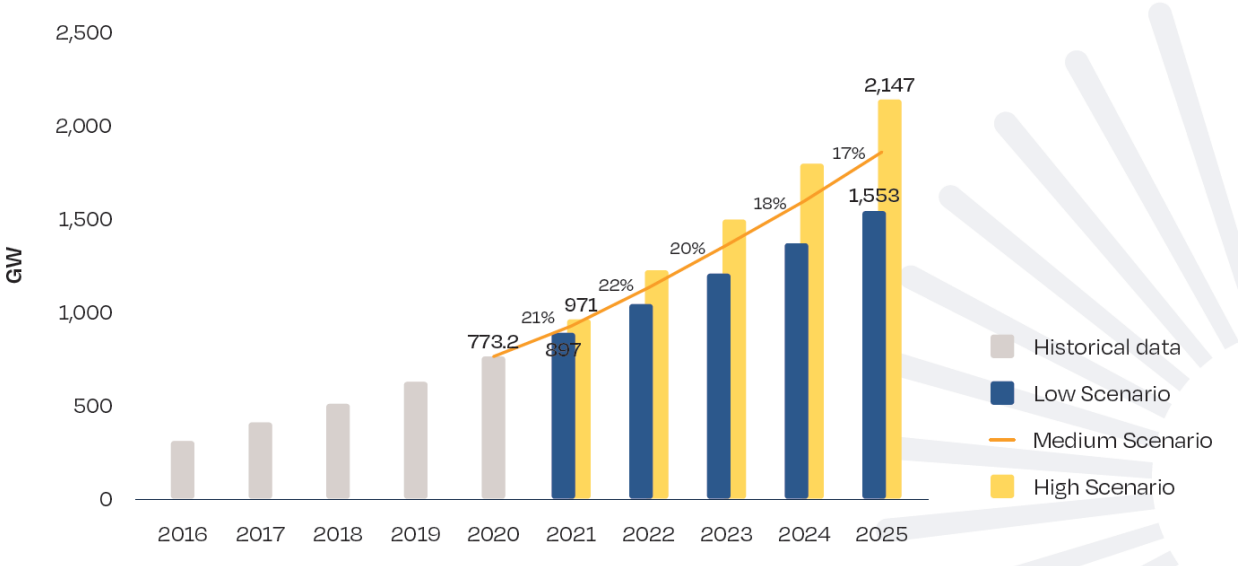

Figure 6. **Annual share of PV installations by type**. Source: IEA-PVPS 2020

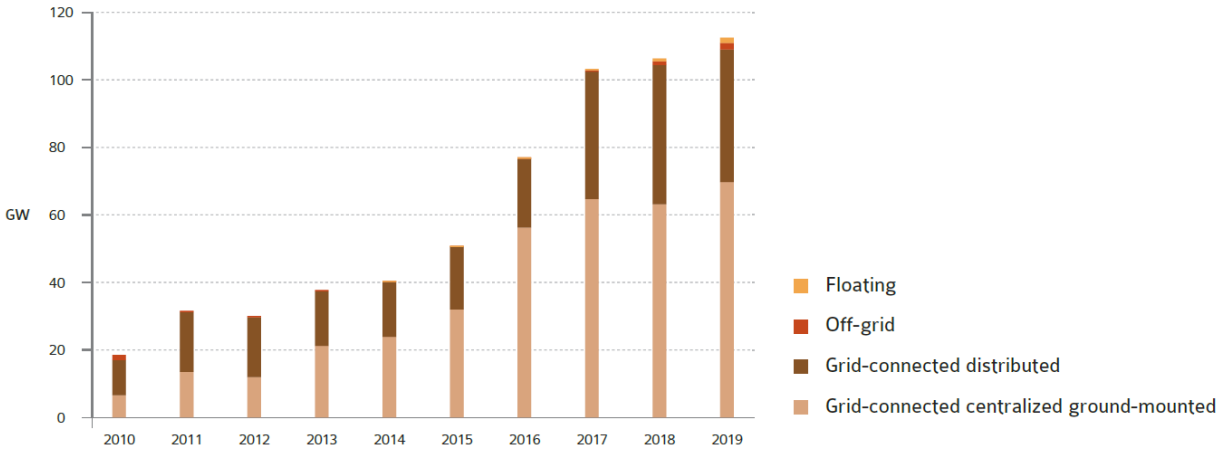

EU members states installed 18.2 GW of solar power capacity in 2020, an 11% improvement over the 16.2 GW deployed in the previous year. 2020 was the second-best year ever for solar in the EU, only topped by 2011, when 21.4 GW was installed [9].

Figure 7. **EU27 Cumulative Solar PV installed capacity 2000-2020**. Source: SolarPower Europe 2021

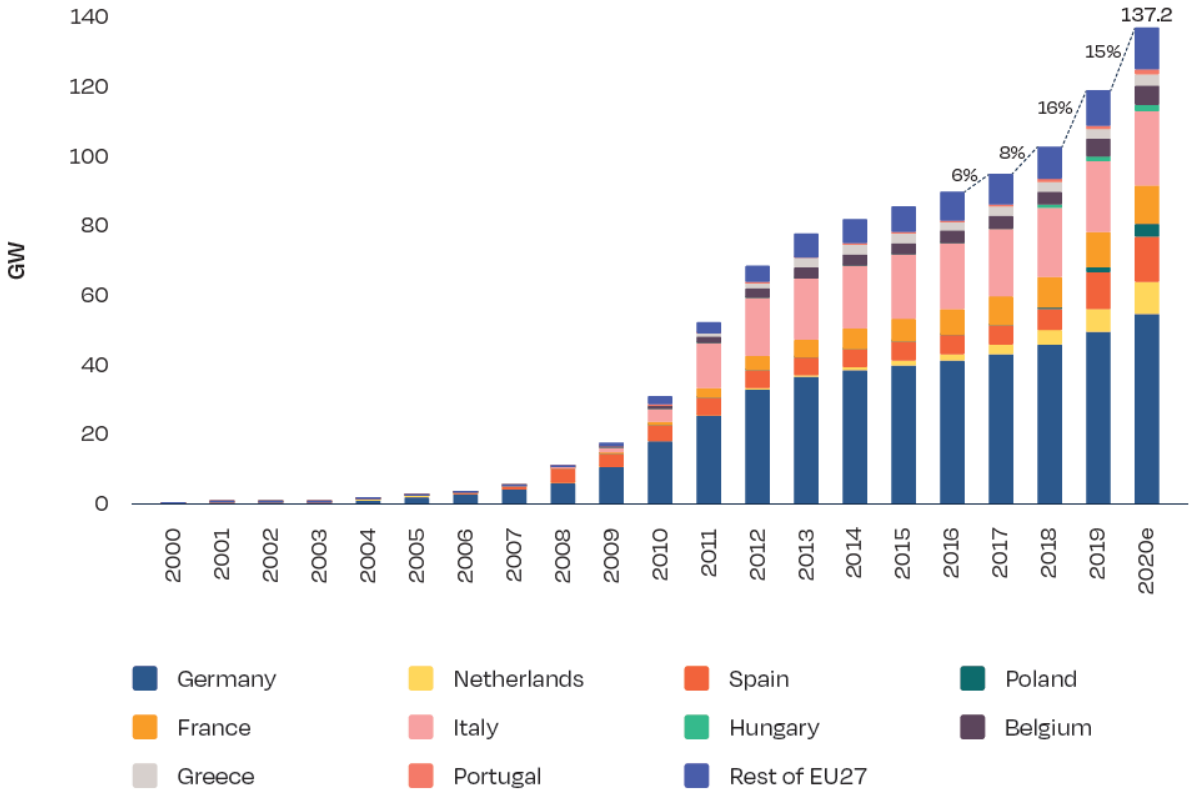

1.3 About BayWa r.e.

BayWa r.e. delivers end-to-end project solutions involving planning, development, construction, and ongoing operations management. Using innovation, creativity and expertise, it has successfully brought over 4 GW of renewable energy online and manages over 10 GW of renewable energy assets, ensuring they operate at peak efficiency. It is also an Independent Power Producer with a growing portfolio and an expanding energy trading business.

Figure 8. **BayWa r.e. overview**

BayWa r.e. is working with businesses and organisations worldwide to provide tailored renewable solutions that reduce carbon footprints and drive down energy costs. Operating 100% carbon neutral, it is also committed to the global sustainability journey by driving forward multiple social, environmental and economic initiatives.

As a leading global supplier to the solar distribution market, it provides a comprehensive range of products and industry leading customer support. Through first in class training, logistical expertise and online services, BayWa r.e. is a preferred partner for thousands of installers and contractors.

Based in 27 countries, with revenues of almost €2.5 billion and sustained growth throughout the company's history, BayWa r.e. is a leading global renewable energy developer, service provider, distributor and energy solutions provider. Operating throughout Europe, the Americas and Asia-

Pacific, it is strategically investing in emerging markets around the world, actively shaping the future of energy and taking a stand against climate change.

Figure 9. **BayWa r.e. global presence**

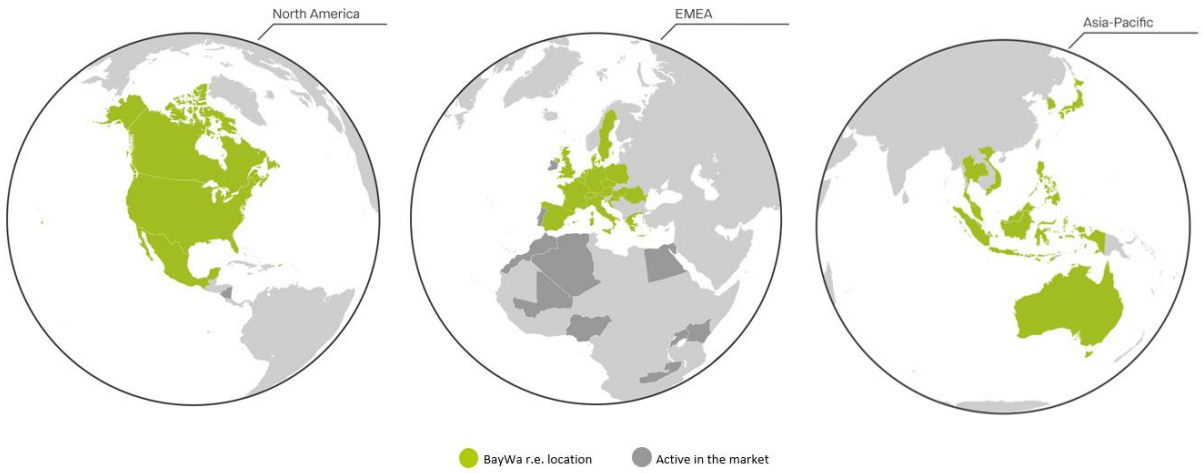

BayWa r.e.'s shareholders are *BayWa AG*, a globally successful business with revenues of €17.2 billion, and *Energy Infrastructure Partners*, a market leader in energy infrastructure investment that manages over €2.6 billion from global investors.

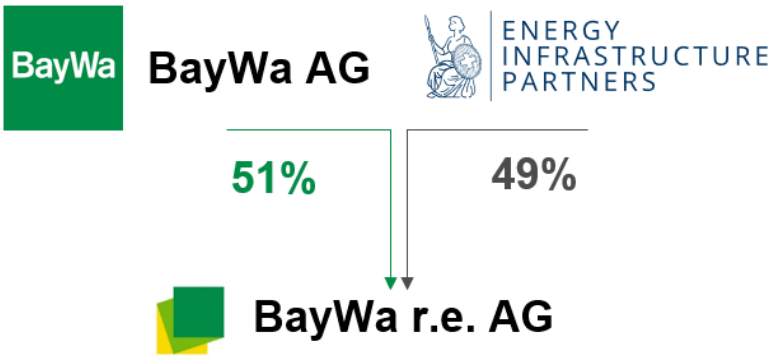

Figure 10. ***BayWa r.e. shareholders***

This thesis was developed under the guidance and knowledge infrastructure of BayWa r.e. Operation Services S.r.l., the Italian legal entity of BayWa r.e. With offices in Rome and Milan, it is responsible for the supply of technical and commercial operation, management and maintenance services for PV plants in Italy, with activities on over 500 sites (see Figure 11), summing up almost one Gigawatt of installed capacity.

Figure 11. **Italian PV portfolio managed by BayWa r.e. Operation Services S.r.l.**

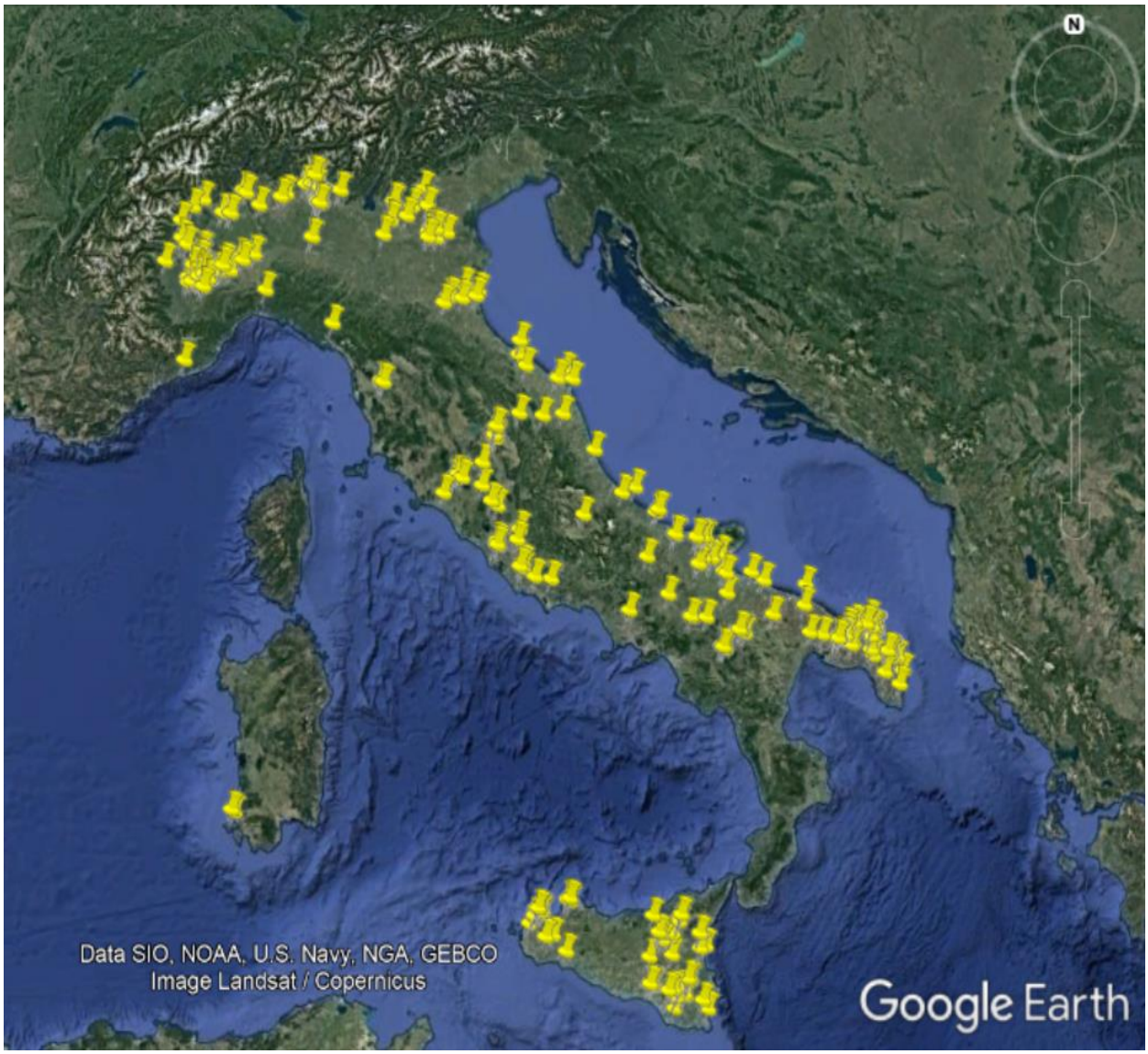

1.4 Operation & Maintenance of PV plants

Operation and Maintenance (O&M) has become a standalone segment within the solar industry and it is widely acknowledged by all stakeholders that high-quality O&M services mitigate potential risks, improve the Levelised Cost of Electricity (LCOE) and Power Purchase Agreement (PPA) prices, and positively impact the return on investment (ROI).

Asset Owners, EPC companies and O&M providers are the key players involved in the funding, design, construction and maintenance of PV plants, which may range from small rooftop arrays to utility-scale plants.

The lifecycle of a PV project can be split up in six stages as illustrated in the figure below, being the O&M phase the longest (30+ years).

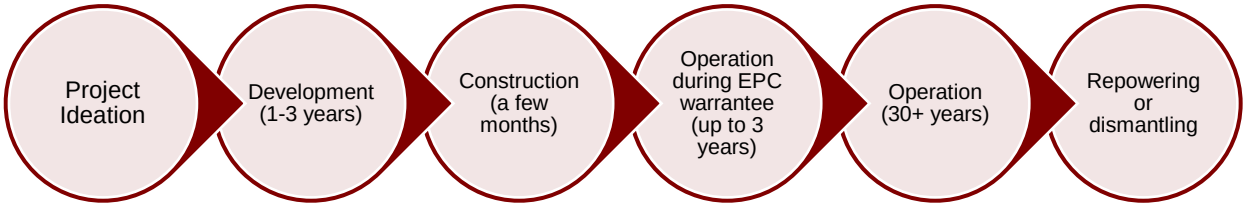

Figure 12. **Lifecycle of a PV plant.** Source: own design

The O&M phase stretches for most of PV systems' lifetime and the ability of O&M providers plays a key role in maintaining high levels of technical and economic performance over the years, mitigating risks and positively impacting the return of investment (ROI).

The scope of work of an O&M contractor falls under a wide umbrella of activities, that might include and not limited to the following: asset management, operations, maintenance, spare parts management, guarantees management and ancillary services (see *Figure 13*).

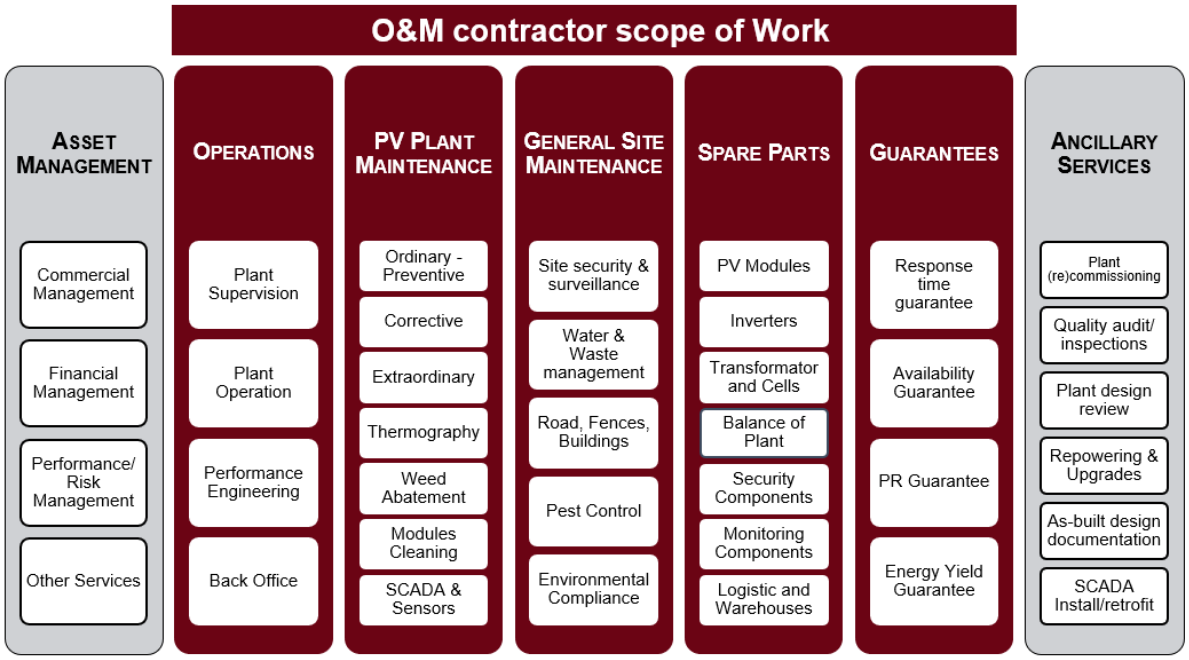

Figure 13. **O&M contractor scope of work**. Source: own design

Operations is about remote monitoring, supervision and control. Power plant operation also involves coordination of the on-site maintenance team. A proper PV plant documentation management system is crucial for Operations. A list of documents that should be included in the as-built documentation set accompanying the solar PV plant (such as PV modules' datasheets), as well as a list of examples of input records that should be included in the record control (such as alarms descriptions), can be found in [10]. Based on the data and analyses gained through monitoring and supervision, the O&M contractor should always strive to improve PV power plant performance. When performed according to the best practice guidelines laid by the industry, *predictive maintenance* could be implemented.

Maintenance activities could be subdivided in preventive, corrective, predictive and extraordinary and they are very comprehensively explained by [10] (see Figure 15).

Beside the above-mentioned basic maintenance activities, additional services, such as vegetation control, modules cleaning, maintenance of buildings, etc., can be included in the O&M scope of work.

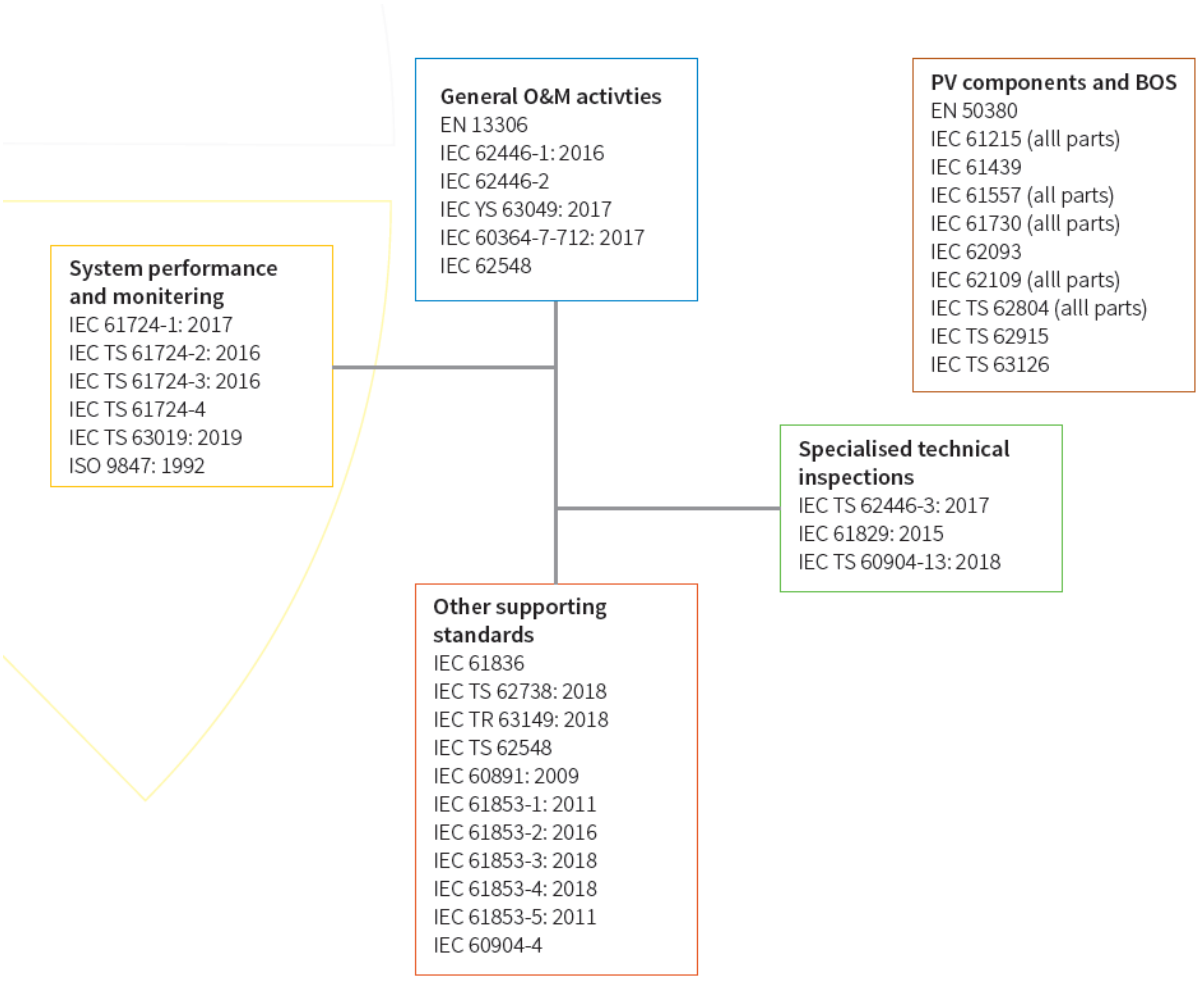

Figure 14. **Applicable International standards for PV O&M**, 2019 status. Source: SolarPower Europe

Due to the fast-growing pace of the solar industry, it has been a big challenge to define standard legal and technical frameworks for a smooth development of the market. Great efforts have been done by the *International Electrotechnical Commission* (IEC) and a list of standards related to the PV O&M sector is summarized in *Figure 14*. On the legal side, the *International Renewable Energy Agency* (IRENA) and *Terrawatt Initiative* (TWI) have teamed up to support the rapid and widespread scale-up of solar energy by providing simple and universally applicable legal agreements that make contracting much faster and less costly, the so-called Open Solar Contracts[1].

Figure 15. **Overview of different types of PV plant maintenance**. Source: SPE O&M Best Practice Guidelines

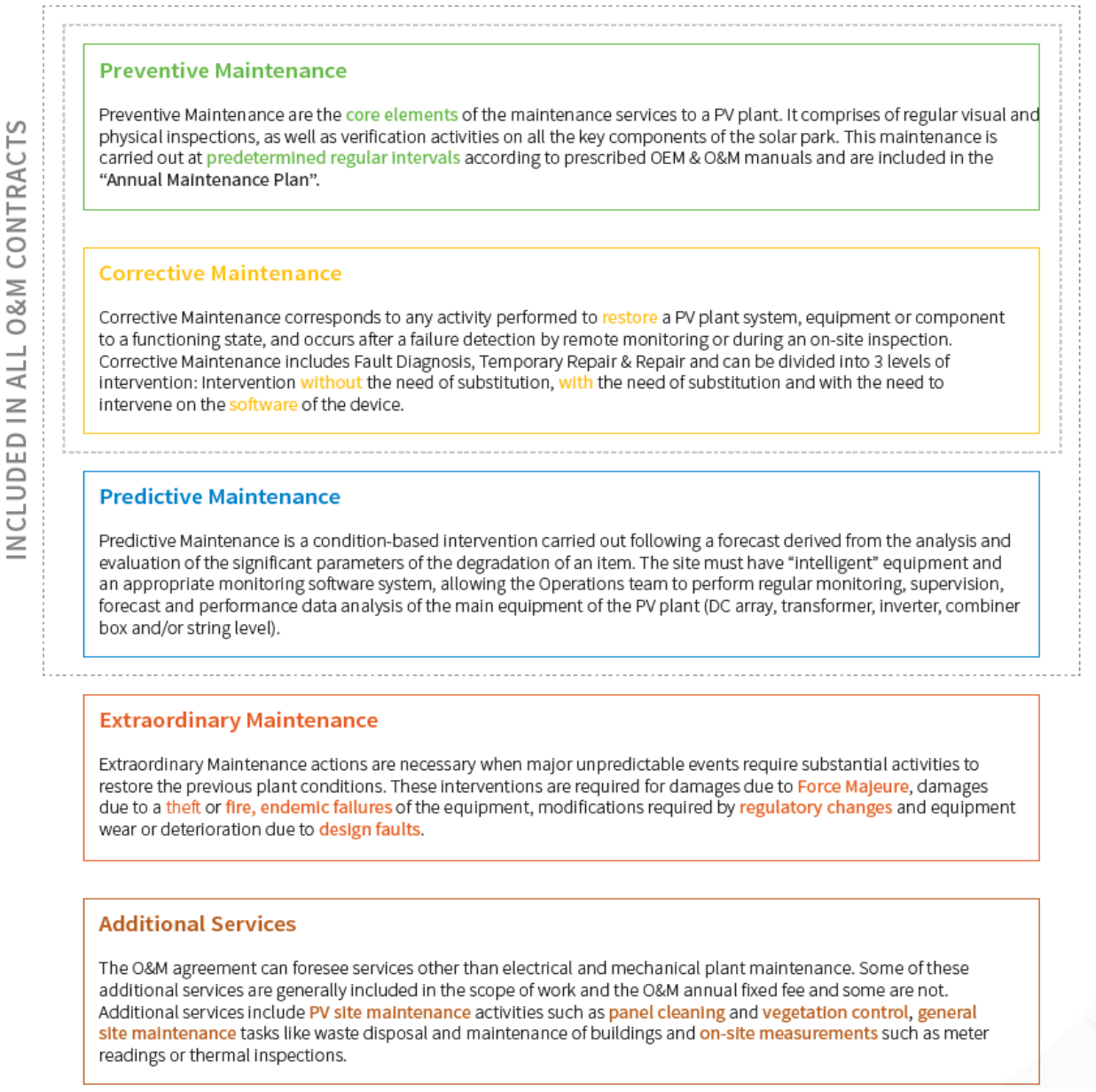

[1] Please refer to https://opensolarcontracts.org/

1.4.1 Monitoring systems

Data acquisition and control is performed through monitoring systems, whose general requirements, as stated in [11], include: “dataloggers capable of collecting data (such as energy generated, irradiance, module temperature, etc.) of all relevant components (such as inverters, energy meters, pyranometers, temperature sensors) and storing at least one month of data with a recording granularity of up to 15 minutes; as well as a reliable Monitoring Portal (interface) for the visualization of collected data and the calculation of KPIs”.

Monitoring systems have diverse purposes, which can include the following:

- Identification of performance trends in an individual PV system
- Localization of potential faults in a PV system
- Comparison of PV system performance to design expectations and guarantees
- Comparison of PV systems of different configurations
- Comparison of PV systems at different locations

The size of the PV plant and the needs of the users define the key components and configuration of the monitoring system: according to the specific scope of work, different sensors and analysis methods may be implemented as part of the system. For example, in order perform fault detection, fine-grained data coming from all sub-levels of the system are required, while for comparing performance to design expectations and guarantees coarser data are needed to perform plant-level analyses. The *International Standard IEC 61724-1:2017* [11] proposes a classification of monitoring systems based on the desired application (see Table *1*).

Table 1. **Monitoring system classifications**, suggested applications and recording interval requirements. Source: International Electrotechnical Commission [11]

Typical applications	Class A High accuracy	Class B Medium accuracy	Class C Basic accuracy
Basic system performance assessment	×	×	×
Documentation of a performance guarantee	×	×	
System losses analysis	×	×	
Electricity network interaction assessment	×		
Fault localization	×		
PV technology assessment	×		
Precise PV system degradation measurement	×		
Maximum recording interval	1 min	15 min	60 min

1.4.2 Performance assessment and KPIs

PV plants' performance assessment is carried out employing Key Performance Indicators (KPIs), metrics which allow the Asset Owner to have a near real-time overview of the systems' status. KPIs are divided into PV plant KPIs (quantitative indicators) and O&M Contractor KPIs (both quantitative and qualitative). The latter are not a subject of this study, thus, in the rest of the dissertation, when talking about KPIs reference is made to PV plant KPIs.

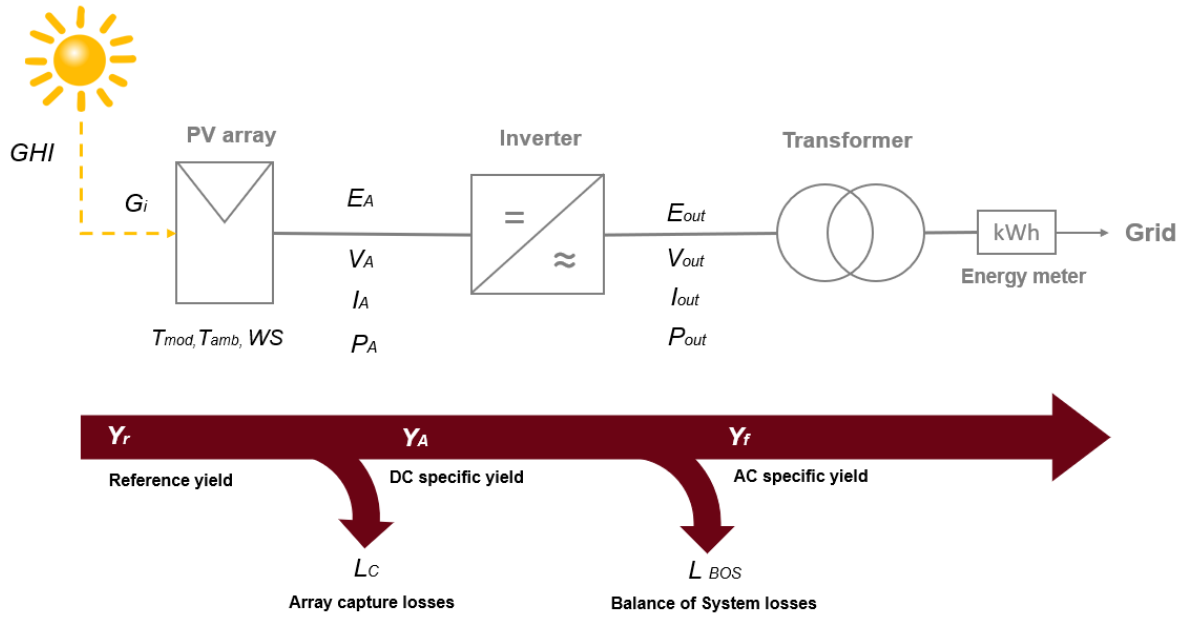

Figure 16. **PV plant parameters and energy flow**. *Source: adapted from SolarPower Europe*

KPIs can be calculated over different time periods, but often they are computed on a monthly or annual basis. Since every plant and every contract are different from one another, the most appropriate metric for a particular system has to be defined according to the system design, user requirements and contractual agreements. Among the contractual KPIs currently used in the solar industry, Performance Ratio (PR) is one of the most common (see *Annex A: PV performance metrics* for a comprehensive review of the metrics used to assess PV plant performance).

1.5 The role of Machine Learning

The distributed nature of PV plants leads to the generation of huge amounts of digital information: while a 1 GW fossil or coal-based power plant generates on average around 10,000 data streams and a similarly sized wind farm produces 51,000 data streams, when talking of PV, the figures rise up at about 439,000 data streams [12].

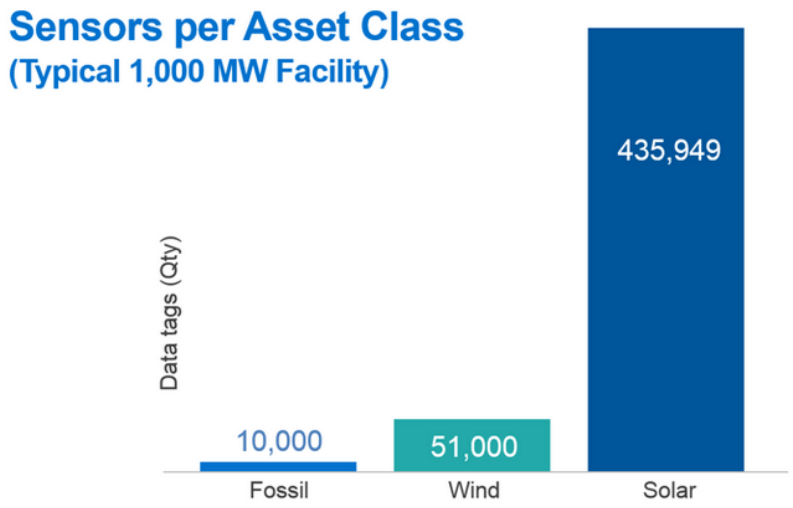

Figure 17. **Sensors per asset class**. Source: *www.renewableenergyworld.com* [12]

Each component of the system, from the individual panel to inverters and meters, produces information about power production, temperature and many other parameters which flood the monitoring systems with continuous streams of data. Without an infrastructure able to handle and timely analyse this information, both Asset Owners and O&M contractors may be overwhelmed by data, unable to exploit all the knowledge hidden in it.

This is a fertile ground for *Machine Learning*: ML is a method of data analysis based on the idea that it is possible to build mathematical models based on sample data which can perform specific tasks without being explicitly programmed for that purpose. These models can learn the relation between past inputs and outputs of a system and, based on this, try to predict future outputs based on future inputs. Thus, once big amounts of data become available, ML algorithms can be exploited to systematically scan it, identify patterns and extract information which may be completely hidden to human eyes.

Machine Learning applications have reached high levels of maturity in many sectors, with *Deep Learning* currently paving the way for the introduction of *Artificial Intelligence* (AI) in our everyday lives, but in the PV plant O&M sector ML applications are still far from common use.

Machine Learning systems can be grouped into four major categories [13]:

- *Supervised learning:* the training data fed to the algorithm includes the desired outputs (labelled data)
- *Unsupervised learning:* the training data fed to the algorithm does not include the desired outputs (unlabelled data)

- *Semi supervised learning*: the training data fed to the algorithm includes both labelled and unlabelled data
- *Reinforcement learning*: the system learns the best strategy by trial and error, getting reward or penalties at every choice.

Supervised learning tasks are classified according to the nature of the target variable: when the desired output is quantitative, the problem is defined as *regression*, while when the labels are qualitative it is called *classification*.

Many ML applications in the PV field revolve around two major topics:

a) PV energy or power forecasting – regression task
b) Fault detection, diagnostics and prognostics - mainly classification task

The ML application which is going to be presented in this dissertation a regression problem (supervised learning approach).

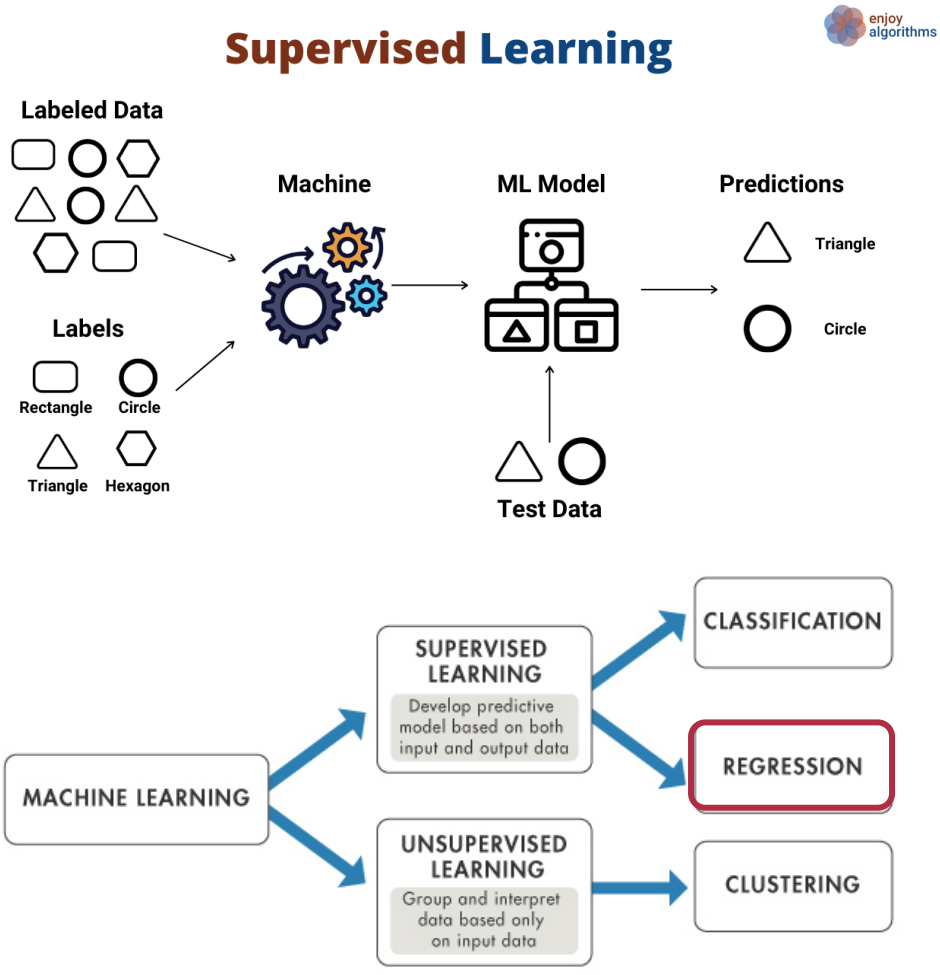

Figure 18. **Machine learning approaches**

2 Methodology and data

In this chapter, the tools, the methodology and data employed are explained. After introducing the research objectives, the methodology and the limitations, the case study and the performance metrics are presented.

2.1 Data science tools

All data handling, processing and computations described hereinafter have been performed employing the programming language *Python 3.7.3* (www.python.org) included in *Anaconda Distribution* (www.anaconda.com), a renowned open-source development environment for data science. *Spyder 3.3.6* (www.spyder-ide.org) was used as programming interface and many widely used scientific python libraries were employed, such as: *Pandas, Numpy, Matplotlib, Scikit-learn, Scipy* and *pvlib* (pvlib-python.readthedocs.io).

pvlib python is a community supported tool that provides a set of functions and classes for simulating the performance of photovoltaic energy systems. pvlib python was originally ported from the PVLIB MATLAB toolbox developed at Sandia National Laboratories and it implements many of the models and methods developed at the Labs (pvpmc.sandia.gov) [15].

Figure 19. **The data science toolkit**

2.2 Methodology overview

The main objective of this work is to improve the quality of PV performance analysis by minimizing the negative effects of using incomplete and/or corrupted time-series as input for the calculation of PV plant KPIs (such as Performance Ratio and Availability). This objective is achieved through the assessment of different data sources with different intrinsic quality. First, raw data from on-

site sensors is compared with satellite-derived data (three different sources are benchmarked). Special emphasis is given to irradiance sensors (usually pyranometers), being the plane of array (POA) irradiance one of the variables with the greatest impact on performance evaluation. Later, a consistent *data quality analysis* is proposed to assess the sensors' health status to proceed with the corresponding cleaning procedure. At this stage, the concept of *'virtual sensor'* is introduced, that solves the problem of having incomplete raw data by generating time-series with no missing data that efficiently combine on-site measurements with satellite data. Furthermore, the advantage of performing *data imputation* using Machine Learning (ML) techniques is demonstrated by applying three good-performing algorithms (*Random Forest, Bagging and Gradient Boosting Regressor*) to replace missing data with highly accurate predicted values.

With the aim of improving the quality of PV performance analysis, this study investigates how irradiance and power time-series coming from different sources and being processed in various manners can affect the calculation of KPIs. For this work, one representative plant located in central Italy was chosen. *Figure 20* summarizes the methodology. First, before KPIs calculation and benchmark, the following steps are performed:

a) Preliminary analysis: uncertainty of satellite data

The three available satellite sources are compared against the calibrated references for the quantification of both, GHI and POA, percentage differences (errors) to validate and corroborate their measurement uncertainty and therefore their usefulness and constraints when used for KPI calculations.

b) Data Quality Check (DQC)

The available time-series, power at plant level (meter data) and inverter level (DC and AC side), irradiance and ambient and module temperature (when available), are processed through the DQC, which performs an integrity evaluation based on the number of missing values. A cleaning process is then performed which identifies the most common types of anomalies (e.g., missing values, missing logs, outliers, dead values, etc.)

c) Data imputation with ML

The replacement of missing data with predicted values (so-called *data imputation*) is performed by the application of three Machine Learning algorithms (*Random Forest, Bagging and Gradient Boosting Regressor*) that, according to previous work [15], have already shown promising results for such a task (i.e. high accuracy predictions using RMSE as performance metric).

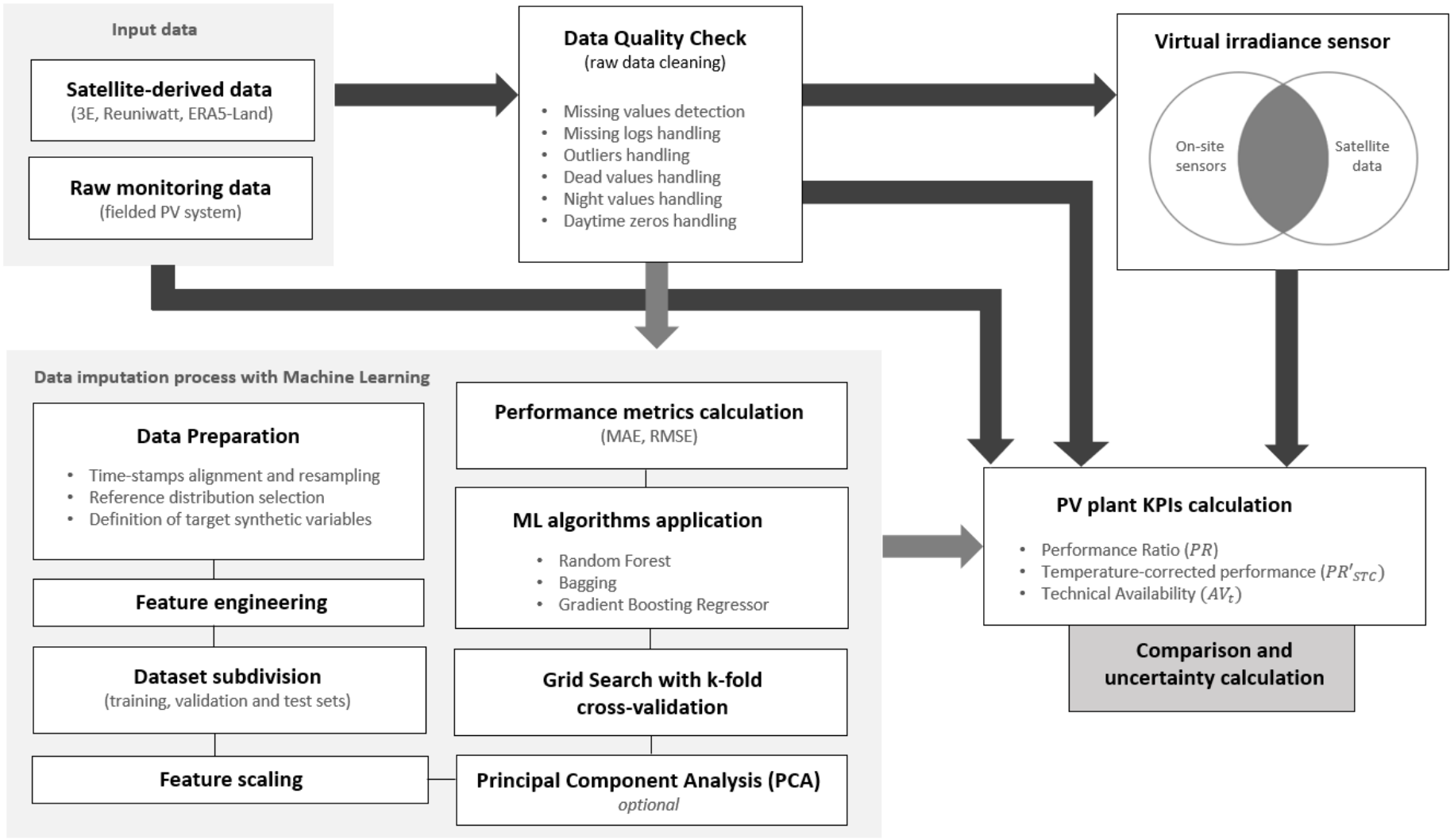

Figure 20. **Methodology overview.** Source: own design

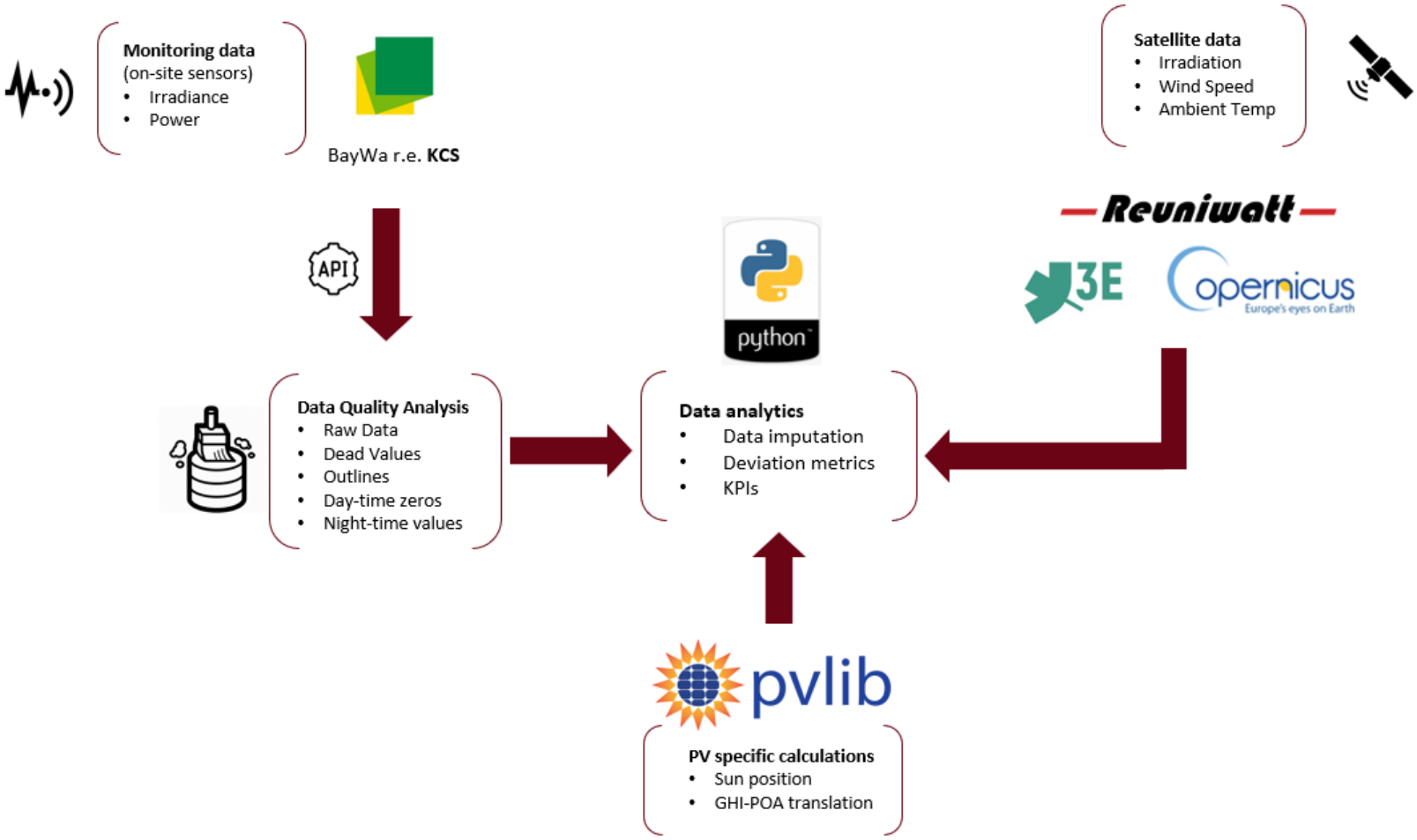

Figure 21. **Data collection and processing.** Source: own design

2.3 Limitations

One PV plant (one location) was selected as case study as the aim was to investigate irradiance sensors in deep, rather than having a more superficial approach focusing on multiple PV plants.

Three satellite data services, two commercial and a free online database, were selected beforehand. A calibrated (research grade) pyranometer was used as reference to retrieve low-uncertainty irradiance time series.

Nine ML models (8 supervised + 1 unsupervised model) were selected with the aim to give an overview of the relative performance of the methods as well as benchmarking them against a consistent satellite-derived dataset rather than investigating a specific model in depth.

2.4 Case study

The plant selected for the case study is located in Lazio region, Italy. It was commissioned in 2013, while BayWa r.e. Operation Services has started the O&M activities in April 2015.

Figure 22. **The case study**: PV plant in central Italy. Source: Google Earth

The main information on the plant is summarized in the following table:

Table 2.1. **Plant metadata**

General information	
Plant area	205,200 m^2
Type of plant	Ground-mounted fixed tilt
Installed capacity	9,019.53 kWp
Altitude	36 m a.s.l.
PV modules	
Modules tilt angle	20°
Modules azimuth	180°
PV module technology	micromorph Si (tandem)
Total number of modules	69,381
Module nominal power	130 W_p
Number of Modules per String	13
Number of Strings per Combiner Box	60
Total number of Strings	5,337
Total number of Combiner Boxes	91
Inverters	
Type of inverter	Central Inverter
Inverter nominal AC power	500 kW
Number of Inverters	17
Energy meters	
Number of Energy meters before transformer	1
Number of Energy meters inverter level	17
Irradiance sensors	
Number of Reference cells[1]	5
Pyranometer model	DeltaOHM LP PYRA 10
Pyranometer type	Secondary Standard
Number of Pyranometers	2

Plant's operation is monitored through a platform developed in-source and owned by BayWa r.e. Operation Services (named KCS).

[1] Since the reference cells' technology (crystalline silicon) differs from the one of the PV modules (thin-film) and the measurement uncertainty of the device is higher than the one of Secondary standard pyranometers, reference cells were considered an unreliable source and thus excluded from the analysis.

Monitoring data coming from the plant have been retrieved through API calls to KCS monitoring system. The maximum temporal resolution available for all the monitoring variables is 5 minutes.

The following table sums up the monitoring variables used.

Table 2.2. **Monitoring variables** retrieved through the plant's monitoring system

Monitoring variable	Source device(s)	Temporal resolution
POA Irradiance	Pyranometers (Cab1, Cab4)	5 minutes
Active Power	Inverters (n. 1 to 17)	
POA Irradiance	Pyranometers (Cab1, Cab4)	
Active power	Meter (Cab 5 Meter 1)	
Day Consumed Energy		
Consumed Energy		
Day Produced Energy		
Produced Energy		
Freq		
Phase A Voltage		
Phase B Voltage		
Phase C Voltage		
Phase A Current		
Phase B Current		
Phase C Current		

3 Uncertainty evaluation of satellite data

3.1 Measuring irradiance

The International Standard IEC 61724-1:2017 defines requirements on measurement uncertainties, referring to "*the combined uncertainties of the measurement sensors and any signal-conditioning electronic*" [11].

Performance indicators reflect the uncertainty deriving from field measurements, hence employing and maintaining a high-level monitoring system guarantees the gathering of high-quality data, which, once processed, enables a better understanding of the real behaviour of the PV plant as well as reducing the final uncertainties in KPIs calculation.

The incoming solar radiation incident on the PV modules is the primary variable involved in PR calculation and its uncertainty is dominated by the one that affects irradiance measurements [16].

The commercial instruments used to perform on-site irradiance measurements can be grouped in three categories:

- Thermopile pyranometers
- Photodiode sensors
- PV reference devices (including reference cells and reference modules)

Figure 23. **Irradiance sensors.** Left: thermopile pyranometer (manufacturer: Hukseflux). Center: photodiode pyranometer (manufacturer: LI-COR). Right: PV reference cell (manufacturer: NES)

The measurement uncertainty of a pyranometer can be described as the maximum expected uncertainty over a defined reference period calculated with respect to a reference, regarded as "absolute truth" [17]. The World Meteorological Organization defines "High Quality" pyranometers as having a maximum uncertainty in the hourly and daily radiation totals respectively of 3% and 2%, with a 95% confidence level [18].

The “Best Practice Guide on Uncertainty in PV Modelling” [19] reports the following typical uncertainty values (95% confidence interval) for the different type of instruments for measuring solar radiation:

Table 3. Typical uncertainty values for irradiance measurements

Typical uncertainty values	
Secondary standard pyranometer	**± 2%**
First class pyranometer	± 5%
Silicon sensor	± 5% - ± 8%
Second class pyranometer	± 10%

Secondary standard thermopile pyranometers can achieve measurement uncertainties of 1% for daily totals and 2% for hourly totals [20], thus they are considered the best type of irradiance sensor available on the market and they are recommended for most solar energy applications [21]. Irradiance measurements can also be retrieved through satellite-derived data, even though the use of on-site sensors is generally preferred [22]. See Table *5* for a detailed comparison.

Satellite-derived data

Satellite-derived irradiance data is retrieved through the application of radiative transfer models to the measurements performed by on-board satellite optical instruments, which measure the radiance reflected by the earth’s surface, filtered by the atmosphere. When choosing from different sources on the market, the following parameters need to be considered:

- Measurement uncertainty reported
- Spatial and temporal resolution
- Geographical coverage
- Irradiance components and other weather data available
- Delay from real time to which data is made available

Table 5. Relevant features for PV application of Satellite data

Satellite-derived data	
Irradiance components measured	GHI (POA can be modelled introducing large uncertainties)
Cleaning	N/A
Calibration	N/A
Measurement uncertainty	19 – 23% for hourly totals [22]
Response time	N/A
Data availability	Near real time
Data integrity	Usually very high (depends on satellite data provider)

Table 5. Comparative table of on-site irradiance sensors for PV applications

Thermopile pyranometers	
Irradiance components measured	GHI, POA
Cleaning	At least once per week (High accuracy), Optional (Medium accuracy) [11]
Calibration	Once per year (High accuracy), Once every 2 years (Medium accuracy), As per manufacturer's requirements (Basic accuracy) [11]
Measurement uncertainty	≤ 3% for hourly totals (High accuracy), ≤ 8% for hourly totals (Medium accuracy), Any (Basic accuracy) [11]
Response time	3 – 15 seconds [16]
Data availability	Real time
Data integrity	From very high to very low (depends on sensors, dataloggers, network connection, etc.)
Photodiode sensors	
Irradiance components measured	GHI, POA
Cleaning	At least once per week (High accuracy), Optional (Medium accuracy) [11]
Calibration	Once per year (High accuracy), Once every 2 years (Medium accuracy), As per manufacturer's requirements (Basic accuracy) [11]
Measurement uncertainty	Not applicable (High accuracy), Not applicable (Medium accuracy), Any (Basic accuracy) [11]
Response time	10^{-2} – 10^{3} microseconds [16]
Data availability	Real time
Data integrity	From very high to very low (depends on sensors, dataloggers, network connection, etc.)
PV reference devices	
Irradiance components measured	GHI, POA
Cleaning	At least once per week (High accuracy), Optional (Medium accuracy) [11]
Calibration	Once per year (High accuracy), Once every 2 years (Medium accuracy), As per manufacturer's requirements (Basic accuracy) [11]
Measurement uncertainty	≤ 3% (High accuracy), ≤ 8% (Medium accuracy), Any (Basic accuracy) [11]
Response time	Considered to be zero for photovoltaic sensors even if not explicitly reported by the manufacturer [16]
Data availability	Real time
Data integrity	From very high to very low (depends on sensors, dataloggers, network connection, etc.)

[22] proposed a comprehensive evaluation of satellite-based irradiation data carried out with respect to pyranometer measurements from several meteorological stations, yielding, for the best models, the following results:

Table 7. **Uncertainty (nRMSE) of satellite-derived irradiation** with respect to on-site sensors.

Temporal resolution	Uncertainty of satellite-derived irradiation with respect to on-site sensors			
	GHI		POA	
	Min.	Max.	Min.	Max.
Monthly	3%	6%	5.4%	8.1%
Daily	9%	11%	10.1%	12.3%
Hourly	19%	23%	19.5%	23.6%

Pros and cons

On the one hand, on-site sensors have a well-defined precision and provide measurements actually recorded at the plant location, being exposed at the exact same conditions as the PV modules. They need regular cleaning, maintenance and calibration and they may be subject to faults which can lead to data losses (introduction of missing data in irradiance time-series). Finally, in some cases, small PV plants may not be equipped with irradiance sensors at all. For hourly and daily POA irradiance, well-maintained and calibrated sensors are always to be preferred over satellite-derived data. Same goes for secondary standard pyranometers used to retrieve monthly irradiance measurements [22].

On the other hand, the precision of satellite-derived data may be comparable with the measurements coming from first, second class pyranometers and reference cells and, due to their constant availability, they may be particularly useful as backup measurements in case of consistent data losses or as only data source for those plants that are not equipped with sensors.

While on-site irradiance sensors require regular maintenance and calibration, the use of satellite-derived irradiance data does not require maintenance actions on the O&M contractor's side, thus removing the costs associated with on-site sensors maintenance. Nevertheless, satellite-derived irradiance data present higher measurement uncertainties which are affected by many factors involved in the process of derivation of irradiance from satellite images (terrain properties, state of the atmosphere, cloud transmittance) and depend on the temporal resolution.

3.2 Comparison methodology

Objective

Make a first attempt to choose the most appropriate satellite source to be used for Performance Reporting purposes, whether it is used for yield forecasting, to replace missing or corrupted on-site measurements and/or as reference to detect anomalous deviations of ground sensors.

Calculation steps

a) Comparison of irradiance data (GHI and POA) from three different satellite sources (*3E Data Services*, *Reuniwatt SunSat* and *ERA5-land*), using as reference calibrated ground pyranometers (maintained by EURAC research).
b) Calculation of error (deviation) metrics such as MBE, RMSE and nRMSE.
c) Validation of the *measurement uncertainty* figures reported in the literature and in the marketing material.

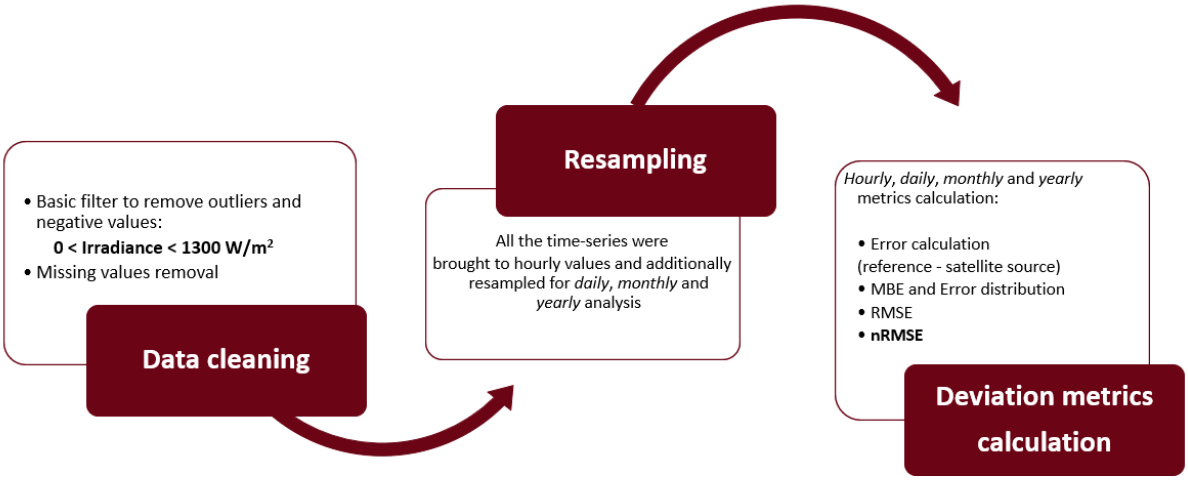

Figure 24. Methodology overview

Limitations

- This analysis was done using data only for the year 2018.
- The results presented here are limited to one location: Bolzano, Italy.

Table 8. **Site metadata for satellite evaluation**

Tilt angle	30°
Azimuth	188.5°
Latitude	46.46
Longitude	11.33

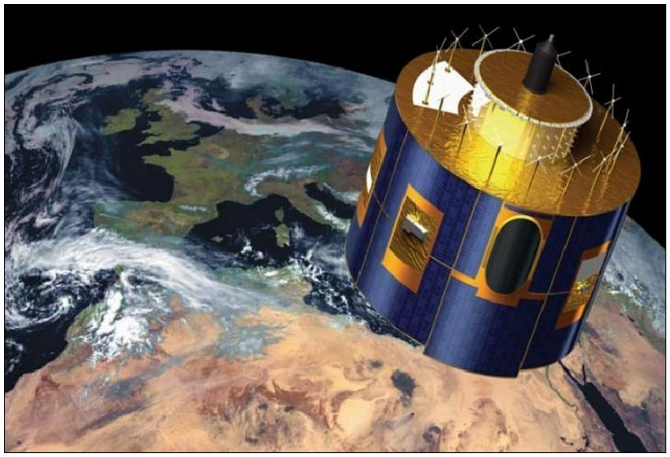

Figure 25. **Meteosat satellites** are spin-stabilised with instruments designed to provide permanent visible and infrared imaging of the Earth. Source: eumetsat.int

Table 9. **Measurement uncertainties** as reported in literature [22]

	GHI	POA
hour	19 - 23%	19,5 - 23,6%
day	9 - 11%	10,1 - 12,3%
month	3 - 6%	5,4 - 8,1%

3.3 Input data sources

Among the satellite-derived data sources available, two commercial services (3E Data Services[1] and Reuniwatt SunSat [2]) and one free dataset (ERA5-Land[3]) were chosen.

Data source	Type of service	Spatial resolution	Temporal resolution	Variables available			
				Global Horizontal Irradiance (GHI)	Plane of Array Irradiance (POA)	Diffuse Horizontal Irradiance (DHI)	Direct Normal Irradiance (DNI)
Ground measurements							
EURAC	research data	NA	15 min	√	√	√	√
Satellite-derived data							
3E Data Services	commercial	3 x 3 km	15 min	√	√	√	√
Reuniwatt SunSat	commercial	1.5 x 1.3 km	15 min	√	√	√	√
ERA5-Land	free database	9 x 9 km	1 h	√	X	X	X

Table 10. **Data sources comparison**

[1] 3E Data Services: https://solardata.3e.eu
[2] Reuniwat SunSat: https://reuniwatt.com/en/
[3] Copernicus Climate Change Service: https://climate.copernicus.eu/climate-reanalysis

ERA5-Land is a replay of the land component of the ERA5 climate reanalysis, but with a series of improvements making it more accurate for all types of land applications [23]. ERA5 is a climate reanalysis dataset providing a numerical description of the recent climate by combining models with observations, which is being developed through the Copernicus Climate Change Service. ERA5, which stands for "'ECMWF ReAnalysis", is the fifth major global reanalysis produced by the European Centre for Medium-Range Weather Forecasts (ECMWF) [24-25].

The ERA5-Land dataset contains fifty variables, available either as accumulations or instantaneous parameters, which are divided into eight categories: Temperature; Lakes; Snow; Soil Water; Radiation and Heat; Evaporation and Runoff; Wind, Pressure and Precipitation; Vegetation. The variables retrieved from that dataset and used throughout the study are the following:

- 2 Metre temperature [K]
- 2 Metre dewpoint temperature [K]
- Surface pressure [Pa]
- Surface solar radiation downwards - GHI [J/m^2]

The maximum temporal resolution available is1 hour**.**

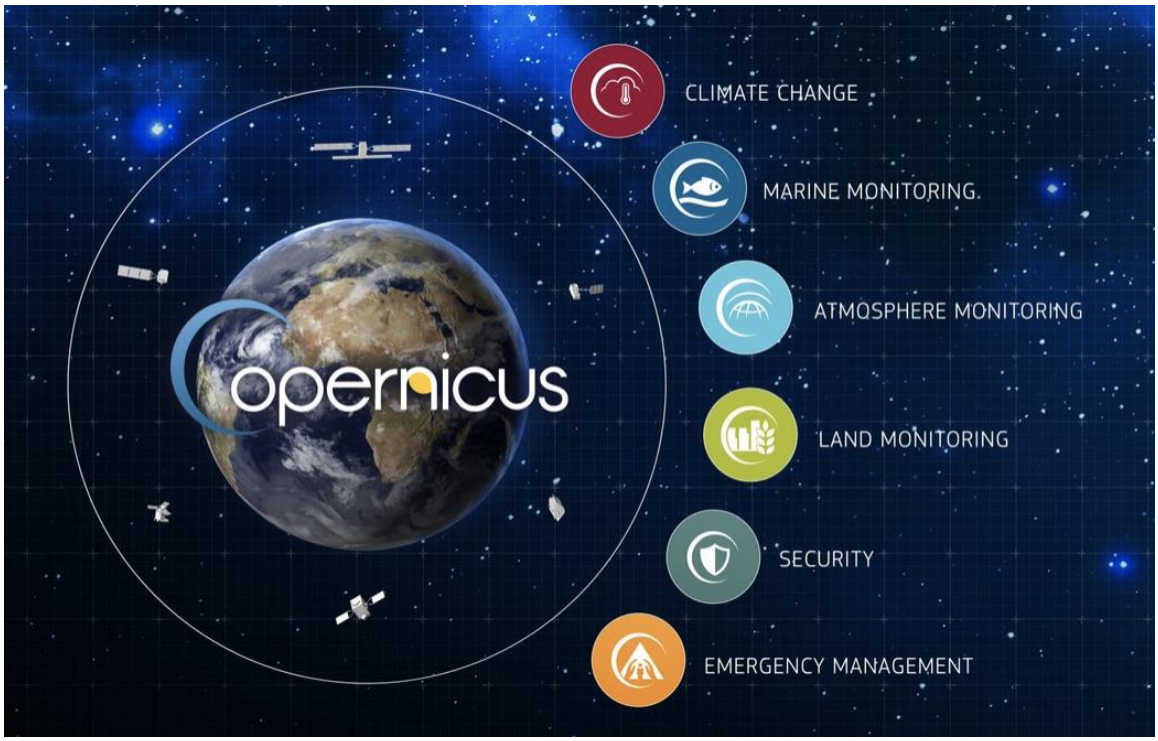

Figure 26. ERA5-Land Source: cds.climate.copernicus.eu

3E Data Services and **Reuniwatt SunSat**, on the other hand, offer products specifically designed for the solar industry and, for the scope of this work, historical and near real-time solar resource data were retrieved.

These services offer the retrieval of seven variables:

- Global Horizontal Irradiation – GHI [Wh/m^2]
- Plane of array Irradiation – POA [Wh/m^2]
- Diffuse Horizontal Irradiation – DHI [Wh/m^2]
- Direct Normal Irradiation – DNI [Wh/m^2]
- Ambient temperature (at 1.5 m) [°C]
- Wind speed (at 10 m) [m/s]
- Wind direction (at 10 m) [°]

The maximum temporal resolution available is 15 minutes**.**

Satellite-derived irradiance data is retrieved through the application of radiative transfer models to the measurements performed by on-board satellite optical instruments, which measure the radiance reflected by the earth's surface, filtered by the atmosphere.

The main differences between the two data sources are the spatial resolution, the maximum temporal resolution, the temporal coverage, the irradiance components retrievable and the delay from real time to which data are made available to the user.

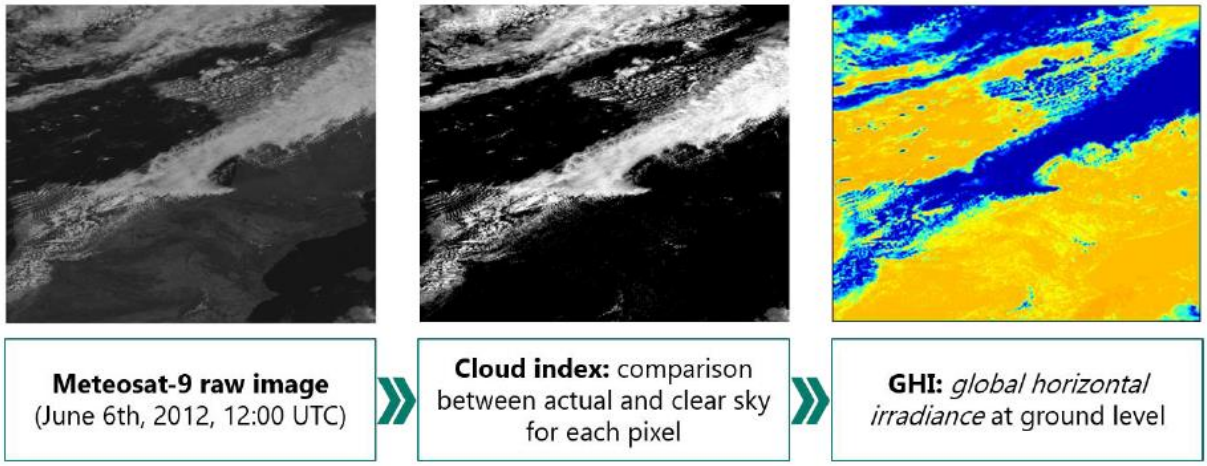

Figure 27. Satellite data: from raw images to GHI. Source: Reuniwatt

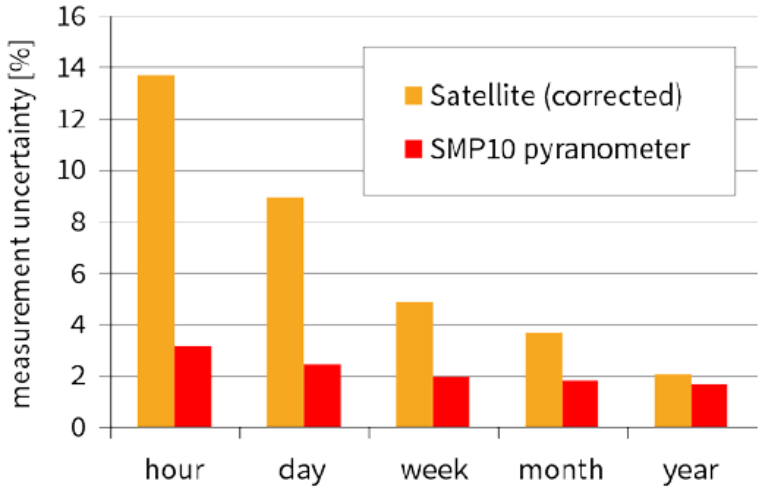

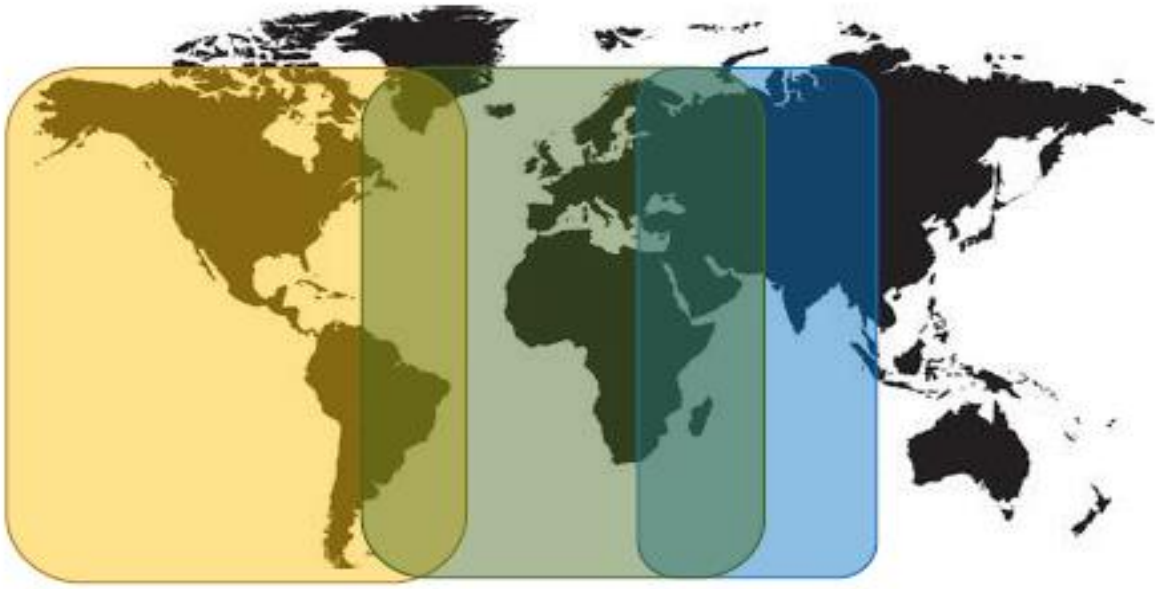

	Data Source	Spatial resolution	Temporal coverage	Time resolution
	Meteosat (PRIME) - CPP algorithm	3 km²	From 2004 to date	
	GOES EAST & WEST Extended Northern Hemisphere & Full Disk	3 km²	From 2014 to date*	15 minutes
	Meteosat (IODC) – CPP algorithm (Available in Q3 2019)	3 km²	From 2019 to date	

* Continuously expanding down to 2009

Figure 28. **3E Data services**: Reported ,measurement uncertainty, geographical and temporal coverage

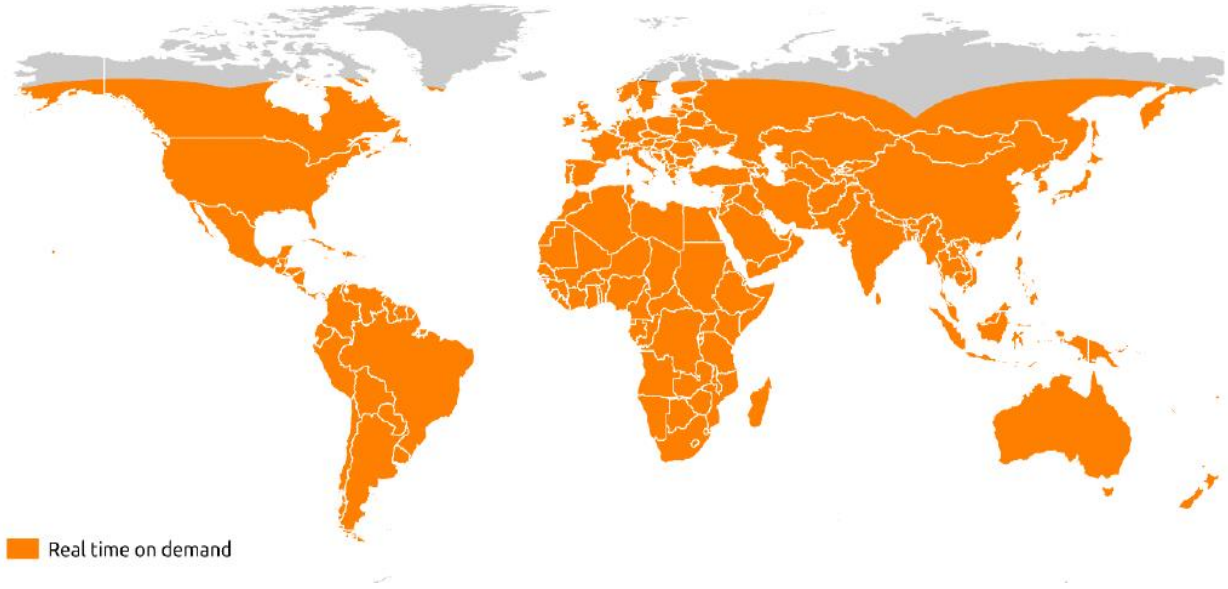

Area	America	Europe-Africa	Middle East / Indian Ocean	Western Pacific / Oceania
Spatial resolution	0.5-1 km	1-3 km	1-3 km	0.5-1 km
Finest time sampling	15 min. (5min. for USA)	15 min.	15 min.	10 min.

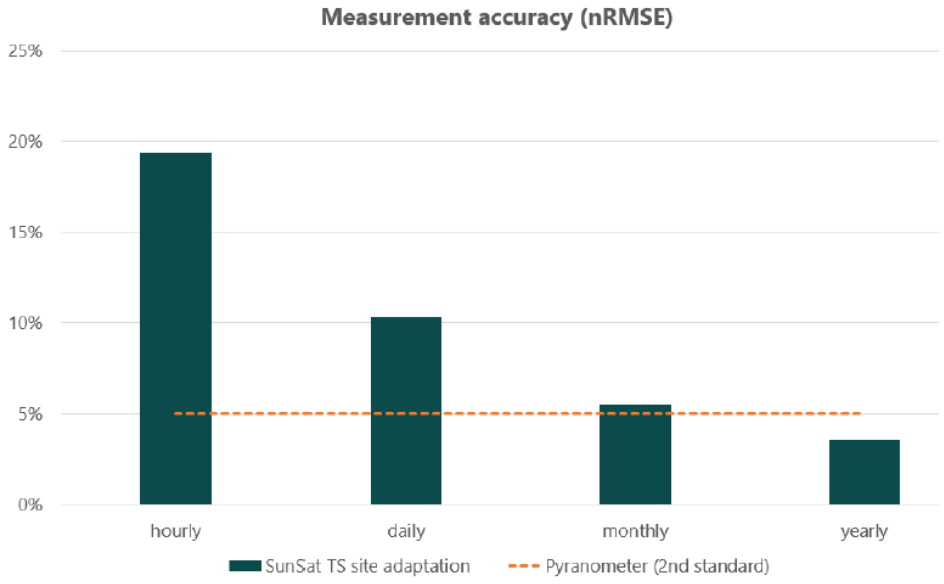

Figure 29. **Reuniwatt SunSat**: Reported measurement uncertainty, geographical and temporal coverage

3.4 The error as a measure of uncertainty

The ISO/IEC GUIDE 98-3 [18] defines the *uncertainty of a measurement* as "*a measure of the possible error in the estimated value of the measurand (particular quantity subject to measurement) as provided by the result of a measurement*", thus linking the concept of error to the concept of measurement uncertainty.

To evaluate how good a satellite-derived irradiance time-series is, it is a good practice to compare it to the measurements recorded (over the same period and in the same location) by a secondary standard pyranometer (properly calibrated and maintained). This comparison is carried out subtracting the measurements vector ($\hat{\boldsymbol{y}}$) from the reference vector (y).

The result of this operation is the vector of residuals, which contains information about how far every single satellite-derived value is from the corresponding pyranometer value, i.e. quantifies the magnitude of the error which the satellite service is doing in estimating the real irradiance from satellite images.

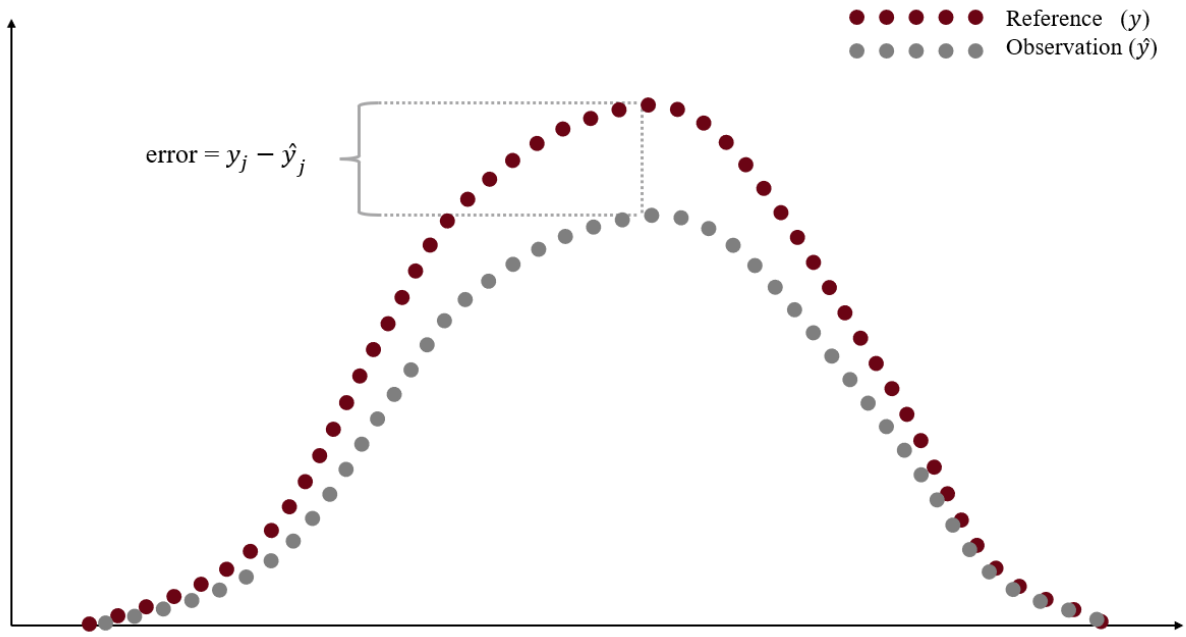

Figure 30. **Error as a measurement of uncertainty**

In this analysis three metrics are employed in order to have a single figure representing the error, instead of the vector of residuals.

3.5 Error metrics applied

Mean Bias Error (MBE)

Quantifies the average magnitude of the errors, considering their direction (sign). It captures therefore the average bias of the dataset. A positive bias represents an underestimation and negative bias represents an overestimation. It expresses the error in units of the variable of interest (in this case W/m^2). It gives useful average information on the bias but should be interpreted cautiously because positive and negative errors will cancel out.

$$MBE = \frac{1}{n}\sum_{j=1}^{n}\left(y_j - \hat{y}_j\right)$$

Root Mean Square Error (RMSE)

It is a quadratic scoring rule that, as the MBE, also measures the average magnitude of the error, but without considering their direction. It expresses the error in units of the variable of interest (in this case W/m^2). Taking the square root of the average squared errors has some interesting implications: since the errors are squared before they are averaged, the RMSE gives a relatively high weight to large errors. This means the RMSE is more useful when large errors are particularly undesirable.

$$RMSE = \sqrt{\frac{1}{n}\sum_{j=1}^{n}\left(y_j - \hat{y}_j\right)^2}$$

Normalized Root Mean Square Error (nRMSE)

It is a metric that normalizes (brings to the same scale) the RMSE. In this report we normalize using the mean of the distribution. It is often expressed as a percentage (%). It facilitates the comparison between datasets or models with different scales.

$$nRMSE = \frac{\sqrt{\frac{1}{n}\sum_{j=1}^{n}\left(y_j - \hat{y}_j\right)^2}}{\bar{y}}$$

Where

n: number of observations
y_j: reference value of j-th observation
$\hat{y}_j$: predicted value of j-th observation
$\bar{y}$: mean of the reference distribution

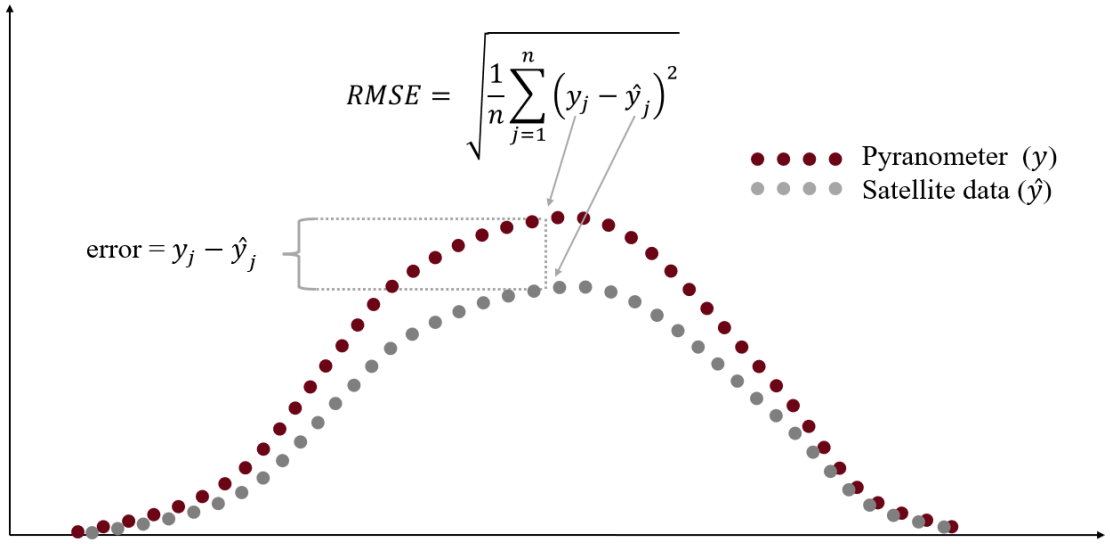

Figure 31. **Example of RMSE calculation**.

3.6 Clean data comparison

During this stage, the raw time series were loaded in the system and underwent the transformations described below.

a) **Timestamp alignment**

The satellite sources are in UTC time zone (Greenwich Mean Time, UTC+00) and they were converted to UTC+01 time zone in order to allow the execution of further modelling steps.

b) **Measurement unit alignment**

Among the variables retrieved from ERA5-Land dataset, 2 Metre temperature and 2 Metre dewpoint temperature (retrieved as instantaneous values) were converted from Kelvin to Celsius, while GHI irradiance (Surface solar radiation downwards, retrieved as accumulations)

was converted from J/m^2 to W/m^2 (considering that the accumulation period is 1 hour – 3,600 seconds) and subsequently converted to instantaneous values. 3E's irradiation, expressed as energy (Wh/m^2), was converted to power (W/m^2).

c) **Irradiance outliers filtering**

In accordance with International Standard IEC 61724-1:2017, values recorded outside the daylight hours (night values) were filtered out (replaced with zero) from both time series. For this purpose, sunrise and sunset hours are calculated for each day (with pvlib) and night values are detected by comparing the timestamps of the time series with calculated sunrise and sunset time.

d) **Resampling**

ERA5-Land variables have a maximum temporal resolution of 1 hour, while 3E's and Reuniwatt's irradiance time-series maximum data granularity is 15 minutes, thus the latter were resampled to 1 hour: the mean of the values over 1 hour intervals were calculated, rendering a timestamp denoting the beginning of the interval together with the mean value (missing values are discarded from the process).

e) **Calculation of deviation/error metrics**

As explained in the previous section.

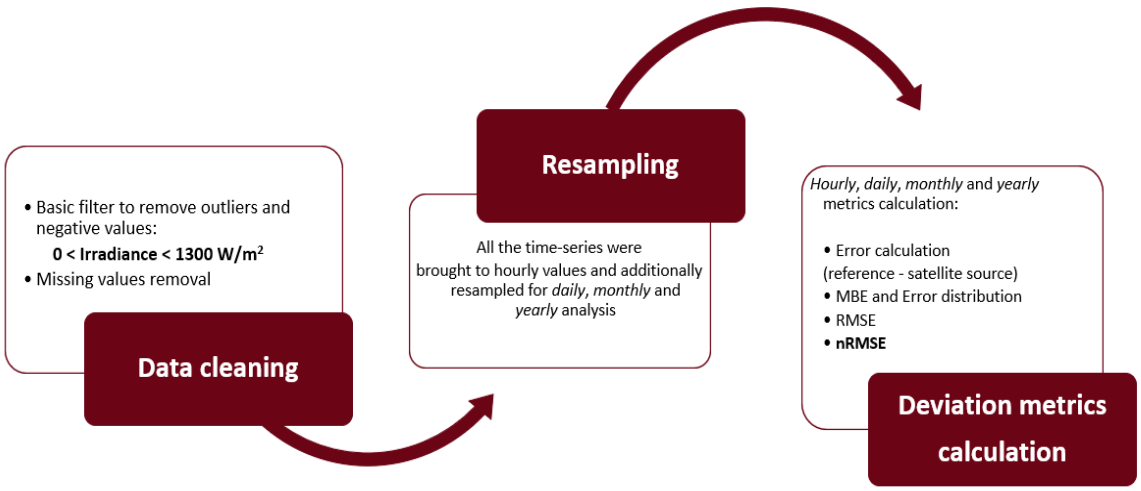

Figure 32. Methodology overview

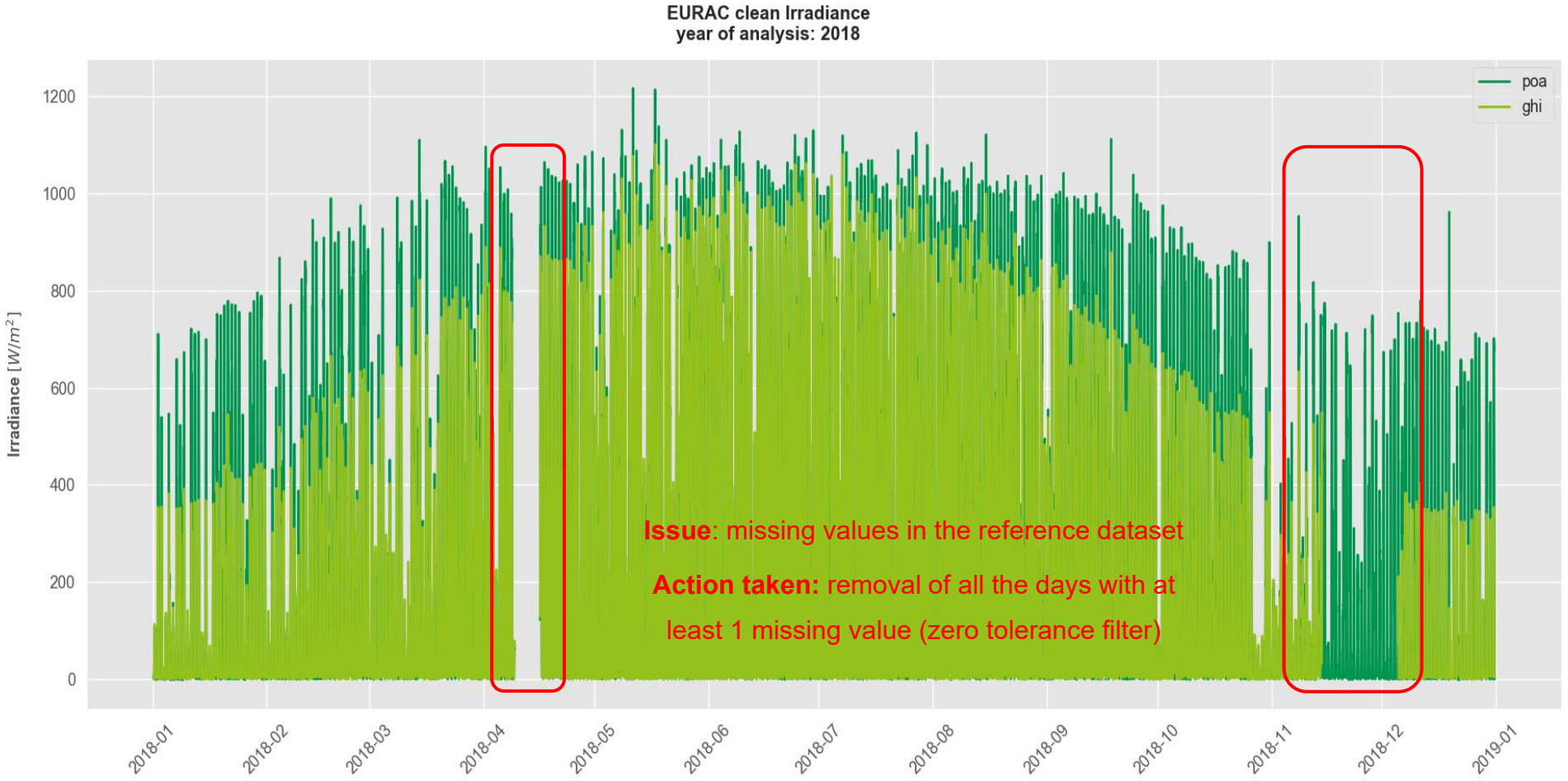

Figure 33. **Reference dataset**: research-grade pyranometers

3.6.1 Global Horizontal Irradiance

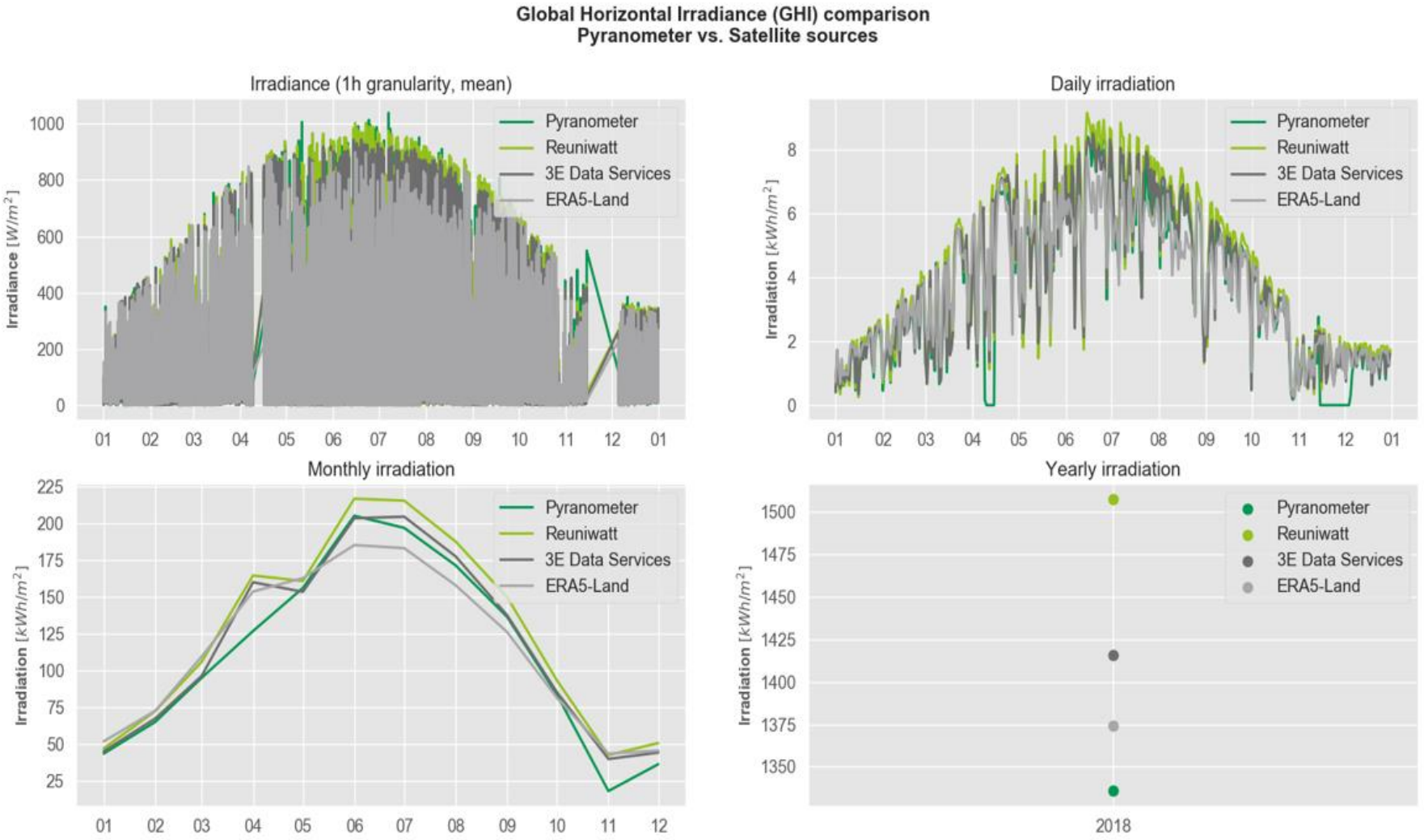

Figure 34. **Clean GHI data summary**

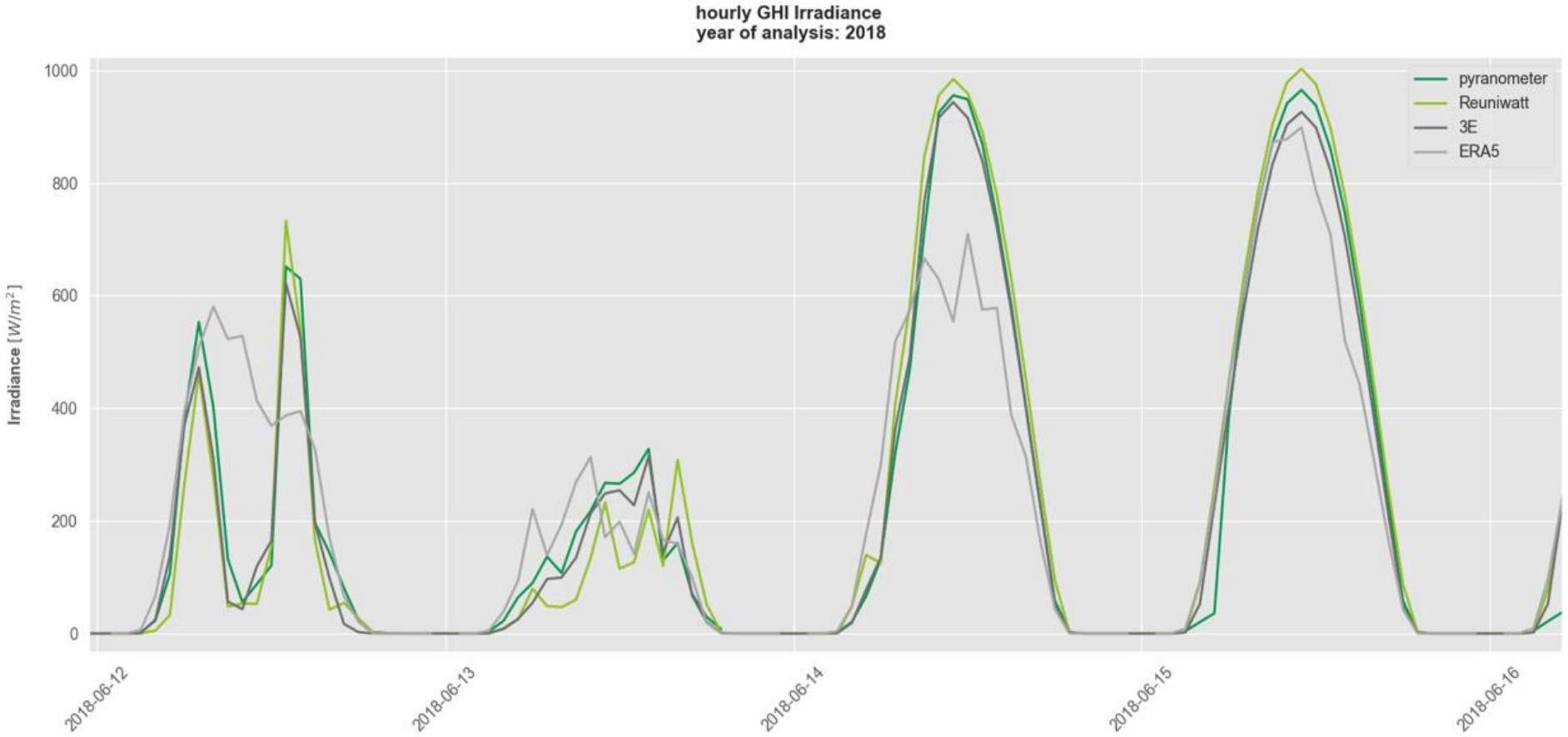

Figure 35. **Clean GHI data**: example of summer days

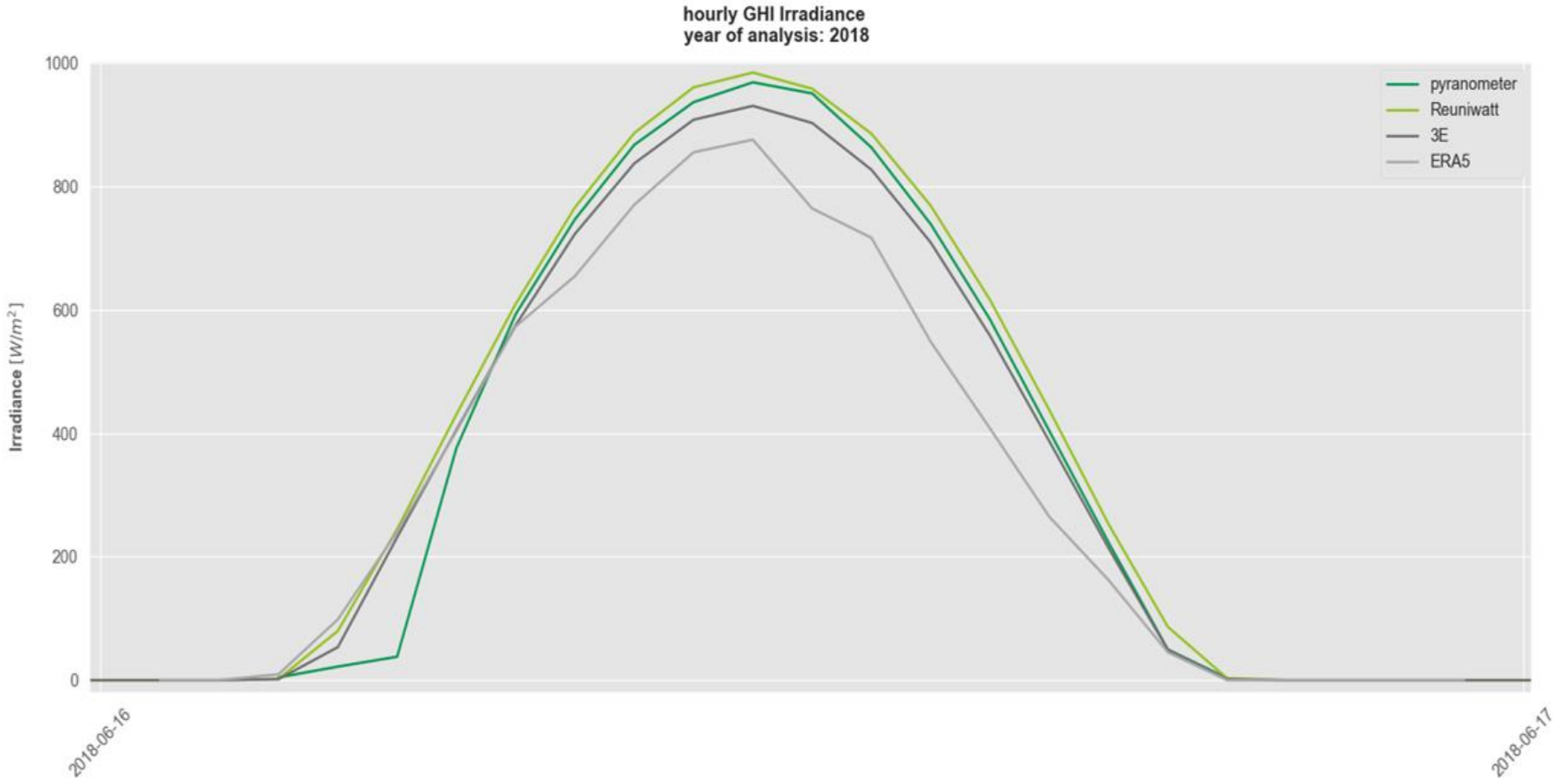

Figure 36. **GHI clean data** – example of a clear summer day

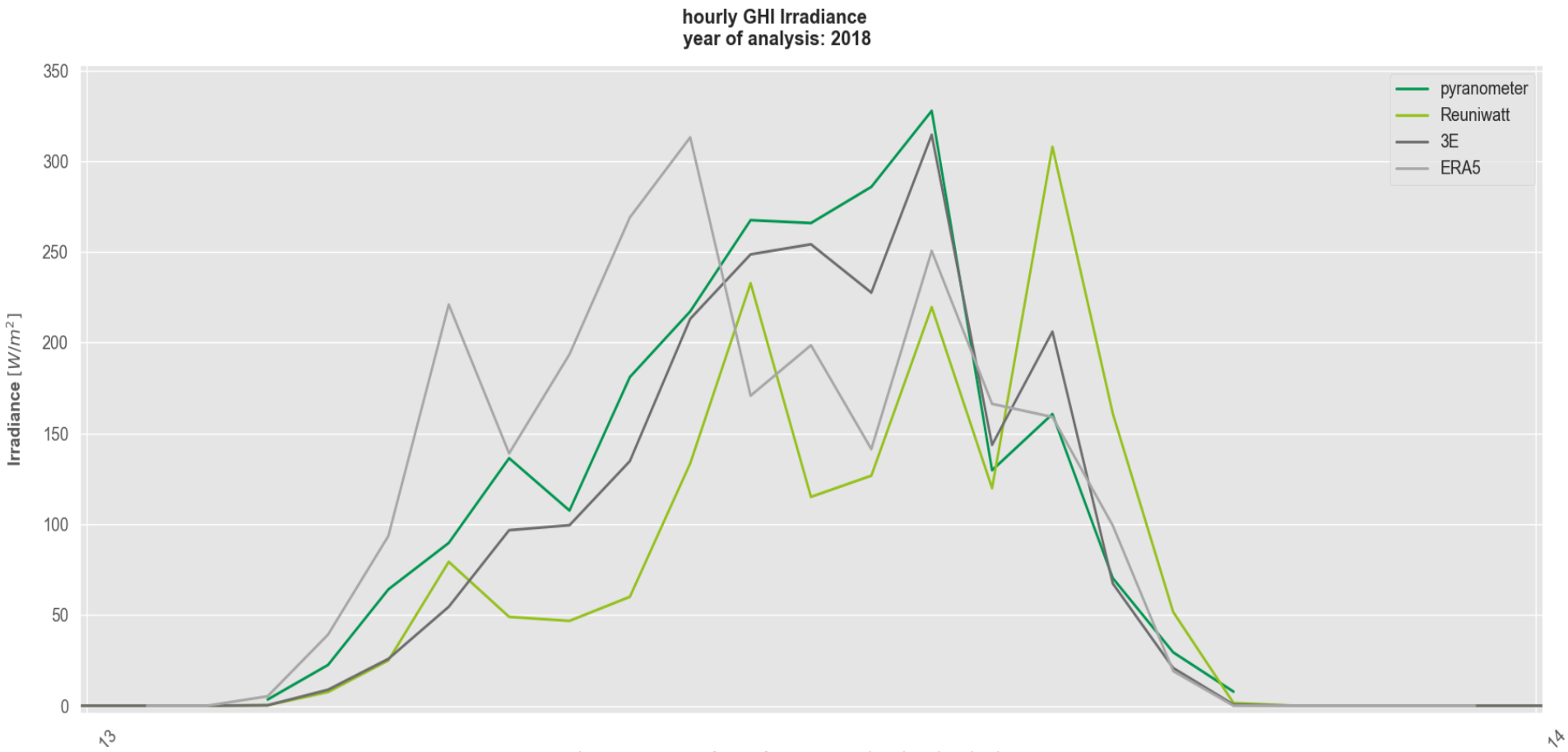

Figure 37. **GHI clean data**: example of a cloudy day

3.6.2 Plane of Array Irradiance

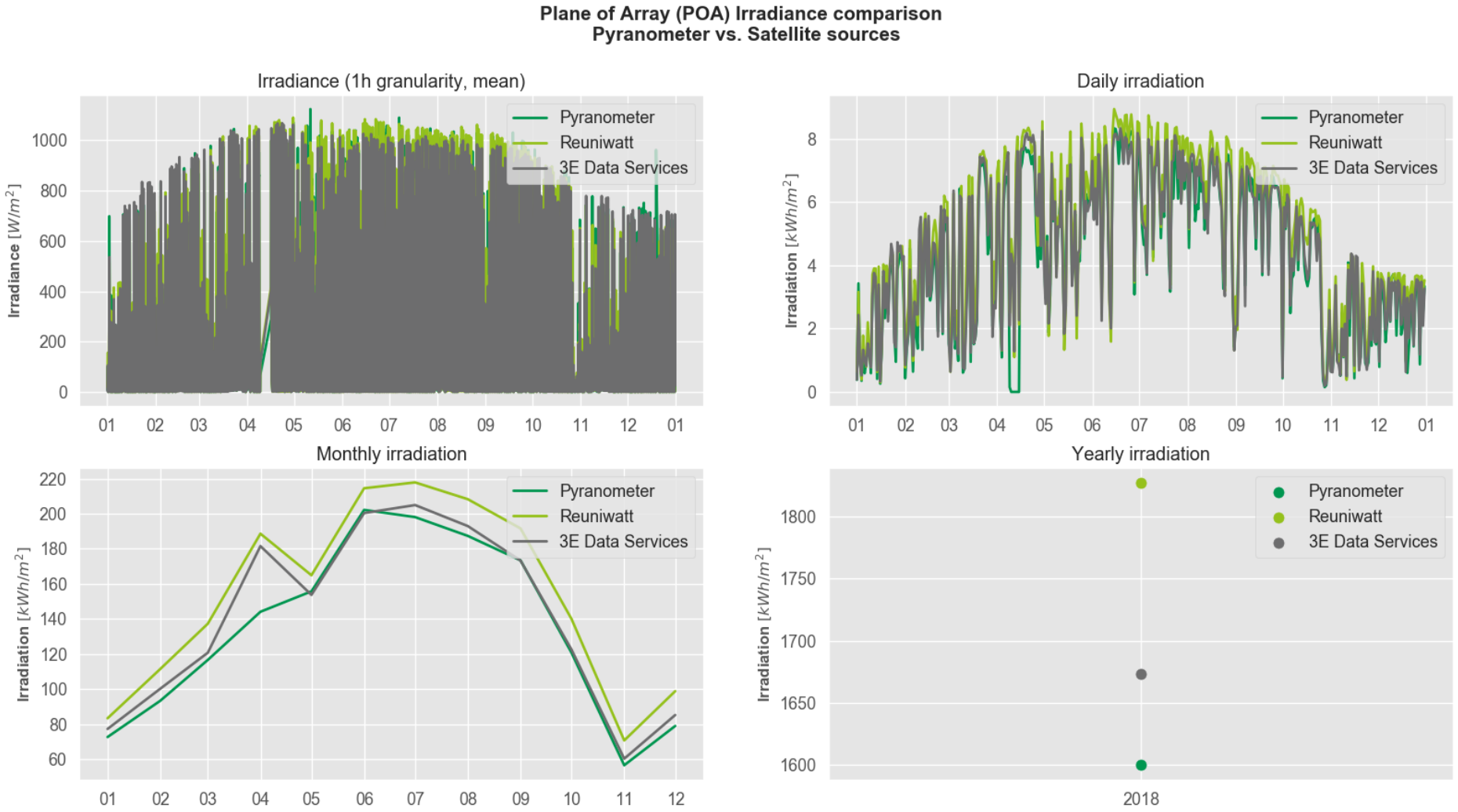

Figure 38. **Clean POA** data summary

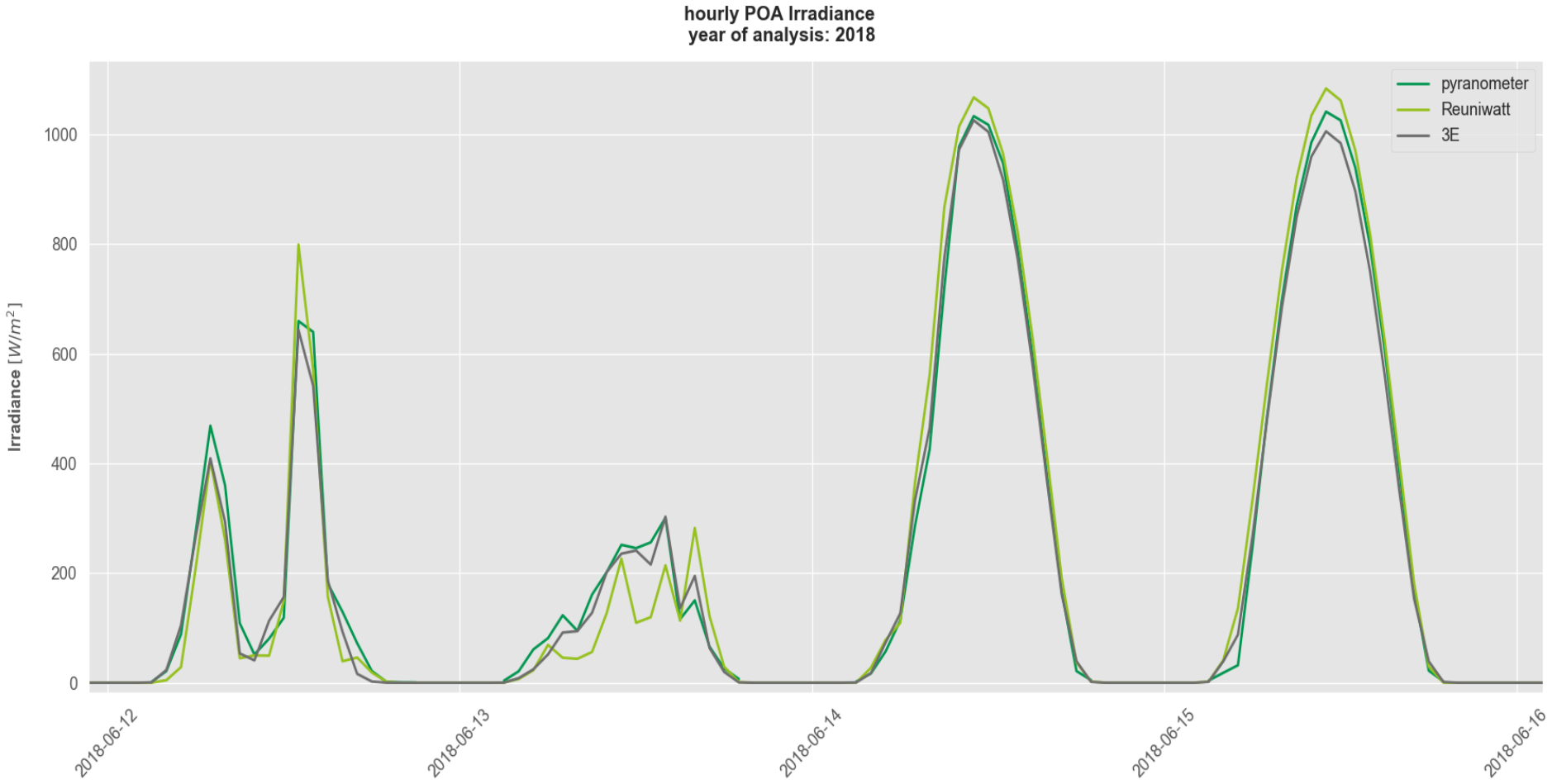

Figure 39. **Clean POA data**: example of summer days

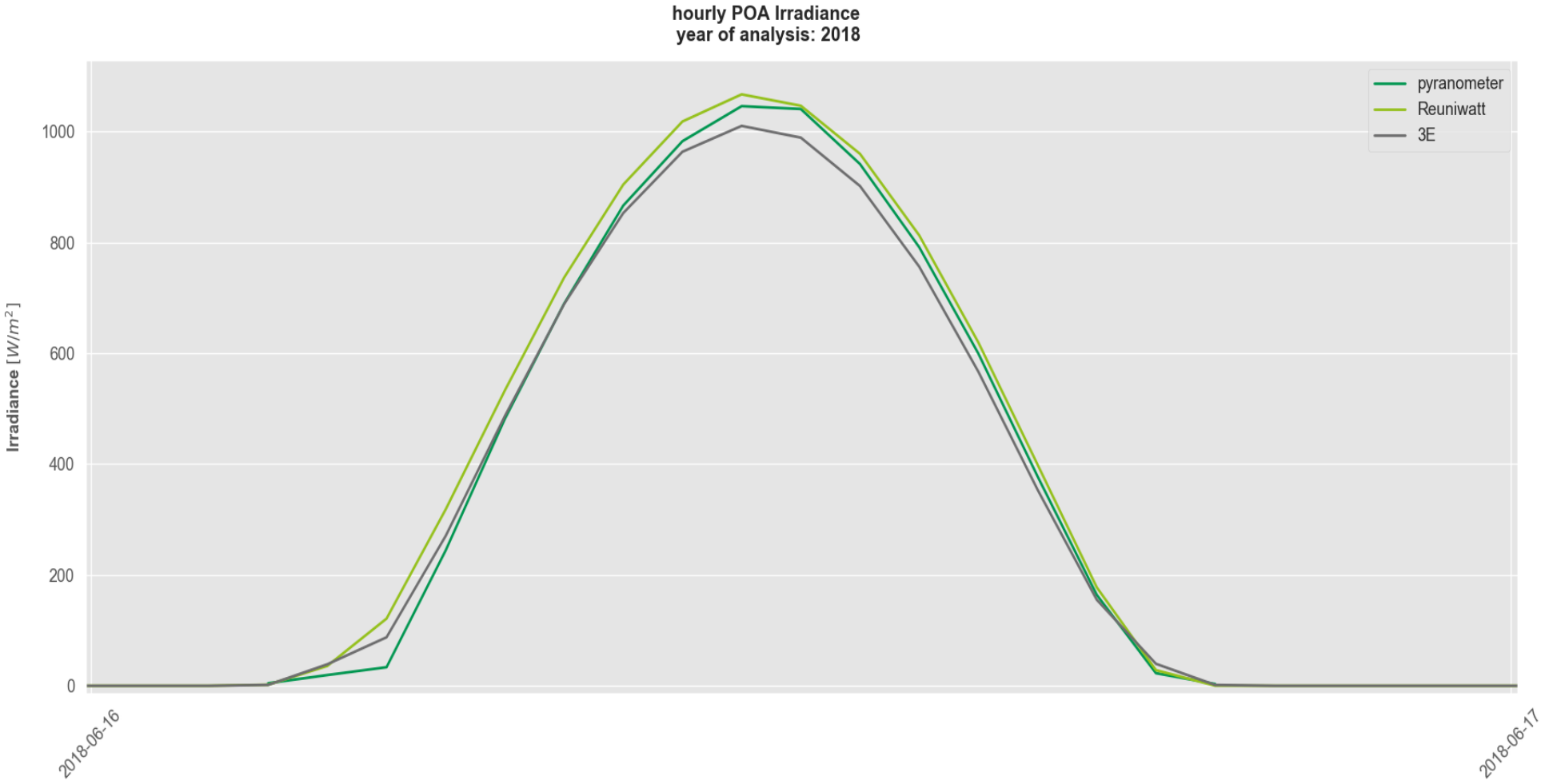

Figure 40. **Example of a clear summer day**

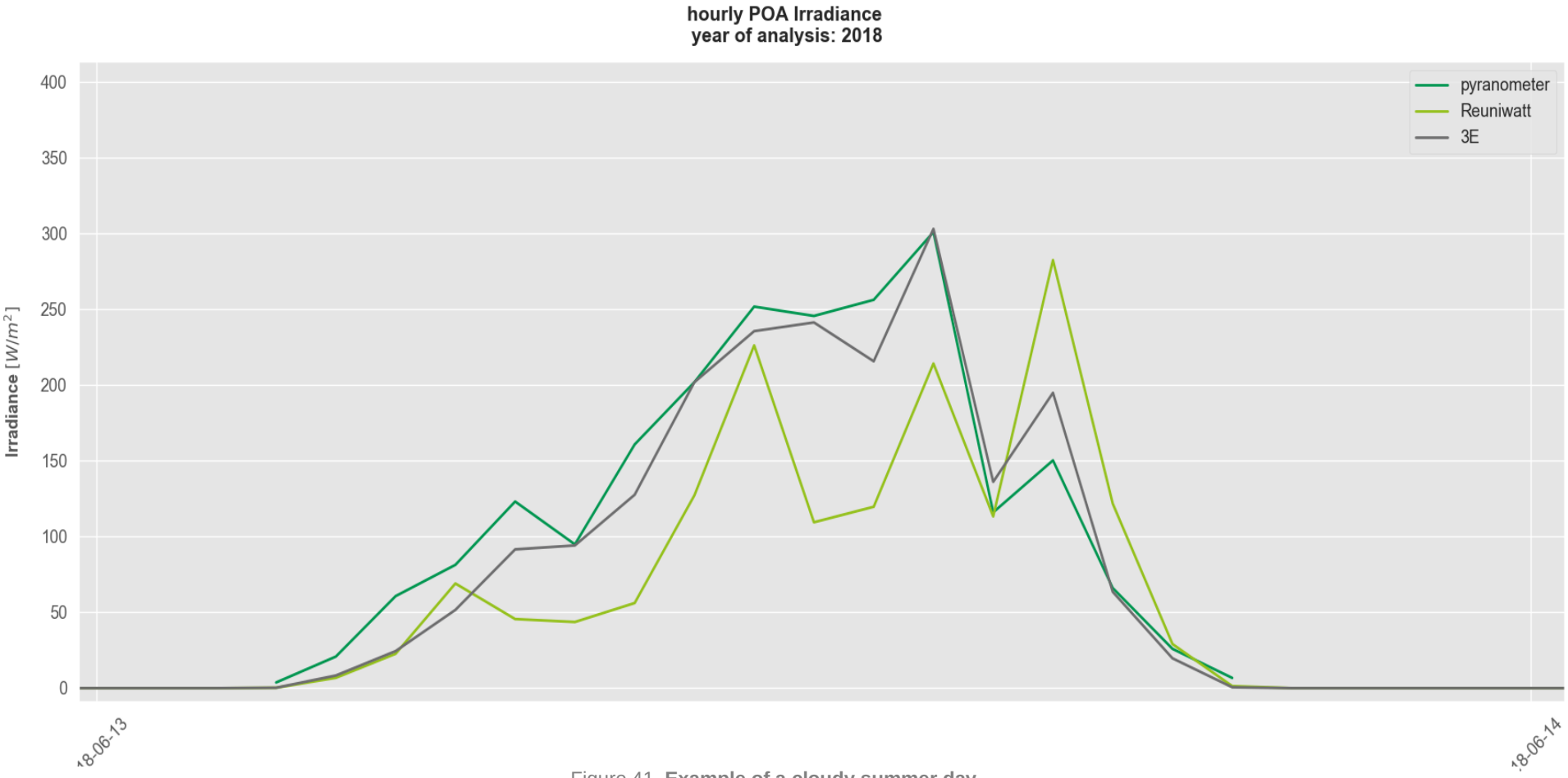

Figure 41. **Example of a cloudy summer day**

3.7 Results and discussion

3.7.1 GHI and POA monthly data comparison

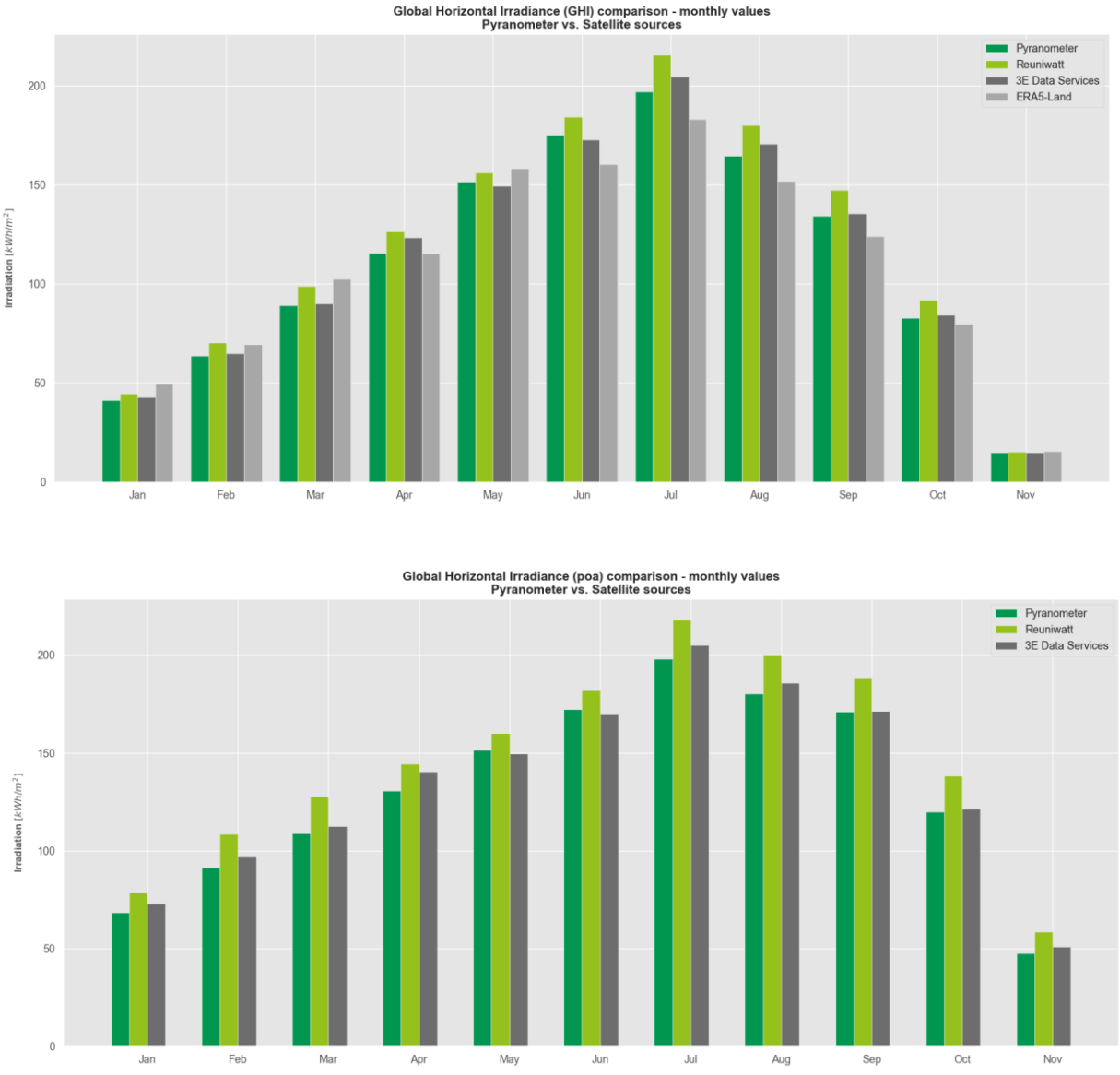

Figure 42. **GHI and POA monthly data**

3.7.2 GHI error distribution

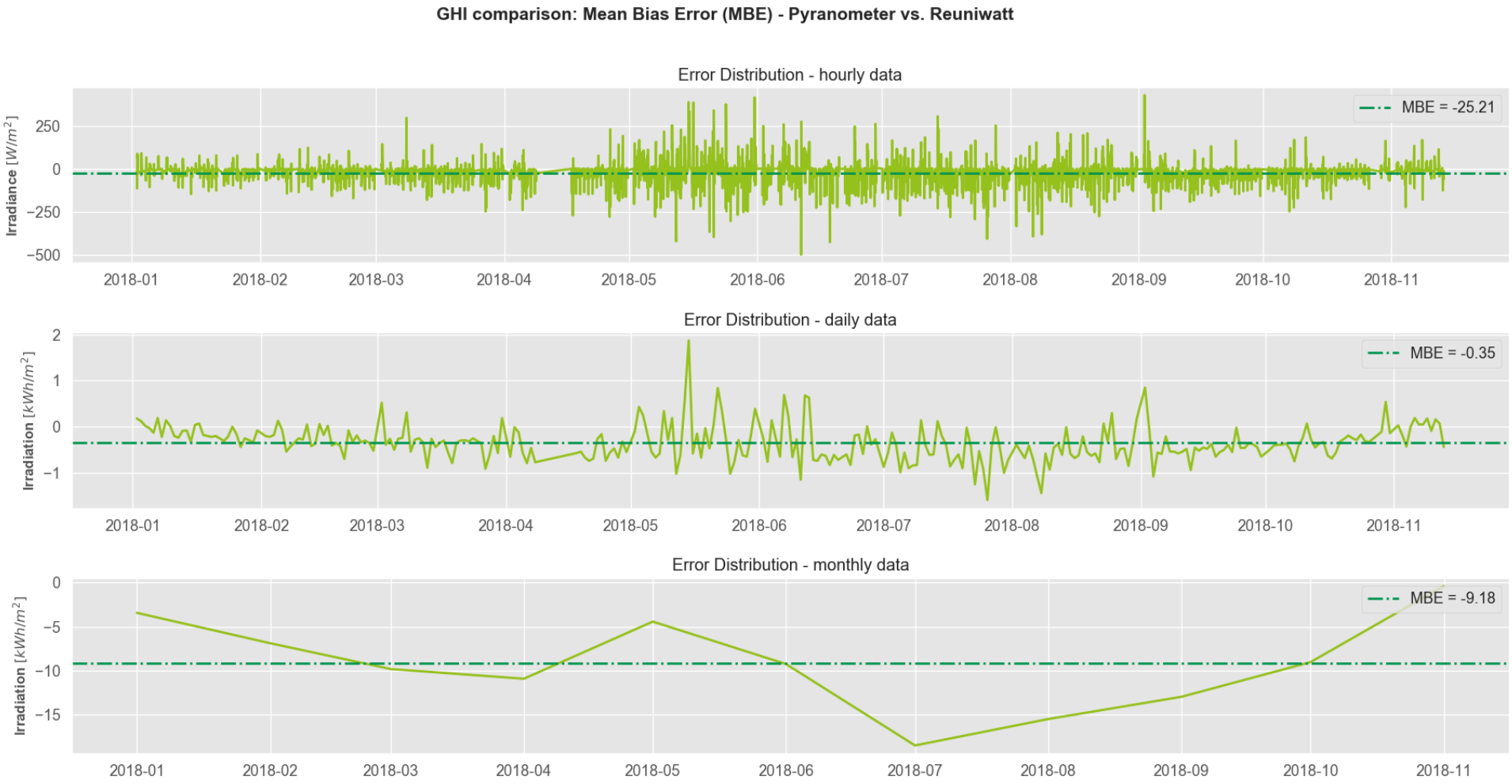

Figure 43.**GHI error distribution:** Reuniwatt SunSat

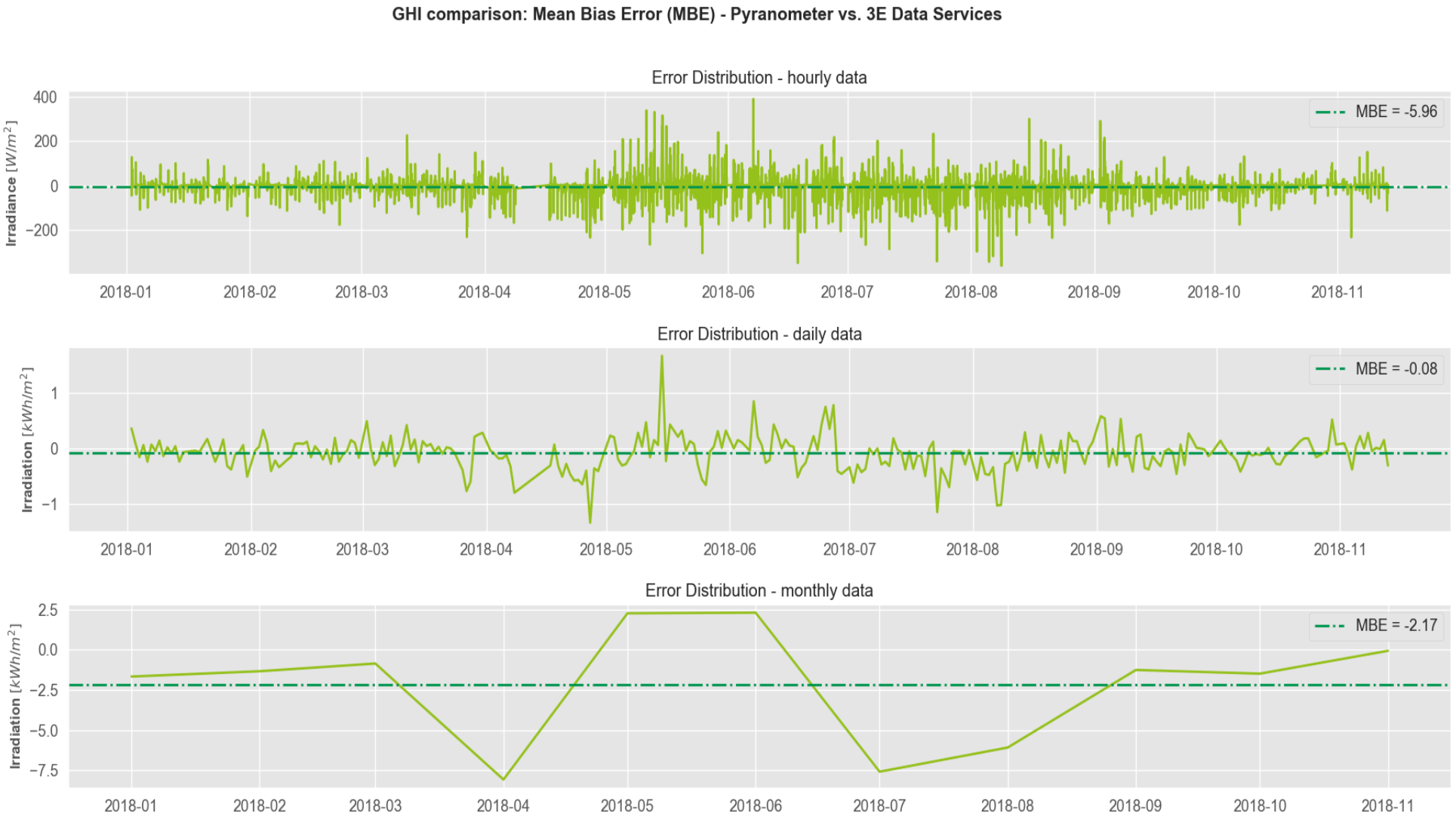

Figure 44. **GHI error distribution:** 3E Data Services

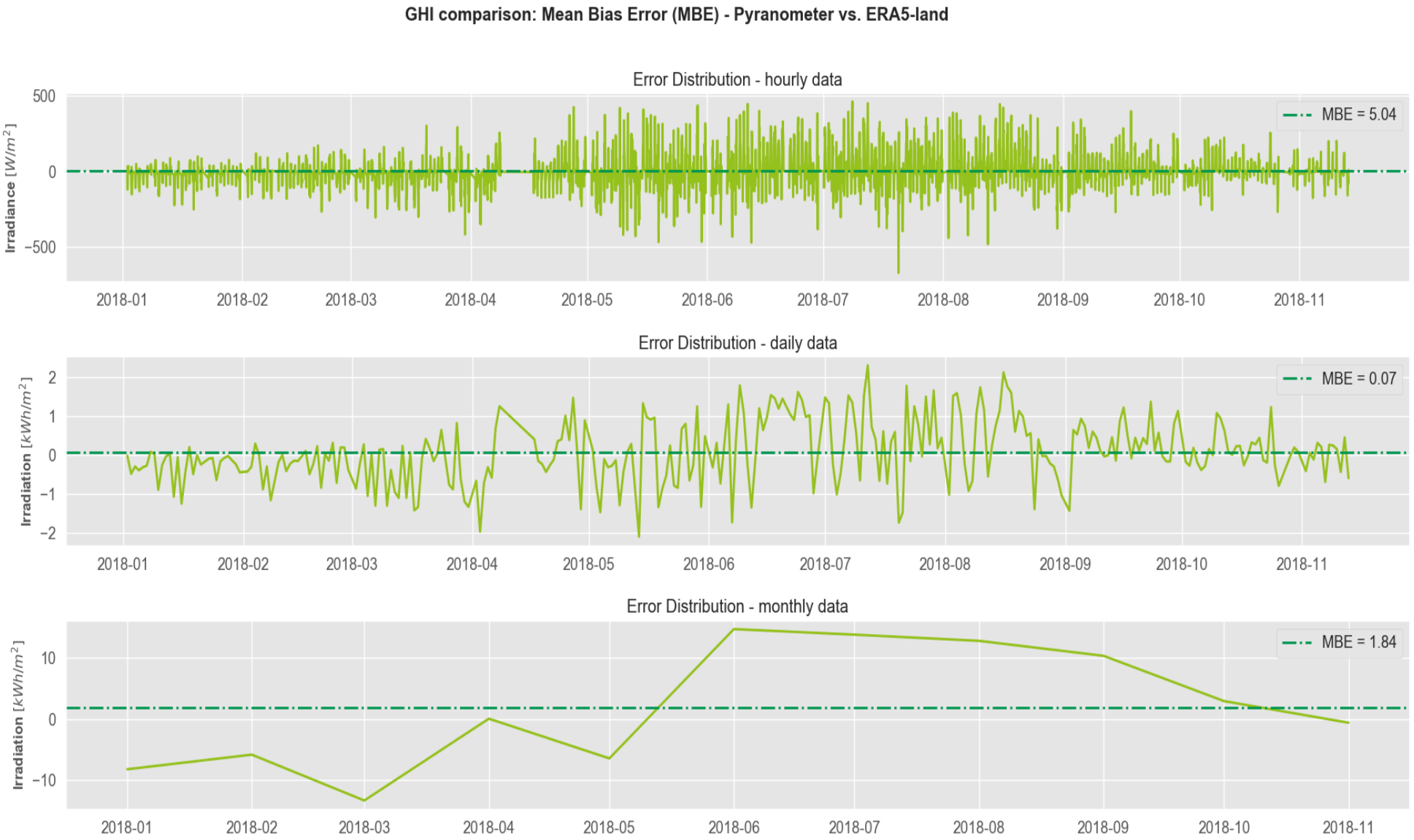

Figure 45. **GHI error distribution:** ERA5-land

3.7.3 POA error distribution

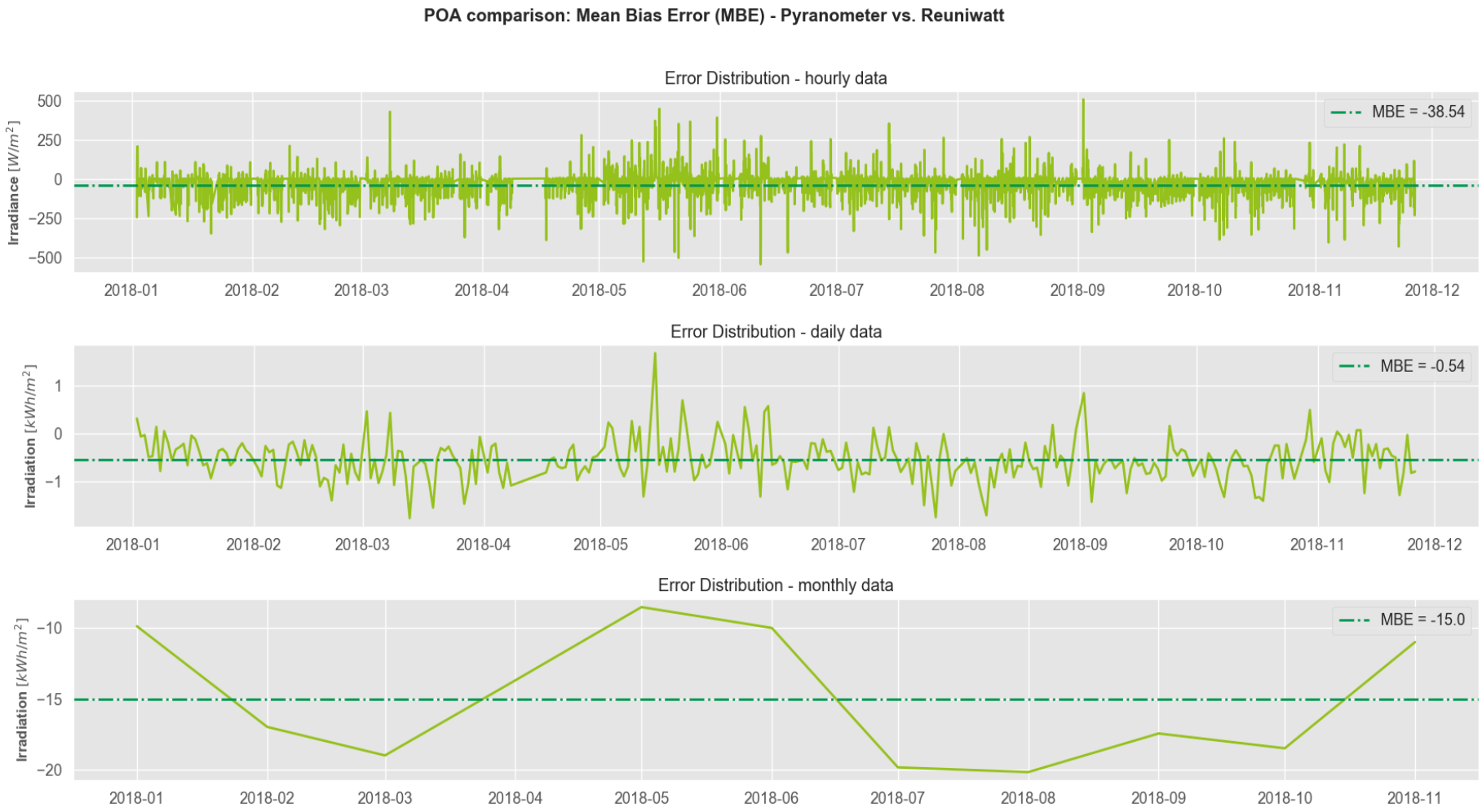

Figure 46. **POA error distribution**: Reuniwatt SunSat

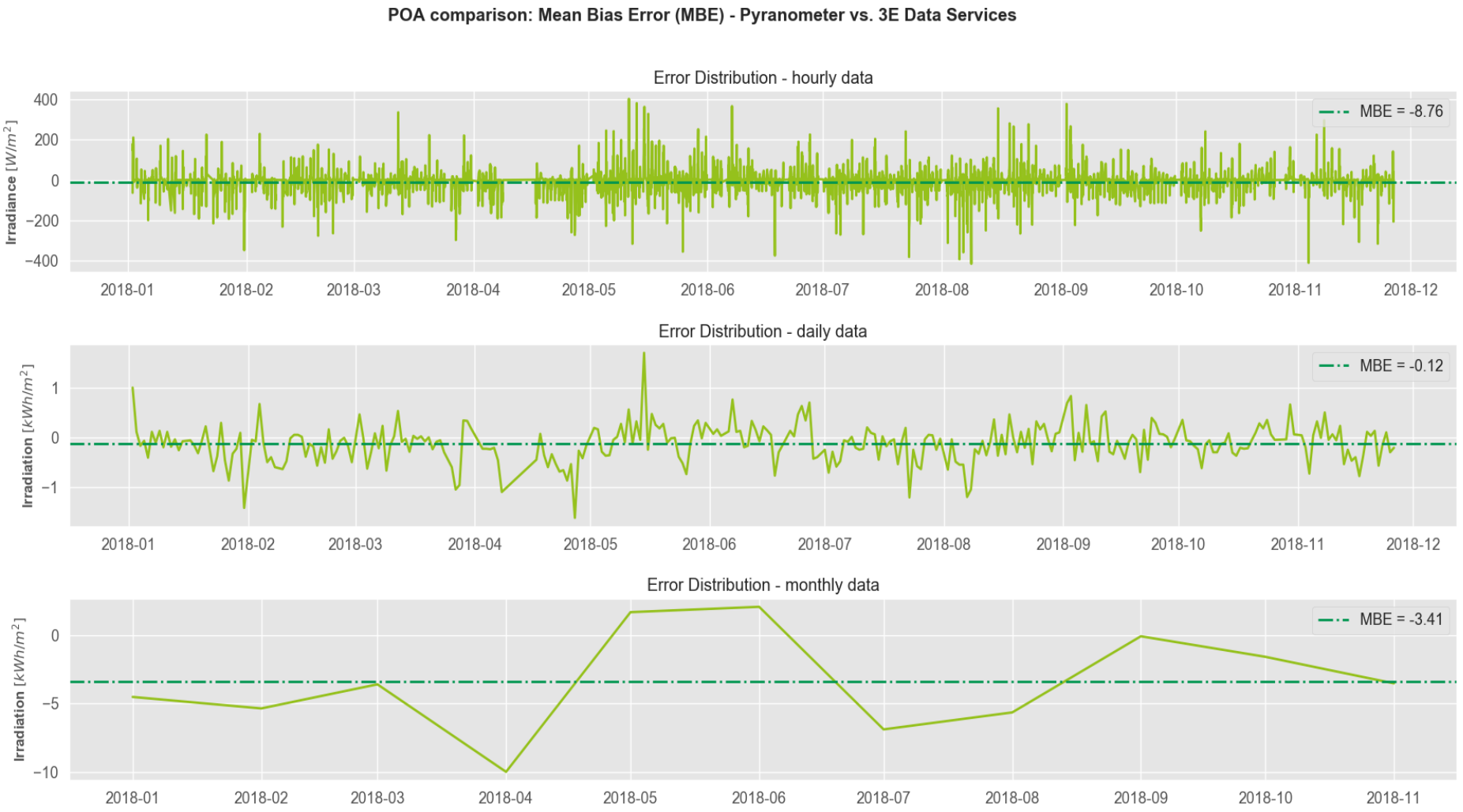

Figure 47. **POA error distribution**: 3E Data Services

3.7.4 MBE and RMSE

Mean Bias Error (MBE)

		Reuniwatt	3E Data Services	ERA5-land
GHI	year (Wh/m²)	-100.95	-23.87	20.21
	month (Wh/m²)	-9.18	-2.17	1.84
	day (Wh/m²)	-0.35	-0.08	0.07
	hour (W/m²)	-25.21	-5.96	5.04
POA	year (Wh/m²)	-164.98	-37.49	*NA*
	month (Wh/m²)	**-15**	**-3.41**	*NA*
	day (Wh/m²)	-0.54	-0.12	*NA*
	hour (W/m²)	-38.54	-8.76	*NA*

- A positive bias represents an underestimation (i.e. satellite < pyranometer)
- A negative bias represents an overestimation (i.e. satellite > pyranometer)
- It can be seen that in all cases both commercial datasets overestimate (in average) the pyranometer's values, whereas the free data set underestimates.

Root Mean Square Error (RMSE)

		Reuniwatt	3E Data Services	ERA5-land
GHI	year (kWh/m²)	100.95	23.86	20.20
	month (kWh/m²)	10.47	4.03	9.54
	day (kWh/m²)	0.51	0.31	0.80
	hour (W/m²)	74.31	56.77	119.40
POA	year (kWh/m²)	164.98	37.49	*NA*
	month (kWh/m²)	**15.58**	**4.89**	*NA*
	day (kWh/m²)	0.69	0.39	*NA*
	hour (W/m²)	92.04	65.23	*NA*

- For most cases, it can be seen that *3E Data Services* yielded the lowest error.
- Especial attention is paid to POA monthly values because they are particularly useful for Performance Reporting.

3.7.5 nRMSE

normalized Root Mean Square Error (nRMSE)

		Reuniwatt	3E Data Services	ERA5-land
GHI	year	7.59%	1.90%	1.67%
	month	**8.66%**	**3.54%**	**8.68%**
	day	11.35%	7.41%	19.44%
	hour	22.37%	18.14%	39.56%
POA	year	10.28%	2.54%	*NA*
	month	**10.68%**	**3.64%**	*NA*
	day	13.23%	8.20%	*NA*
	hour	24.56%	18.91%	*NA*

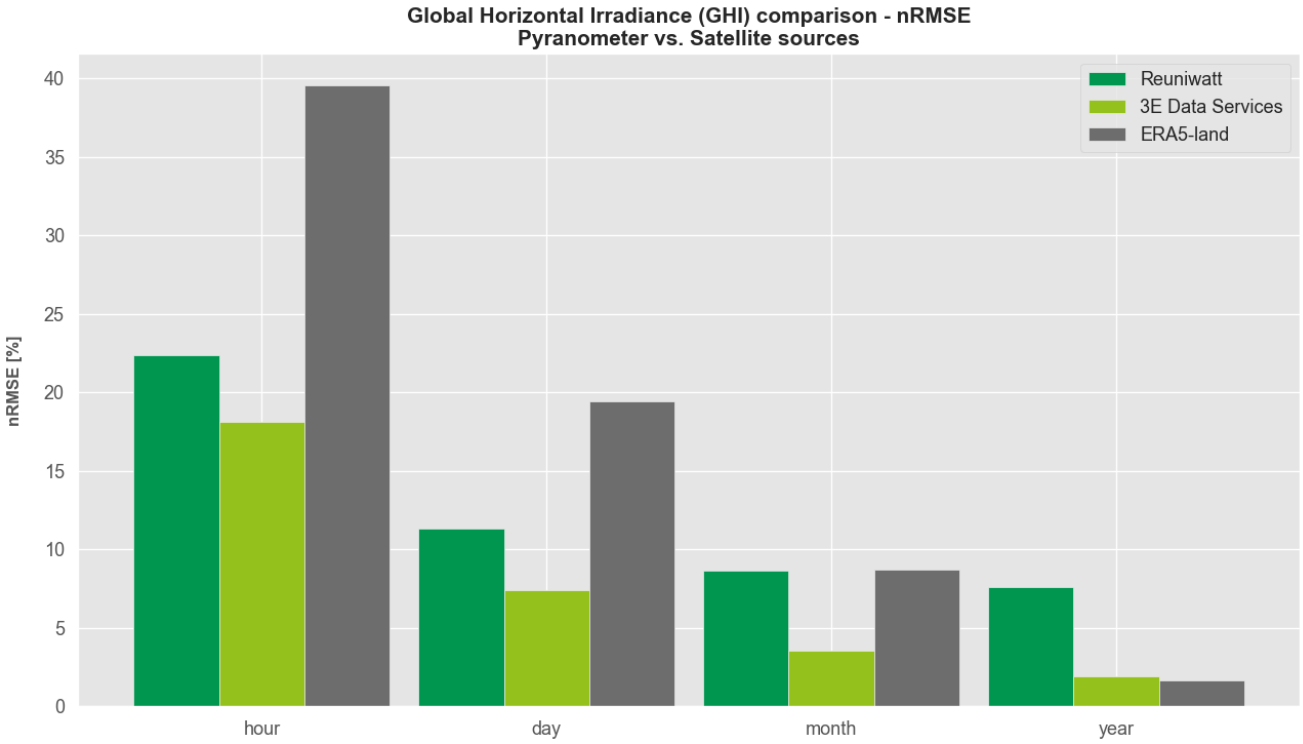

Figure 48. **GHI uncertainty** summary

- For most cases, *3E Data Services* yielded the lowest uncertainty, with the exception of yearly data, where ERA5-land had the lowest value.
- For high granularity values (hour, day), *ERA5-land* resulted the less accurate of the 3 satellite sources analyzed.
- For low granularity values (year), *Reuniwatt* resulted as the less accurate of the 3 satellite sources analyzed.

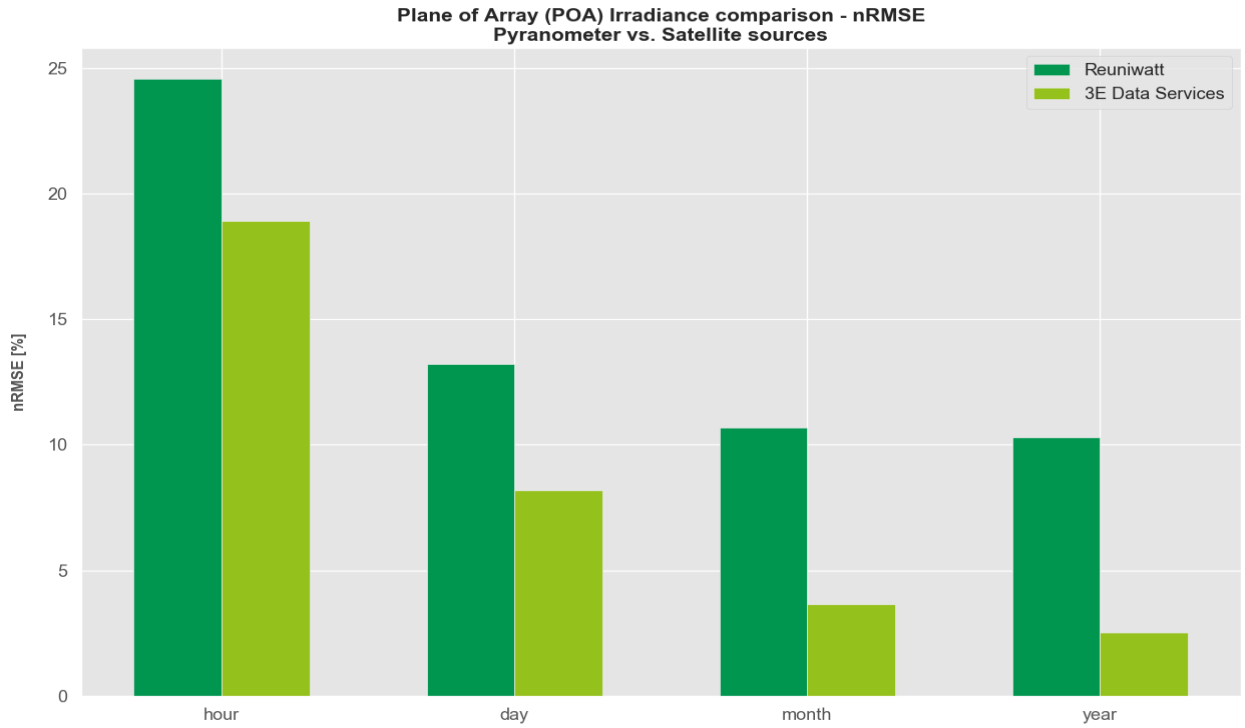

Figure 49. **POA uncertainty summary**

- POA irradiance is not available in the *ERA5-land* dataset, so this comparison was possible only for *Reuniwatt* and *3E*.
- In all the cases, *3E Data Services* resulted the most accurate source.

Interpretation of results

- In all the cases, *3E Data Services* resulted the most accurate source.
- The present analysis gives a general idea of how satellite sources deviate from on-site measurements.
- In 95% of the cases (19/20) satellite data overestimated on-site measurements.
- Satellite data deviates the most from ground measurements under cloudy conditions (commercial solutions based their competitive advantage on how well they deal with this issue).
- Of the three solutions analysed, in 87.5% of the cases (7/8), *3E Data Services* resulted the most accurate source.
- The free available dataset *ERA5-land* resulted the best only for GHI yearly data, but the worst for daily and monthly data.

- The *uncertainty* figures calculated in the present analysis in many cases are twice as big as the reported uncertainties in the literature and in the marketing material of the service providers. This might be mainly due to the fact this analysis was done only for one site for one year (other possible causes might involve the methodology and metrics used).
- Validation should be done more extensively (more sites) to get more precise generic figures, because satellite data is highly sensible to the geographic location and local climates
- Finally, as previously explained, the temporal resolution offered by ERA5-Land (1 hour) may be enough for monthly KPIs calculation, but it could be totally insufficient when a higher granularity is needed, for example in case of fault detection. In this case, employing 3E Data Services is the most viable solution (maximum temporal resolution: 15 minutes), despite the well-known uncertainties.

4 Data Quality analysis

The analysis proposed in this chapter is a consistent data quality control procedure for the assessment of raw measurements and consequently of the sensors' health status.

The procedure consists of three stages:

a) Data pre-processing
b) Data Quality Check
c) The 'virtual sensor' *concept*

Once data have been pre-processed, anomalous records are detected through the execution of multiple consecutive quality checks. Finally, virtual sensors are defined to lower the uncertainties deriving from missing data, which may affect KPIs calculation.

Each step gets as input the time-series processed during the previous stage and outputs a summary reporting on the transformations applied to the data and, when applicable, one or more modified time-series, ready for evaluation. The only exception is the first stage, in which raw data gets loaded and transformed in order to be ready for further processing.

This analysis has been programmed in Python and delivers a report-like document containing valuable insights for technical managers and decision makers.

4.1 Terms and definitions

For ease of reading, terms and definitions used in the rest of the chapter are gathered in this paragraph.

Resampling: modifying the temporal interval of a time series averaging the values over the chosen temporal interval. For example, aggregation of 5-minutes data into 15-minutes data: in this process the mean of the values over 15 minutes intervals are calculated, rendering a timestamp denoting the beginning of the interval together with the mean value (missing values are discarded from the process).

Timestamp	POA (W/m²)
2018-01-01 13:00:00+01:00	158.1
2018-01-01 13:05:00+01:00	127.5
2018-01-01 13:10:00+01:00	142.8
2018-01-01 13:15:00+01:00	NaN
2018-01-01 13:20:00+01:00	71.4
2018-01-01 13:25:00+01:00	40.8

⇒

Timestamp	POA (W/m²)
2018-01-01 13:00:00+01:00	142.8
2018-01-01 13:15:00+01:00	56.1

Missing value (NaN): no value available for a specific variable at a specific time. The timestamp is present in the time series.

	cab1	cab4
2018-03-19 23:55:00+01:00	0.0	4.0
2018-03-20 00:00:00+01:00	NaN	4.0
2018-03-20 00:05:00+01:00	0.0	4.0

Missing log: no records are available for all the variables at a specific time. The timestamp is absent from the time series.

	2018-01-04 15:05:00+01:00	284.0
	2018-01-04 15:10:00+01:00	268.0
15:15 missing →	2018-01-04 15:20:00+01:00	246.0

Missing data: sum of missing values and missing logs

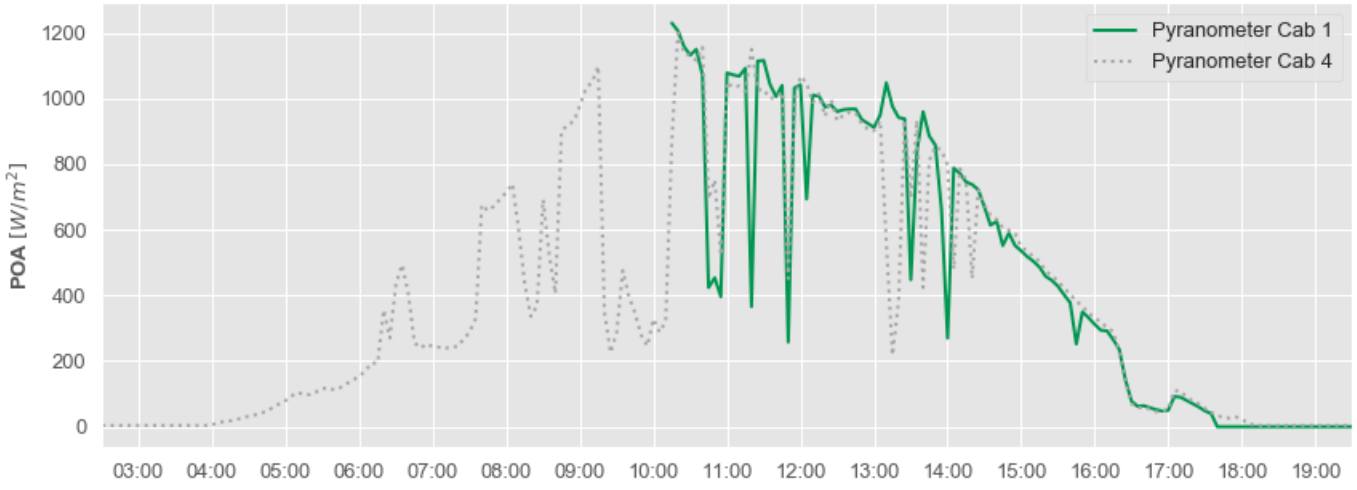

Figure 50. **Example of missing data** in raw irradiance time-series (no distinction between missing values and logs)

Outlier: value which lies outside of reasonable bounds. Two different approaches are defined.

a) Filter IEC standard – irradiance specific: In accordance with *IEC TS 61724-3 Photovoltaic system performance: Part 3: Energy evaluation method* [27], a following outlier filter is defined:

$$-6\ W/m^2 \leq measurement \leq 1500\,W/m^2$$

Table 11. **IEC filtering criteria** [27, table 3]

		Suggested criteria for flag (15 min data)			
Flag type	**Description**	**Irradiance W/m²**	**Temperature °C**	**Wind speed m/s**	**Power (AC power rating)**
Range	Value outside of reasonable bounds	< –6 or > 1 500	> 50 or < –30	>32 or < 0	> 1,02 × rating or < –0,01 × rating
Missing	Values are missing or duplicates	n/a	n/a	n/a	n/a
Dead	Values stuck at a single value over time. Detected using derivative.	< 0,0001 while value is > 5	< 0,0001	?	?
Abrupt change	Values change unreasonably between data points. Detected using derivative.	> 800	> 4	> 10	> 80 % rating
May be adjusted depending on the tilt of the system and the season of data acquisition.					

b) Filter adjusted to local conditions – *empirical:* to take into account local conditions, the bounds for irradiance have been defined as follows:

$$0\ W/m^2 \leq measurement \leq 1.3 \cdot max(reference\ distribution)\ W/m^2$$

The maximum irradiance value is increased by 30% in order to take into account the uncertainty related to satellite data measurements as stated in literature (19-23%) for hourly irradiation [22.]

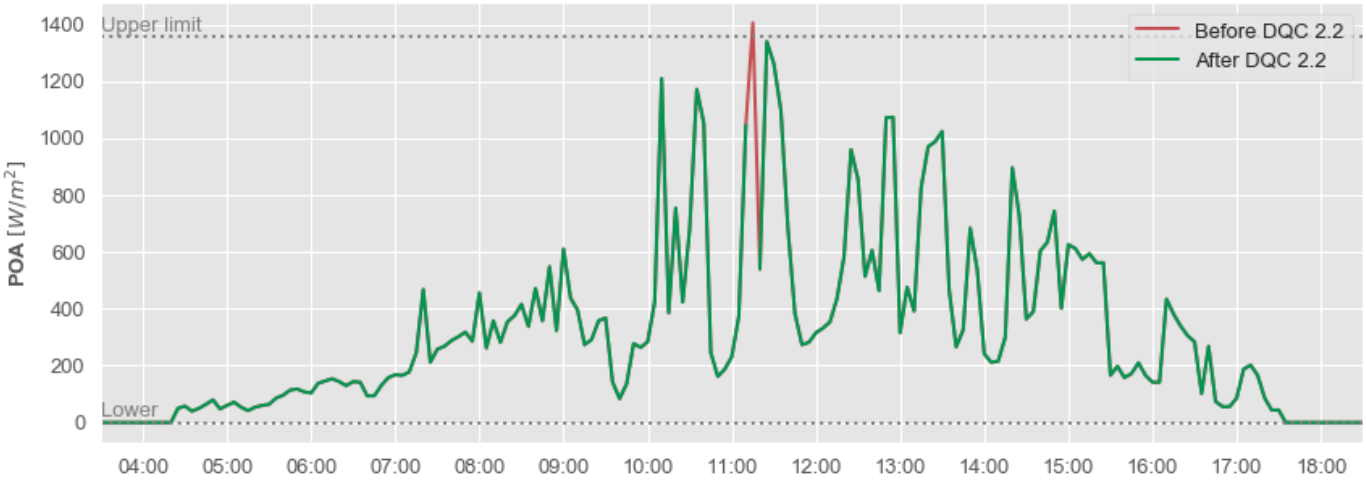

Figure 51. **Example of outlying data** detection (focus on a single day)

Dead value: data point which is stuck at a single value over time. Considering the granularity of the dataset (5 minutes), the timespan of interest to identify anomalous data points has been fixed to 15 minutes.

	cab1	cab4
2018-01-01 00:05:00+01:00	0.0	4.0
2018-01-01 00:10:00+01:00	0.0	4.0
2018-01-01 00:15:00+01:00	0.0	4.0
2018-01-01 00:20:00+01:00	0.0	4.0
2018-01-01 00:25:00+01:00	0.0	4.0
2018-01-01 00:30:00+01:00	0.0	4.0

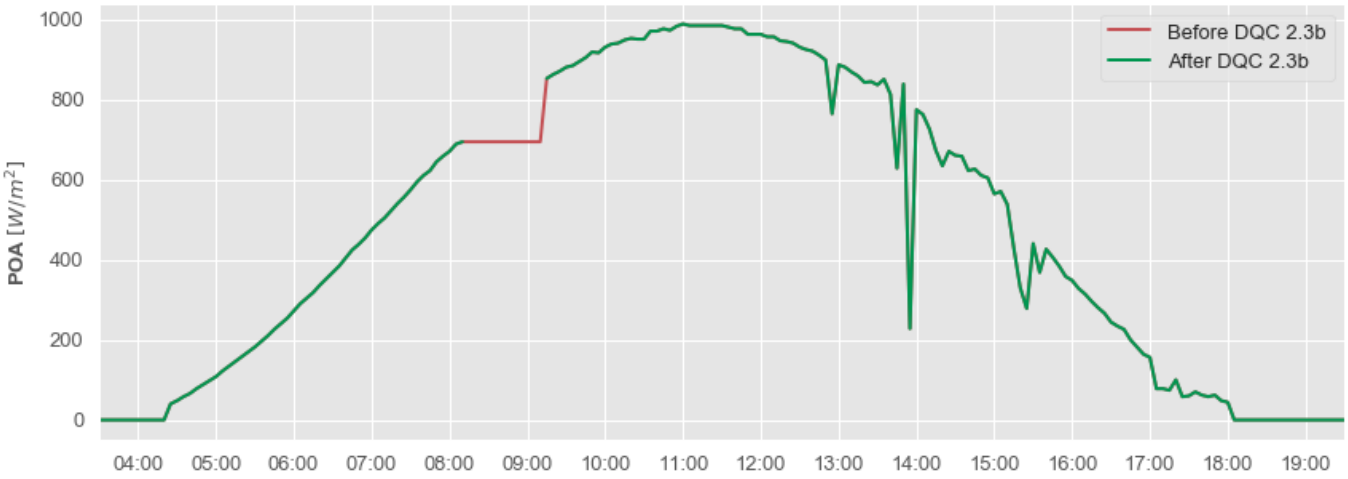

Figure 52. **Example of dead values** detection (focus on a single day)

Night value: in accordance with *International Standard IEC 61724-1:2017*, a night value is defined as a value recorded outside the daylight hours. For this purpose, sunrise and sunset hours are calculated for each day and night values are detected by comparing the timestamps of monitoring data with calculated sunrise and sunset time.

The calculation of sunrise and sunset hours is executed employing Python pvlib library, which contains algorithms that, given the reference period and the coordinates of a location, can compute sunrise and sunset time for each day included in the timespan of interest.

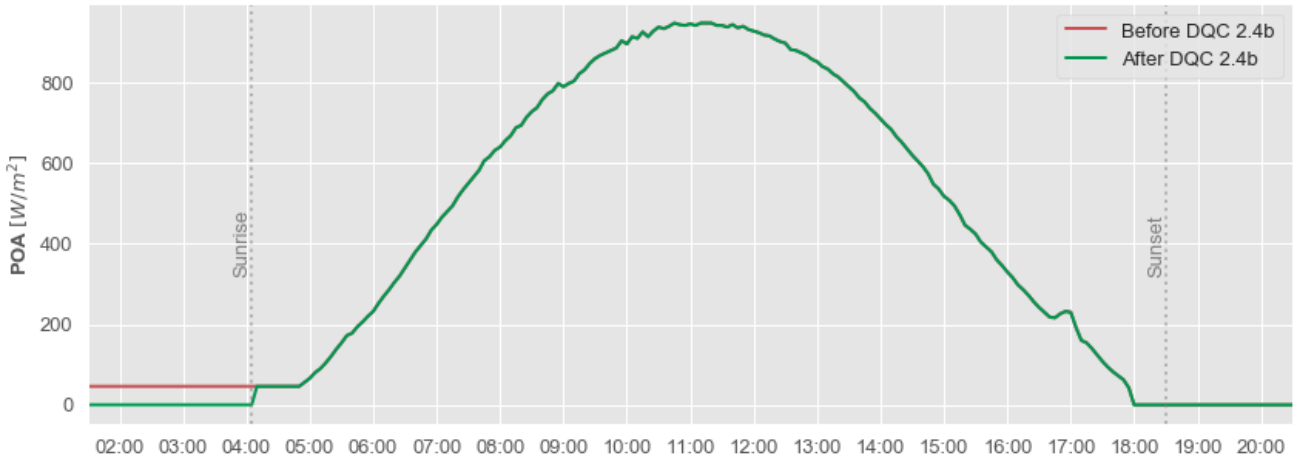

Figure 53. **Example of night values** detection (focus on a single day)

Daytime zero: zero-value recorded during daylight hours. For this purpose, sunrise and sunset hours are calculated for each day as well as the mean AC Power of all inverters for each timestamp. A zero-value irradiance reading recorded in the timespan between sunrise and sunset is labelled as daytime zero when, for the same timestamp, the mean AC Power is non-zero.

	cab1	cab4
2018-12-31 16:20:00+01:00	8.166667	11.0
2018-12-31 16:25:00+01:00	6.666667	0.0
2018-12-31 16:30:00+01:00	5.333333	0.0

Irradiance time-series of the selected sensors suspicious values are highlighted in red

```
date
2018-12-31 16:20:00+01:00    14.758235
2018-12-31 16:25:00+01:00    10.532353
2018-12-31 16:30:00+01:00    7.392353
```

AC Power time-series (mean of AC Power of all inverters): the timestamp identified in (2018-12-31 16:25:00+01:00) reveals a non-zero AC Power value, thus the irradiance value identified above (Irradiance of Pyranometer Cab 4) gets replaced by a missing value

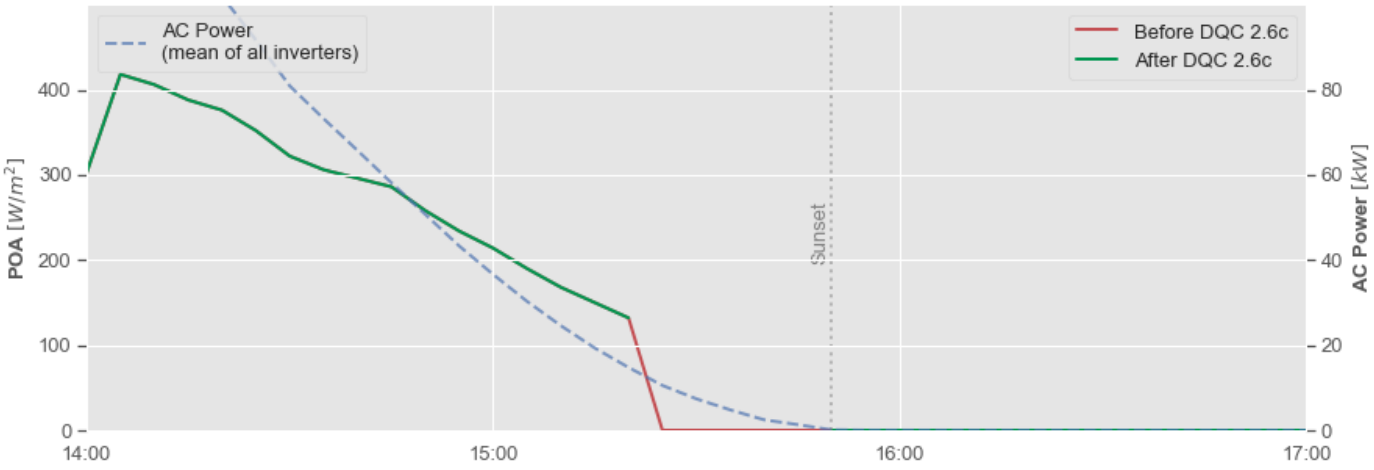

Figure 54. **Example of daytime zeros** detection (focus on a single day)

4.2 Methodology applied

Figure 55. **Irradiance Analysis** flowchart

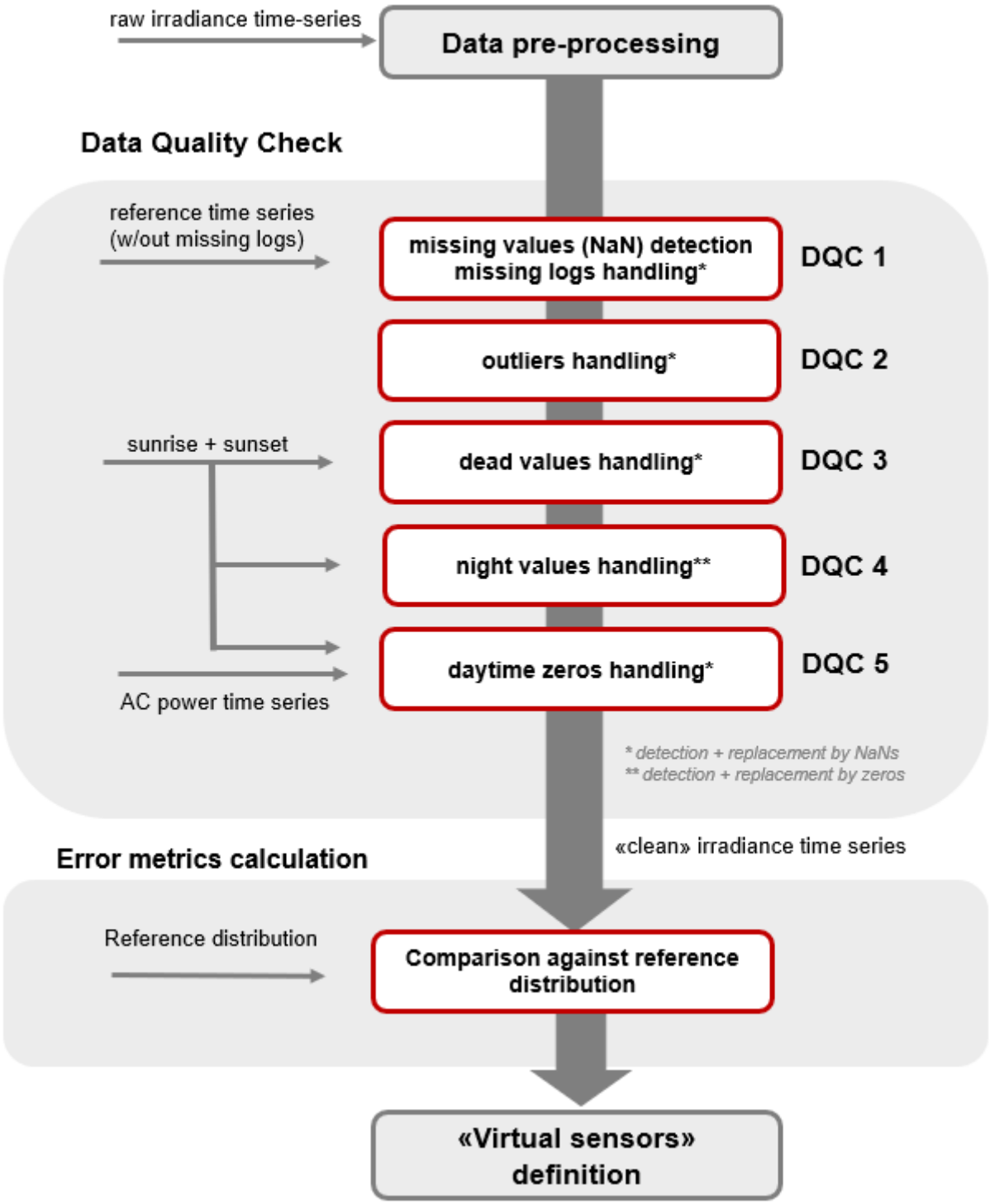

4.3 Input data

The analysis introduced in the present chapter made use of both monitoring and satellite-derived data.

Two criteria were used in order to select the reference period of the analysis: the length of the timespan and the number of missing data in the timespan. The length was chosen so to consider the seasonal variability, while the year was selected in order to minimize the number of missing data recorded by the selected pyranometers:

Data source	Temporal resolution	Reference period		N. of logs analysed
		Start	End	
3E Data Services	15 minutes	01/01/2018	31/12/2018	35,040
KCS monitoring system	5 minutes			105,120

Among the variables made available by 3E Data Services, only POA irradiation was employed in the present analysis, while the following variables were retrieved from KCS monitoring system):

Data source	Monitoring variable	Source device(s)	Temporal resolution
KCS monitoring system	POA Irradiance	Pyranometers (Cab1, Cab4)	5 minutes
	Active Power	Inverters (n. 1 to 17)	

4.4 Data pre-processing

During this stage, raw time series coming from all available sources were loaded in the system and underwent the transformations described below.

3E's POA irradiation, expressed as energy (Wh/m^2), was converted to power (W/m^2) in order to allow comparisons with pyranometers' data, which are already expressed as irradiance in the monitoring system. Monitoring data time series (both from pyranometers and inverters), retrieved through KCS monitoring system, have a temporal resolution of 5 minutes, while 3E's POA irradiance time-series have a temporal resolution of 15 minutes.

Most of the quality checks on irradiance sensors time-series were executed on five-minutes data to allow the identification of anomalous records. Only in the final step of the procedure, which

consists in the comparison between 3E and monitoring data, sensors' time-series were resampled from 5-minutes data into 15-minutes data.

Furthermore, monitoring data are in local time (Central European Time, UTC+01), while 3E time-series are in UTC time zone (Greenwich Mean Time, UTC+00), thus the latter were converted to UTC+01 time zone in order to allow the detection of night values and daytime zeros.

As final pre-processing step, a complete collection of timestamps (with no missing data) ranging from start to end of the reference period was created for each data granularity (5 minutes, 15 minutes) to allow the identification of missing logs.

4.5 Data Quality Check

The *Data Quality Check* (*DQC*) procedure is composed of five consecutive steps:

DQC 1. Missing values detection and missing logs handling
DQC 2. Outlier's handling
DQC 3. Dead values handling
DQC 4. Night values handling
DQC 5. Daytime zeros handling

Each *Data Quality Check* step gets as input the irradiance time-series processed during the previous stage and outputs a summary (composed of a table and two graphs) of the anomalies detected in the individual step and, when applicable, a modified time-series.

4.5.1 DQC 1: Missing values detection and missing logs handling

DQC 1 gets as input the pre-processed data and quantifies the amount of missing data detected in the reference period (year 2018) for the selected irradiance sensors (pyranometer Cabin 1 and Cabin 4). When a missing log is detected, a new record containing only NaNs is inserted in the time-series. *DQC 1* outputs a modified-time series for each sensor (which will be used as input for the next step) as well as a summary table and graphs, which are presented below:

Table 12. **Summary of missing data**, missing values and missing logs detected after DQC 1. Percentages are calculated with respect to the total number of logs analysed (105,120 logs)

		Pyranometer Cab 1	Pyranometer Cab 4
Missing logs *[A]*	*Count*	6,121	1,654
	Percentage	5.82%	1.57%
Missing values *[B]*	*Count*	1	0
	Percentage	0.00%	0.00%
Missing data *[A] + [B]*	*Count*	6,122	1,654
	Percentage	5.82%	1.57%

4.5.2 DQC 2: Outlier's handling

DQC 2 acts identifying outlying data present in the time series of the selected sensors across the reference period and replacing them with missing values. *DQC 2* outputs a modified time series for each sensor (which will be used as input for the next step) as well as a summary table and graphs. The former is presented below, while output graphs are not shown because they are not relevant in this specific case (basically no outliers were detected, the graphs would be empty):

Table 13. **Summary of outlying data** detected after DQC 2. Percentages are calculated with respect to the total number of logs analysed (105,120 logs)

		Pyranometer Cab 1	Pyranometer Cab 4
Outliers	*Count*	5	1
	Percentage	0.00%	0.00%

4.5.3 DQC 3: Dead values handling

DQC 3 acts identifying dead values present in the time series of the selected sensors across the reference period and replacing them with missing values. *DQC 3* outputs a modified time series for each sensor (which will be used as input for the next step) as well as a summary table and graphs, which are presented below:

*Table 14. **Summary of dead values** detected after DQC 3.*
Percentages are calculated with respect to the total number of logs analysed (105,120 logs)

		Pyranometer Cab 1	Pyranometer Cab 4
Dead values	*Count*	52	13,061
	Percentage	0.05%	12.42%

4.5.4 DQC 4: Night values handling

DQC 4 acts identifying night values present in the time series of the selected sensors across the reference period. Night values are replaced by missing values and subsequently substituted with zeros. *DQC 4* outputs a modified time series for each sensor (which will be used as input for the next step) as well as a summary table and graphs, which are presented below:

Table 15. **Summary of non-zero night values** detected after DQC 4.
Percentages are calculated with respect to the total number of logs analysed (105,120 logs)

		Pyranometer Cab 1	Pyranometer Cab 4
Night values	*Count*	0	7.237
	Percentage	0.00%	6.88%

4.5.5 DQC 5: daytime zeros handling

DQC 5 acts identifying daytime zeros present in the time series of the selected sensors across the reference period and replacing them with missing values.*DQC 5* outputs a modified time series for each sensor (which will be used as input for the next step) as well as a summary table and graphs, which are presented below:

Table 16. **Summary of daytime zeros detected** after DQC 5.
Percentages are calculated with respect to the total number of logs analysed (105,120 logs)

		Pyranometer Cab 1	Pyranometer Cab 4
Daytime zeros	*Count*	6,376	4,241
	Percentage	6.07%	4.03%

4.5.6 DQC summary

Once *DQC 5* has been performed, the results of each step are presented together with an overview of the whole process (**Error! Reference source not found.**).

Table 17. **Data Quality Check summary**

	Pyranometer Cabin 1		**Pyranometer Cabin 4**	
	N. of Missing Data	% of Missing Data	N. of Missing Data	% of Missing Data
DQC 1	6,122	5.82	1,654	1.57
DQC 2	5	0.00	1	0.00
DQC 3	52	0.05	13,061	12.42
DQC 4	0	0.00	7,237	6.88
DQC 5	6,376	6.07	4,241	4.03
Total	**12,555**	**11.94**	**26,194**	**24.90**

The following graphs summarize how missing data are distributed with respect to the above-mentioned issues, enabling a preliminary assessment of sensors' health status.

Figure 56. **Pyranometer Cabin 1**: distribution of missing data with respect to the identified issues

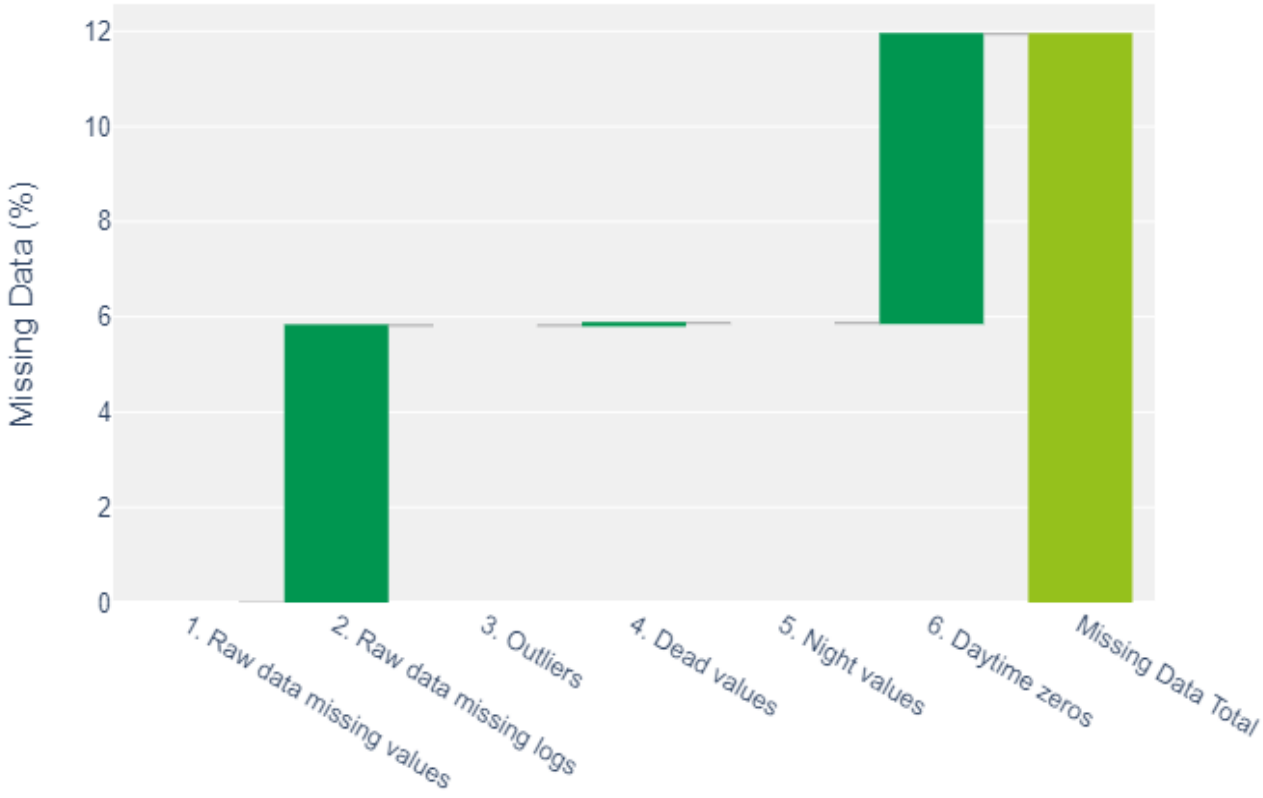

Figure 57. **Pyranometer Cabin 4**: distribution of missing data with respect to the identified issues

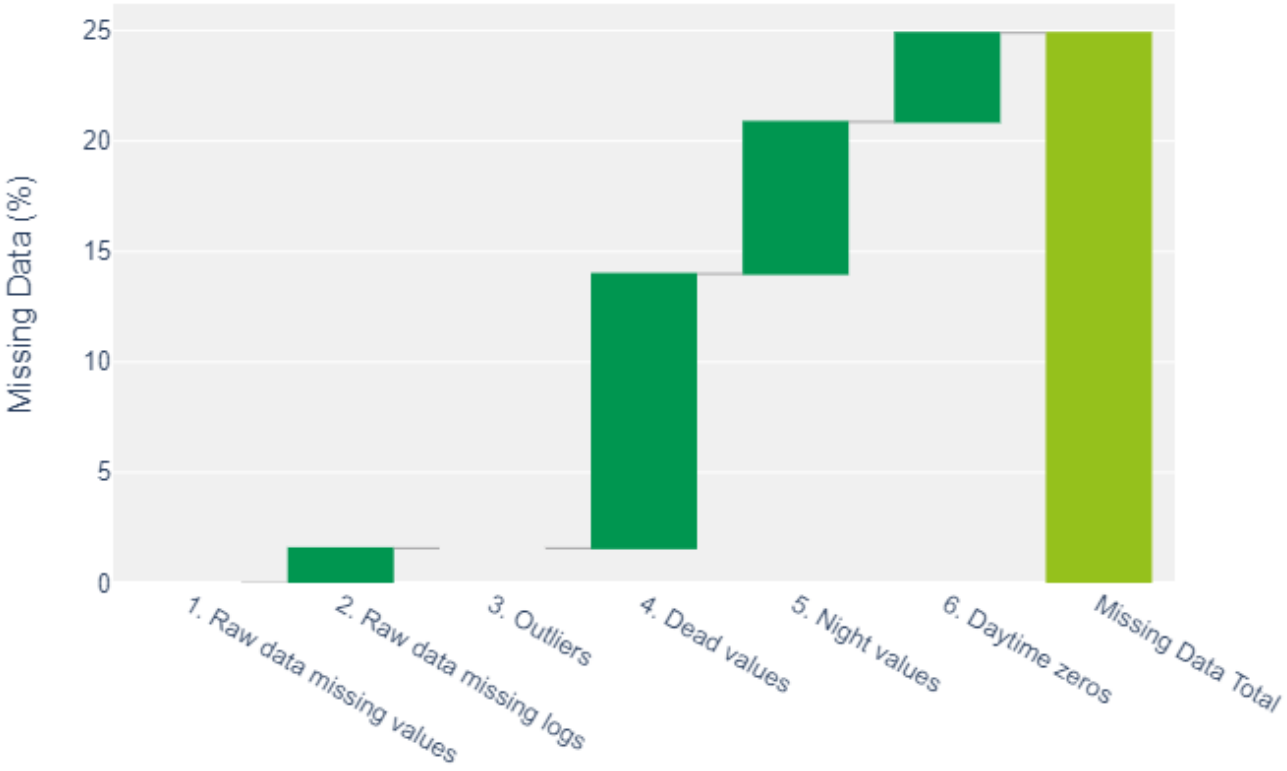

4.6 The 'virtual sensor' concept

The idea which stands behind the concept of **virtual sensor** is to the make the most out of the available data (on-site measurements and satellite data) to improve the data integrity by minimizing the percentage of missing values. This is of great importance for the reliable calculation of KPIs. Since on-site measurements are prone to be affected by a number of issues (as discussed in the previous section), virtual sensors tackle this problem by blending on-site sensors measurements and satellite data.

The available inputs for KPIs calculation are:

a) on-site sensors, which may bear uncertainties deriving from missing data (after being processed through the *Data Quality Check*)
b) virtual sensors, which aim at lowering the uncertainties deriving from missing data by blending on-site sensors measurements and satellite data

Within the framework of this thesis, two approaches were studied:

1) Virtual sensor 1: when 2 or more on-site sensors are available, but no satellite data
2) Virtual sensor 2: when 2 or more on-site sensors are available and also satellite data

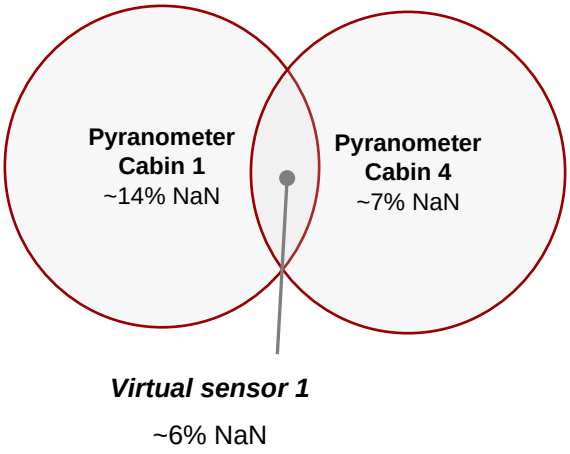

The *virtual sensor 1* is created by comparing the measurements of the sensors record by record. If a sensor at a certain time shows a missing value, then it gets discarded and the measurement of the other sensor is taken. If all readings are valid (no missing values), then the mean of the measurements is calculated. If all sensors show missing values, then also the "*virtual sensor 1*" will show the missing value.

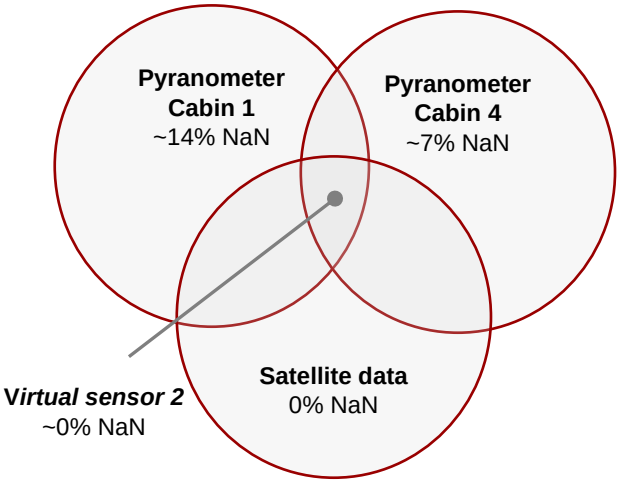

The *virtual sensor 2* is created by comparing the measurements of the sensors record by record. If a sensor at a certain time shows a missing value, then it gets discarded and the measurement of the other sensor is taken. If all readings are valid (no missing values), then the mean of the measurements is calculated. If all sensors show missing values, then 3E satellite data are employed to fill in the gaps.

Figure 58. **Missing data comparison**: On-site sensors vs. virtual sensors

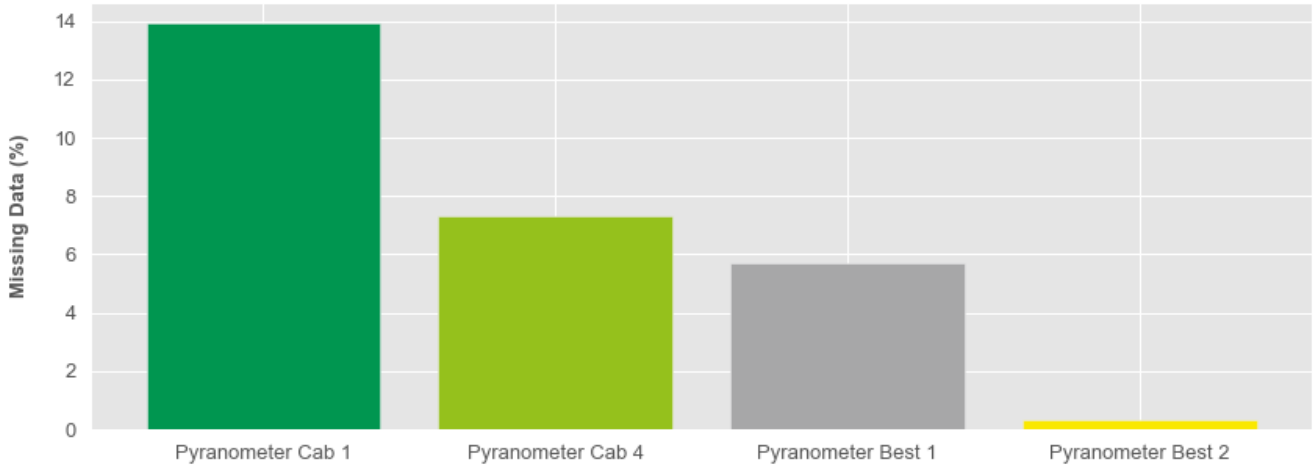

4.7 Results and discussion

The *Data Quality Check* procedure presented enables the detection of anomalous records and unlocks the possibility to compare on-site sensos between each other based on the identified issues.

- While pyranometer Cabin 1 shows mainly raw data missing logs (5.82%) and daytime zeros (6.07%), pyranometer Cabin 4 showcases a wider range of anomalies: raw data missing logs (1.57%), dead values (12.42%), night values (6.88%) and daytime zeros (4.03%).
- Comparing the total percentage of missing data after the *DQC*, pyranometer Cabin 1 seems to show a better general behaviour over the reference period (11.94% of missing data) than pyranometer Cabin 4 (24.90% of missing data).

Furthermore, the application of the 'virtual sensor' concept has proven to bring down the percentage of missing values to almost zero, but its effectiveness is clearly limited by and highly dependent on the quality and availability of sensors on-site (the more sensors the better).

5 Data imputation with ML techniques

Supervised learning tasks are classified according to the nature of the target variable: when the desired output is quantitative, the problem is defined as *regression*, while when the labels are qualitative it is called *classification*.

Many of the articles concerning ML applications in the PV field revolve around two major topics:

- PV energy or power forecasting – regression task
- Fault detection, diagnostics and prognostics - mainly classification task

The ML application presented in this work is a *regression* problem. On previous research [15], a literature was carried out to analyse the most relevant articles concerning PV energy/power forecasting [28-30] to find out the best performing ML models applied (see Table *18*).

Table 18. **Literature review.** ML application in the PV sector

Input variables	Output variables	Models	Best performing models
GHI, DHI, POA, ambient temperature, wind speed	Power	DBN, SVR, RFR	DBN, RFR
GHI, ambient temperature, relative humidity, wind direction, wind speed, solar azimuth and elevation	Power	ANNs, SVR, RT	FFNN
21 NWP variables, such as ambient temperature, total cloud cover, wind speed, wind direction, clear sky radiation, etc.	Energy	Lasso regression, ARIMA, KNN, GBR, ANN	GBR, ANN

Despite the importance of having accurate and reliable irradiance measurements available, it is very common for O&M operators to deal with plants which are not equipped with irradiance sensors or which are equipped with unreliable ones. The lack of regular cleaning and calibration may be responsible for sensor recording substantial deviations from the actual incoming solar radiation incident on the panels (lowering the data quality), while sensor outages (even though the root cause may not lie in the sensor itself, e.g. network connection error) may be responsible for the introduction of missing data (lowering the data integrity), which may compromise the correct interpretation of system's performance.

In this framework, if there are no backup sensors available on site, measurements recorded in nearby plants or weather stations may be used for KPIs calculation, paving the way for growing uncertainties and misleading performance evaluation.

As analysed in chapter 3, satellite-derived irradiance data may be used, when available, as backup even though operators must be aware of the uncertainties which this approach may introduce.

In this chapter an alternative approach based on MLL techniques is explored: additional monitoring data coming from other on-site devices (in addition to irradiance sensors) are used as input variables for several ML algorithms in order to perform **POA irradiance missing values imputation**. This imputation issue is a typical regression problem that can be tackled with a supervised learning approach, where the training set fed to the algorithm includes the desired solutions (in this case, POA irradiance). Once the algorithm has been trained, its task is to predict irradiance measurements (quantitative target variable) which were missing in the original time series coming from field sensors.

This data-driven approach is particularly useful for plants which only have one irradiance sensor (suspected to be unreliable) but there are other monitoring variables available (e.g. power, voltage, current, energy, etc.).

The predictions obtained by the best performing algorithms analysed have been subsequently evaluated against commercial satellite derived-irradiance data, resulting in 60 to 70% lower MAE and RMSE.

5.1 Methodology applied

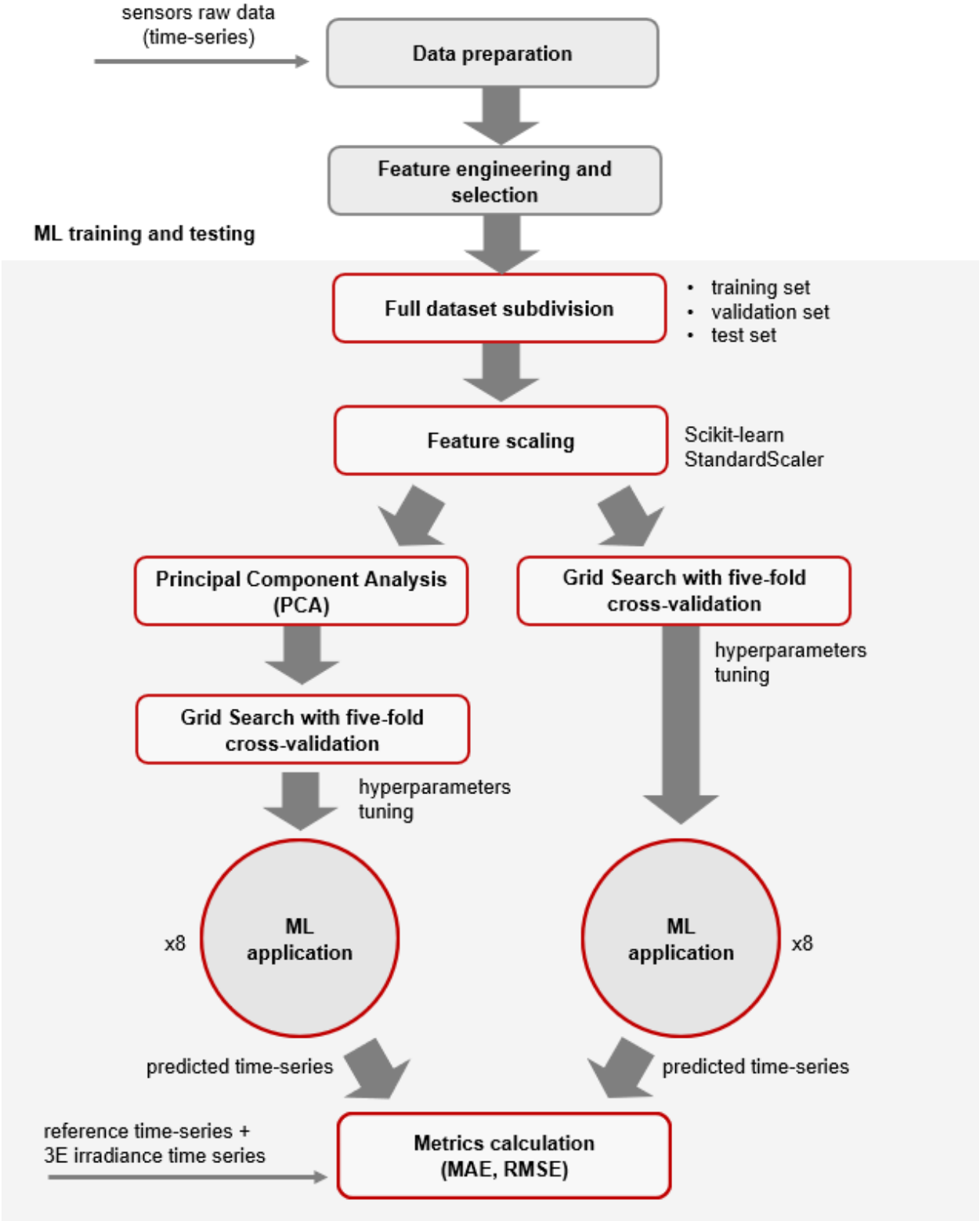

Figure 59. **ML application workflow**

5.2 Input data

The analysis introduced in the present chapter made use of both raw monitoring (not processed through *DQC* – section 4.5) and satellite-derived data.

The length of the reference period was extended so to exploit the biggest amount of monitoring data retrievable through KCS monitoring system and subsequently allow the ML algorithms to be trained on the largest available dataset.

Table 19. **Key features of the analysed datasets**

Data source	Temporal resolution	Reference period		N. of logs analysed
		Start	End	
3E Data Services	15 minutes	08/11/2016	13/08/2019	96,772
KCS monitoring system	15 minutes			96,772

Among the variables made available by 3E Data Services, only POA irradiation was employed in the present analysis, while the following variables were retrieved from KCS monitoring system:

Table 20. **Monitoring variables retrieved**

Data source	Monitoring variable	Source device(s)	Temporal resolution
KCS monitoring system	POA Irradiance	Pyranometers (Cab1, Cab4)	5 minutes
	Active power	Meter (Cab 5 Meter 1)	
	Day Consumed Energy		
	Consumed Energy		
	Day Produced Energy		
	Produced Energy		
	Freq		
	Phase A Voltage		
	Phase B Voltage		
	Phase C Voltage		
	Phase A Current		
	Phase B Current		
	Phase C Current		

5.3 Data preparation

Before entering in the details of the machine learning algorithms employed, data preparation steps are briefly described.

5.3.1 Time-stamps alignment and resampling

Monitoring data time series (both from pyranometers and meters), retrieved through KCS monitoring system, have a temporal resolution of 5 minutes, while 3E's POA irradiance time series have a temporal resolution of 15 minutes, thus monitoring time series were resampled to 15 minutes: the mean of the values over 15 minutes intervals are calculated, rendering a timestamp denoting the beginning of the interval together with the mean value (missing values are discarded from the process – see section 4.1).

Furthermore, 3E time-series are in UTC time zone (Greenwich Mean Time, UTC+00), while monitoring data are in local time (Central European Time, UTC+01), so the latter were converted to UTC time zone.

5.3.2 Reference distribution selection

The analysis has been restricted to one field pyranometer to take into account the worst conditions experienced by the on-site sensors across the timespan of interest, so to benchmark the ML algorithms with respect to the worst-case scenario faced by the available field instruments. The selection of the pyranometer was made based on three criteria detected in the time-series: the total number of missing data, the number of days without missing data and the number of consecutive days with missing data (i.e. missing data distribution).

The following table sums up the first two criteria described above:

	Pyranometer Cabin 1		**Pyranometer Cabin 4**	
	Count	Percentage	Count	Percentage
Missing data	8,261	8%	1,451	1%
Days with no missing data	879	87%	941	93%

The following graphs display the missing data distribution for the two pyranometers:

Figure 60. **Missing data distribution** of the field pyranometers across the reference period (raw data)

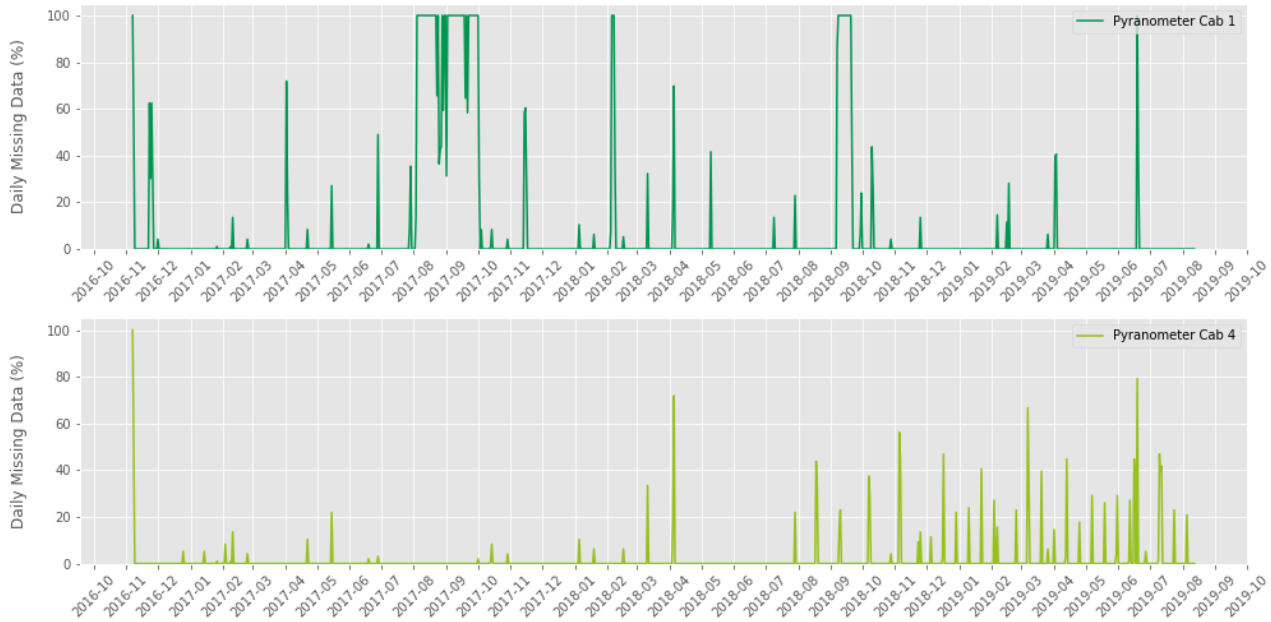

Pyranometer Cabin 1 was selected both because of the highest rate of missing data and because it includes the worst-case scenario of multiple consecutive days without valid data.

In this framework, a reference distribution coming from a calibrated pyranometer would serve as gold standard, allowing for the correct evaluation of the predictions yielded by the ML algorithms as well as of the satellite-derived irradiance data. Due to the lack of a dedicated pyranometer to be used as gold standard, the pyranometer Cabin 1 was selected as reference by deleting from the time-series all the logs corresponding to days containing at least one record with missing data, increasing the percentage of missing data from 8% to about 13%.

Figure 61. **Reference distribution**: POA irradiance recorded by pyranometer Cabin 1 across the reference period, deprived of the days with missing data

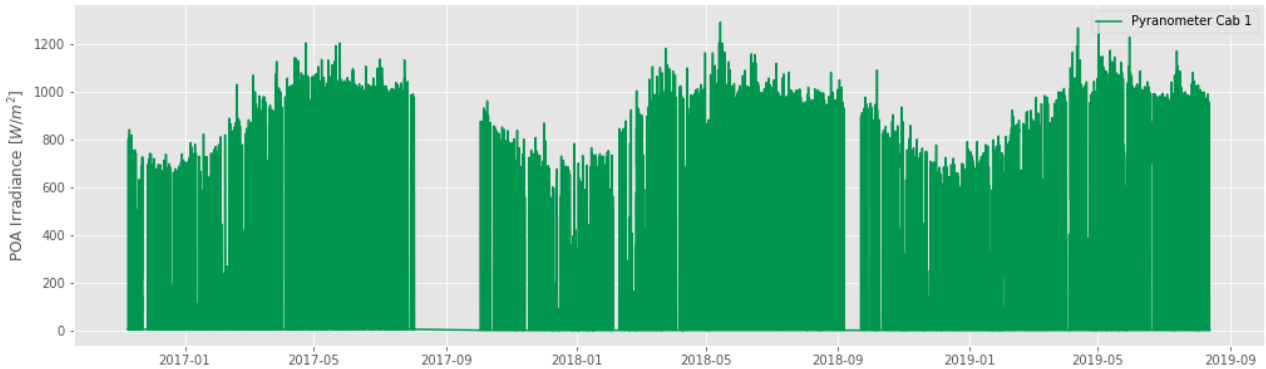

5.3.3 Definition of target synthetic POA irradiance time-series

To simulate the anomalous behaviour of a virtual pyranometer based on the above-defined reference distribution (real pyranometer Cab 1 readings across the reference period, containing only days without missing data), two synthetic distributions, named “A” and “B”, were created by mimicking the missing data distribution of pyranometer Cabin 1.

In synthetic distribution “A” were introduced about 9% of additional missing data (reaching a total of about 22% of missing data), according to the following steps:

1) A copy of the reference distribution was created
2) The missing data distribution of pyranometer Cabin 1 was shifted onwards by 70 days (“*shifted distribution*”)
3) Missing values were introduced in the copy of the reference distribution replicating the above-mentioned “*shifted distribution*” and thus obtaining the synthetic distribution “A”

Figure 62. **Reference distribution vs synthetic distribution “A”**

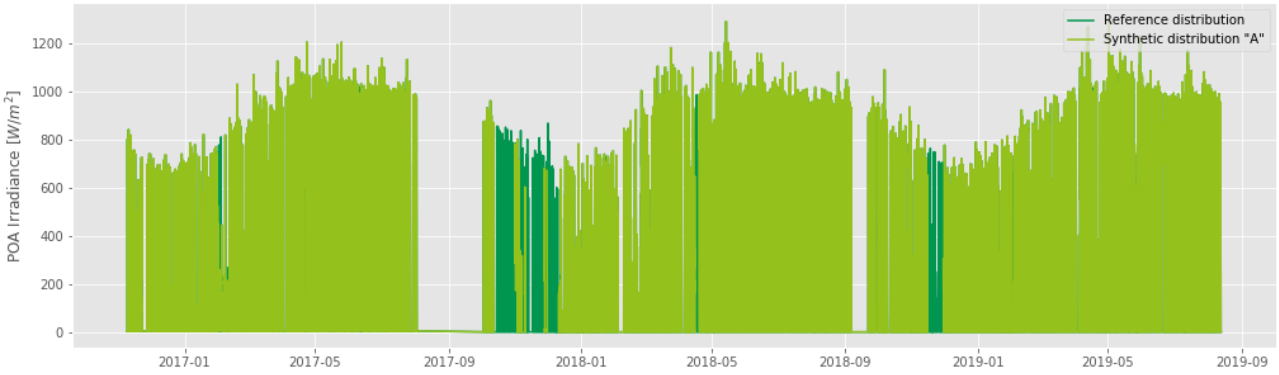

In synthetic distribution “B” were introduced about 20% of additional missing data, by replicating the above-described steps and adding an additional 11% of missing data randomly (reaching a total of about 33% of missing data).

Figure 63. **Reference distribution vs synthetic distribution “B”**

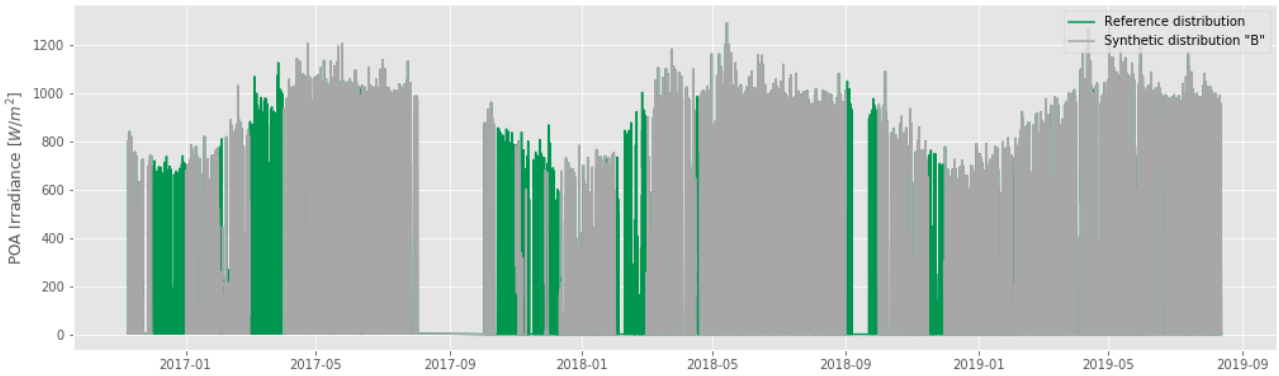

The synthetic distributions, representing POA irradiance readings across the reference period, will be used as **target variable** for the machine learning algorithms described in the following sections.

5.4 Feature engineering and selection

5.4.1 Feature selection

The electrical parameters referring to a single meter (Active power, Day Consumed Energy, Consumed Energy, Day Produced Energy, Produced Energy , Freq, Phase A Voltage, Phase B Voltage, Phase C Voltage, Phase A Current, Phase B Current, Phase C Current) were used as input variables.

After calculating the percentage of missing data of all the plant's meters, *Cabin 5 Meter 1* was selected as the meter which showed the lowest percentage on all the available variables (electrical parameters).

5.4.2 Feature engineering

Once *Cabin 5 Meter 1* was selected, its time series were pre-processed as follows:

a) Days having more than ten consecutive records with missing data (empirical threshold) were discarded both in meter's and target synthetic time series (previously defined in section 5.3.3) for aligning their timestamps
b) The gaps in the time series (maximum ten consecutive missing data) were filled by employing linear interpolation to avoid potential issues in ML processing of time series with missing data

Furthermore, exploiting the information contained in the time series index four additional features were generated: "month", "day", "hour" and "minute".

The full dataset is hence composed by sixteen input variables and one target variable, as summarized in the following table:

Table 21. **Input and target variables**

N.	Input variable	Unit
1	Month	-
2	Day	-
3	Hour	h
4	Minute	min
5	Active power	kW
6	Day Consumed Energy	kWh
7	Consumed Energy	kWh
8	Day Produced Energy	kWh
9	Produced Energy	kWh
10	Freq	Hz
11	Phase A Voltage	V
12	Phase B Voltage	V
13	Phase C Voltage	V
14	Phase A Current	A
15	Phase B Current	A
16	Phase C Current	A
N.	**Target variable**	**Unit**
1	Plane of array irradiance	W/m^2

Once the reference period had been identified and input variables and target variable had been pre-processed, the selected ML algorithms could be trained and subsequently run on the test set to get **POA irradiance predictions** where the synthetic distributions presented missing data.

5.5 ML models training and testing

Eight ML algorithms were employed:

1. Linear Regression
2. Polynomial Regression – degree 2
3. Stochastic Gradient Descent Regressor
4. Linear Support Vector Regression
5. Decision Tree Regressor
6. Random Forest Regressor
7. Bagging Regressor
8. Gradient Boosting Regressor

The models were applied both on the full dataset and on the dataset pre-processed through the application of Principal Component Analysis (PCA).

Principal Component Analysis is a dimensionality reduction algorithm which is used for deriving a low-dimensional set of features from a large set of variables. PCA identifies the hyperplane that lies closest to the data (input variables) and then projects the data onto it, creating a new set of input variables, smaller than the original one. The selection of the right hyperplane is done so that the projection preserves the maximum amount of variance, which means losing less information than other projections. It is possible to adjust the amount of information (variance) lost in the process, so to find the optimal trade-off between information lost and algorithms performance [13][38].

Each synthetic distribution was split in two subsets: all the observations without missing data were placed in the first subgroup, which was subsequently divided into **training set** (80%) and **validation set** (20%). The second subgroup, containing all the observations having a missing value as target variable, was used as **test set** (see Figure 64 and Figure 65).

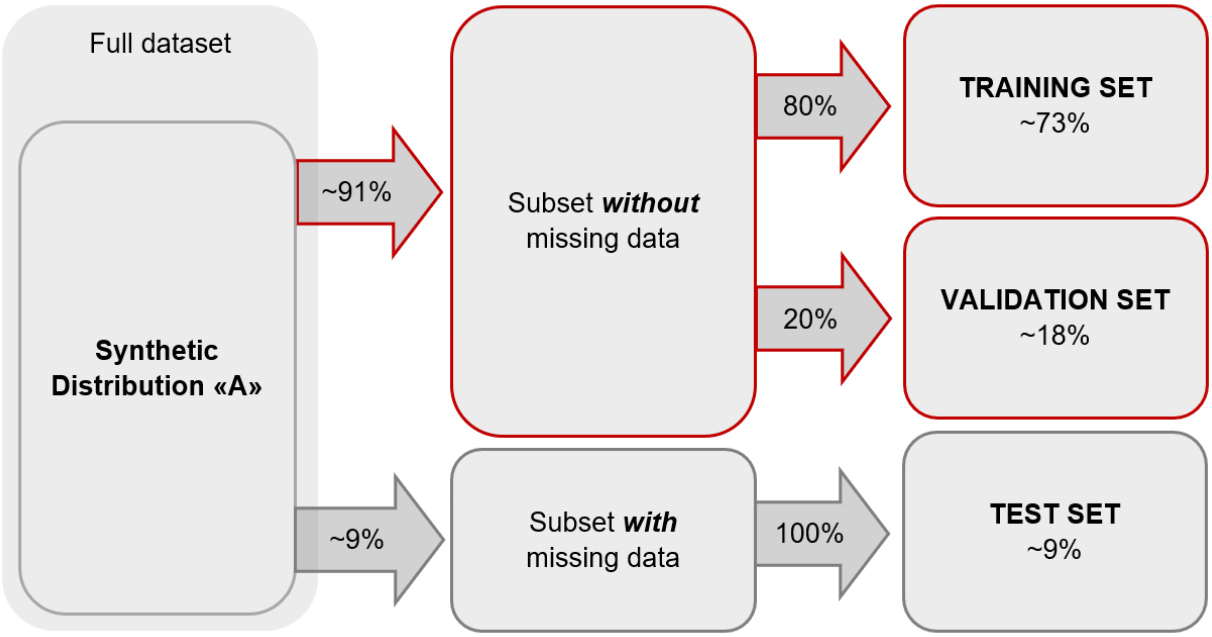

Figure 64. **Synthetic distribution "A**": training-validation-test set flowchart

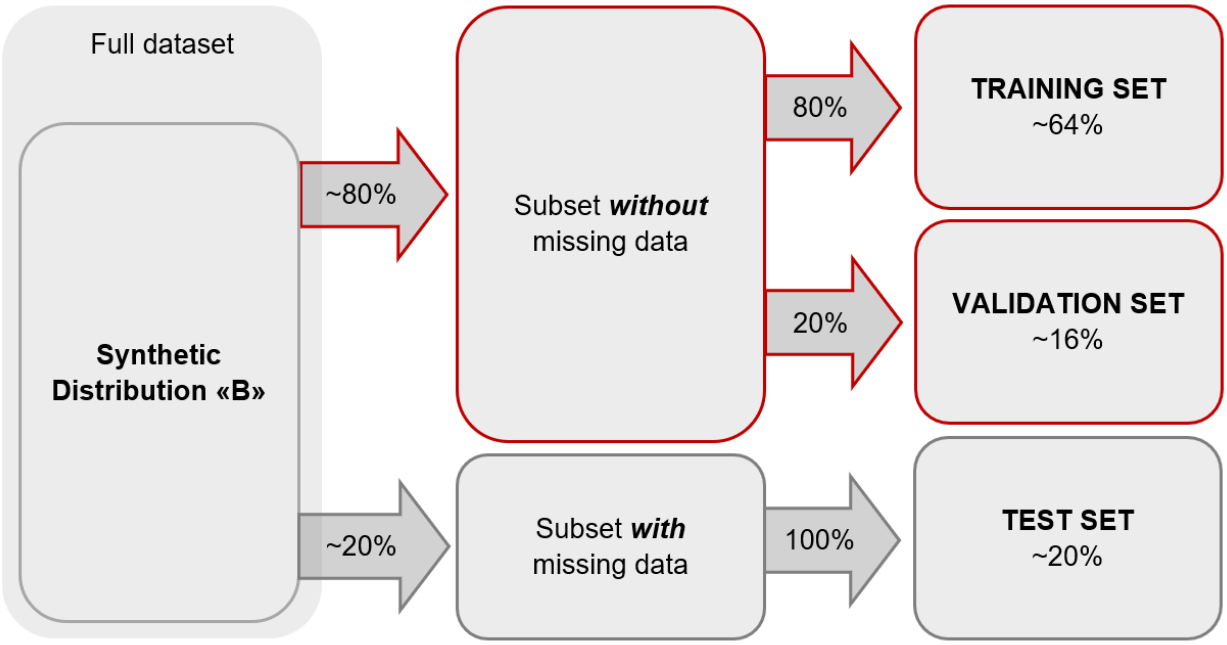

Figure 65. **Synthetic distribution "B":** training-validation-test set flowchart

Table 22. **Training, validation and test sets** split for synthetic distribution "A" and "B"

	Synthetic distribution "A"		Synthetic distribution "B"	
	Observations Count	Observations Percentage	Observations Count	Observations Percentage
Training Set	61,360	73%	53,988	64%
Validation set	15,341	18%	13,497	16%
Test set	7,395	9%	16,611	20%
Total	84,096	100%	84,096	100%

Before applying any ML model, the input variables belonging to the two subsets were brought to common scale in order to allow for a better performance of the algorithms: the *Scikit-learn* class *StandardScaler* was applied on the features in order to remove the mean and scale to unit variance (*StandardScaler* was fit to the training input variables and subsequently used to transform the training input variables as well as the validation and test input variables).

Models evaluation was executed by calculating both RMSE and MAE on the training, validation and test set. Five-fold cross-validation was applied on the training set obtaining an array of five evaluation scores, whose mean and standard deviation were subsequently analysed.

Furthermore, **3E POA irradiance** time series was evaluated against the reference distribution by calculating RMSE and MAE over the timespan of interest defined by the test set. The results are summarized in the following table:

3E POA irradiance	MAE	RMSE
Test set synthetic distribution “A”	43.44	91.04
Test set synthetic distribution “B”	49.12	96.78

In the end, the values of the performance metrics calculated on the test set for each algorithm and each synthetic distribution were compared with the values shown here.

5.5.1 Models applied on the full dataset

For each synthetic distribution, performance metric and algorithm, *Grid Search* with five-fold cross-validation was employed to search for the best combination of hyperparameters. A selection of hyperparameters for each algorithm with a range of tentative values were passed to *Scikit-learn*’s *GridSearchCV* class, which evaluates all the possible combinations of hyperparameter values using cross-validation.

The collection of hyperparameters tested are presented in Annex B: Hyperparameters tuning. The results obtained for the best performing models are shown in the following *Tables 23-26*.

Table 23. **Models evaluation: synthetic distribution “A”** – performance metric: RMSE (W/m^2)

Model	Training set		Validation set	Test set	3E	% Change
	RMSE mean	RMSE STD	RMSE	RMSE [A]	RMSE [B]	([A] - [B]) / [B]
Linear Regression	73.52	1.64	73.62	46.44	91.04	-49%
Polynomial Regression – Degree 2	69.69	1.66	70.16	46.42		-49%
Stochastic Gradient Descent Regressor	74.22	1.49	73.89	46.03		-49%
Linear Support Vector Regression	80.96	2.21	80.29	48.68		-47%
Decision Tree Regressor	49.20	0.90	48.47	43.19		-53%
Random Forest Regressor	42.84	0.98	42.00	33.92		-63%
Bagging Regressor	46.10	1.04	45.29	32.77		-64%
Gradient Boosting Regressor	42.21	1.24	41.02	33.71		-63%

Table 24. **Models evaluation: synthetic distribution "A"** – performance metric: MAE (W/m^2)

Model	Training set		Validation set	Test set	3E	% Change
	MAE mean	MAE STD	MAE	MAE [A]	MAE [B]	([A] - [B]) / [B]
Linear Regression	30.72	0.36	30.76	24.73	43.44	-43%
Polynomial Regression – Degree 2	33.43	0.38	33.72	28.57		-34%
Stochastic Gradient Descent Regressor	31.44	0.57	31.67	23.72		-45%
Linear Support Vector Regression	25.89	0.44	25.41	17.96		-59%
Decision Tree Regressor	18.17	0.21	17.45	15.46		-64%
Random Forest Regressor	14.89	0.35	14.21	12.34		-72%
Bagging Regressor	15.61	0.31	14.92	12.53		-71%
Gradient Boosting Regressor	14.79	0.35	14.09	11.84		-73%

Table 25. **Models evaluation: synthetic distribution "B"** – performance metric: RMSE (W/m^2)

Model	Training set		Validation set	Test set	3E	% Change
	RMSE mean	RMSE STD	RMSE	RMSE [A]	RMSE [B]	([A] - [B]) / [B]
Linear Regression	75.64	2.63	73.85	53.85	96.78	-44%
Polynomial Regression – Degree 2	71.37	2.52	69.88	56.19		-42%
Stochastic Gradient Descent Regressor	76.07	2.79	74.19	53.99		-44%
Linear Support Vector Regression	83.03	3.15	80.02	60.01		-38%
Decision Tree Regressor	48.89	0.43	48.84	53.16		-45%
Random Forest Regressor	42.98	0.28	43.26	47.16		-51%
Bagging Regressor	46.78	0.79	46.39	43.36		-55%
Gradient Boosting Regressor	41.96	0.74	41.42	47.10		-51%

Table 26. **Models evaluation: synthetic distribution "B"** – performance metric: MAE (W/m^2)

Model	Training set		Validation set	Test set	3E	% Change
	MAE mean	MAE STD	MAE	MAE [A]	MAE [B]	([A] - [B]) / [B]
Linear Regression	32.14	0.65	31.63	22.42	49.12	-54%
Polynomial Regression – Degree 2	35.01	0.59	34.49	30.23		-38%
Stochastic Gradient Descent Regressor	32.39	0.45	32.79	23.26		-53%
Linear Support Vector Regression	26.97	0.74	26.04	18.36		-63%
Decision Tree Regressor	18.51	0.13	17.59	17.60		-64%
Random Forest Regressor	15.20	0.12	14.79	14.40		-71%
Bagging Regressor	18.40	0.36	17.76	13.83		-72%
Gradient Boosting Regressor	15.05	0.16	14.56	14.37		-71%

5.5.2 Models applied on the dataset pre-processed through PCA

On both datasets, referring to the synthetic distributions, was applied **Principal Components Analysis** (PCA).

PCA was fit to the training set and the components with variance less than 1 were dropped (Kaiser criterion), thus only six components were selected, summing up to a cumulative proportion of explained variance of 80.9%. Afterwards, training, validation and test set data were projected onto the selected components, obtaining the lower dimensional datasets on which ML models were applied.

For each synthetic distribution, performance metric and algorithm, Grid Search with five-fold cross-validation was employed to search for the best combination of hyperparameters.

The collection of hyperparameters tested are presented in the Annex A, section 8.2.

The results obtained for the best performing models are shown in the following tables.

Table 27. **Models evaluation: synthetic distribution "A"** – performance metric: MAE (W/m^2)

Model	Training set		Validation set	Test set	3E	% Change
	MAE mean	MAE STD	MAE	MAE [A]	MAE [B]	([A] - [B]) / [B]
Linear Regression	36.22	0.45	36.18	26.20	43.44	-40%
Polynomial Regression – Degree 2	31.36	0.39	31.44	22.25		-49%
Stochastic Gradient Descent Regressor	36.21	0.92	36.32	26.02		-40%
Linear Support Vector Regression	32.08	0.48	31.62	23.55		-46%
Decision Tree Regressor	22.69	0.34	22.36	17.13		-61%
Random Forest Regressor	18.00	0.28	17.60	14.15		-67%
Bagging Regressor	19.09	0.30	18.58	15.31		-65%
Gradient Boosting Regressor	19.71	0.31	19.25	15.80		-64%

Table 28. **Models evaluation: synthetic distribution "A"** – performance metric: RMSE (W/m^2)

Model	Training set		Validation set	Test set	3E	% Change
	RMSE mean	RMSE STD	RMSE	RMSE [A]	RMSE [B]	([A] - [B]) / [B]
Linear Regression	75.03	1.70	75.10	47.96	91.04	-47%
Polynomial Regression – Degree 2	72.39	1.77	72.64	44.48		-51%
Stochastic Gradient Descent Regressor	75.50	1.49	75.16	47.88		-47%
Linear Support Vector Regression	80.91	2.12	80.30	50.71		-44%
Decision Tree Regressor	57.57	0.98	58.21	40.40		-56%
Random Forest Regressor	49.71	1.28	49.89	36.43		-60%
Bagging Regressor	50.72	1.09	50.81	36.89		-59%
Gradient Boosting Regressor	52.13	0.91	52.07	39.44		-57%

Table 29. **Models evaluation: synthetic distribution "B"** – performance metric: MAE (W/m^2)

Model	Training set		Validation set	Test set	3E	% Change
	MAE mean	MAE STD	MAE	MAE [A]	MAE [B]	([A] - [B]) / [B]
Linear Regression	37.71	0.58	37.22	27.96	49.12	-43%
Polynomial Regression – Degree 2	32.76	0.56	32.32	24.77		-50%
Stochastic Gradient Descent Regressor	37.40	0.56	37.33	27.98		-43%
Linear Support Vector Regression	33.37	0.71	32.54	25.22		-49%
Decision Tree Regressor	23.50	0.57	22.61	20.84		-58%
Random Forest Regressor	18.61	0.28	18.26	18.09		-63%
Bagging Regressor	20.02	0.30	19.64	19.62		-60%
Gradient Boosting Regressor	20.41	0.35	19.96	20.39		-59%

Table 30. **Models evaluation: synthetic distribution "B"** – performance metric: RMSE (W/m^2)

Model	Training set		Validation set	Test set	3E	% Change
	RMSE mean	RMSE STD	RMSE	RMSE [A]	RMSE [B]	([A] - [B]) / [B]
Linear Regression	77.21	2.56	75.25	56.50	96.78	-42%
Polynomial Regression – Degree 2	74.35	2.53	72.53	54.61		-44%
Stochastic Gradient Descent Regressor	77.38	2.65	75.31	56.57		-42%
Linear Support Vector Regression	82.96	3.10	79.86	61.39		-37%
Decision Tree Regressor	58.14	1.70	57.04	55.44		-43%
Random Forest Regressor	50.34	1.38	51.03	49.47		-49%
Bagging Regressor	51.23	1.43	51.83	50.05		-48%
Gradient Boosting Regressor	52.58	1.85	52.86	55.23		-43%

5.6 Results and discussion

Table *31* provides an overview on the best and worst models for each synthetic distribution, input dataset and performance metric. Percentage change is calculated with respect to 3E POA irradiance error, which is in turn calculated with respect to the reference distribution.

Table 31. **Best and worst models** (percentage change is calculated with respect to 3E POA irradiance error).

		Synthetic distribution "A"				Synthetic distribution "B"			
		Worst		Best		Worst		Best	
		% Change	Model	% Change	Model	% Change	Model	% Change	Model
Full dataset	MAE	**-34%**	**PLR**	**-73%**	**GBR**	-38%	PLR	-72%	BAG
	RMSE	**-47%**	**SVR**	**-64%**	**BAG**	-38%	SVR	-55%	BAG
PCA	MAE	-40%	LR/SGD	-67%	RFR	-43%	LR/SGD	-63%	RFR
	RMSE	-44%	SVR	-60%	RFR	-37%	SVR	-49%	RFR

LR: Linear Regression
PLR: Polynomial Regression (degree 2)
SGD: Stochastic Gradient Descent Regressor
SVR: Linear Support Vector Regression
BAG: Bagging Regressor
RFR: Random Forest Regressor
GBR: Gradient Boosting Regressor

All **machine learning** algorithms employed provide an **improvement over the satellite-derived data** for each of the analysed settings: through ML models it has been possible to obtain lower errors, ranging from 34% to 73% less error than 3E POA irradiance data.

Among the algorithms applied, **ensemble methods**[1] provided the best results, with Random Forest, Bagging and Gradient Boosting Regressor yielding very similar scores.

As expected, the application of dimensionality reduction techniques (PCA) has led to slightly worst performances, while halving the execution time of the algorithms.

Moving from synthetic distribution "A" to synthetic distribution "B", both the dimensions and the statistical properties of training, validation and test set change. These modifications did not

[1] Once a group of predictors, called an *ensemble* (e.g. Decision Tree regressors), has been selected, each one of them can be trained and tested on a random subset of the dataset. The predictions obtained from the individual predictors are then aggregated (e.g. averaged) to form the most efficient predictor. Algorithms that use this strategy are called *ensemble methods*.

particularly affect MAE, while RMSE experienced remarkable variations (around 10%, maybe due the presence of outlying predictions which are highlighted by RMSE).

Despite the fact that some algorithms result in larger percentage changes from 3E reference, from an O&M perspective it is preferable to penalize large deviations in POA irradiance time series, hence the preferred performance metrics to evaluate the ML imputation is the Root Mean Square Error.

In the following graphs the best and worst performing algorithms applied on the full dataset for synthetic distribution “A” are qualitatively compared to the reference distribution as well as to 3E satellite-derived irradiance data over a 14-days Figures 67-70) and over a cloudy and a sunny day (Figures 71 and 72).

Best and worst algorithms have been selected as the ones yielding the biggest and the smallest percentage change, as defined at the beginning of this paragraph:

- Worst performing algorithms: Linear Support Vector Regression (RMSE) and Polynomial Regression - degree 2 (MAE)
- Best performing algorithms: Bagging Regressor (RMSE) and Gradient Boosting Regressor (MAE)

Figure 67. **Synthetic distribution "A": reference distribution vs.3E satellite-derived irradiance data** (RMSE: 91.04 W/m^2, MAE: 43.44 W/m^2)

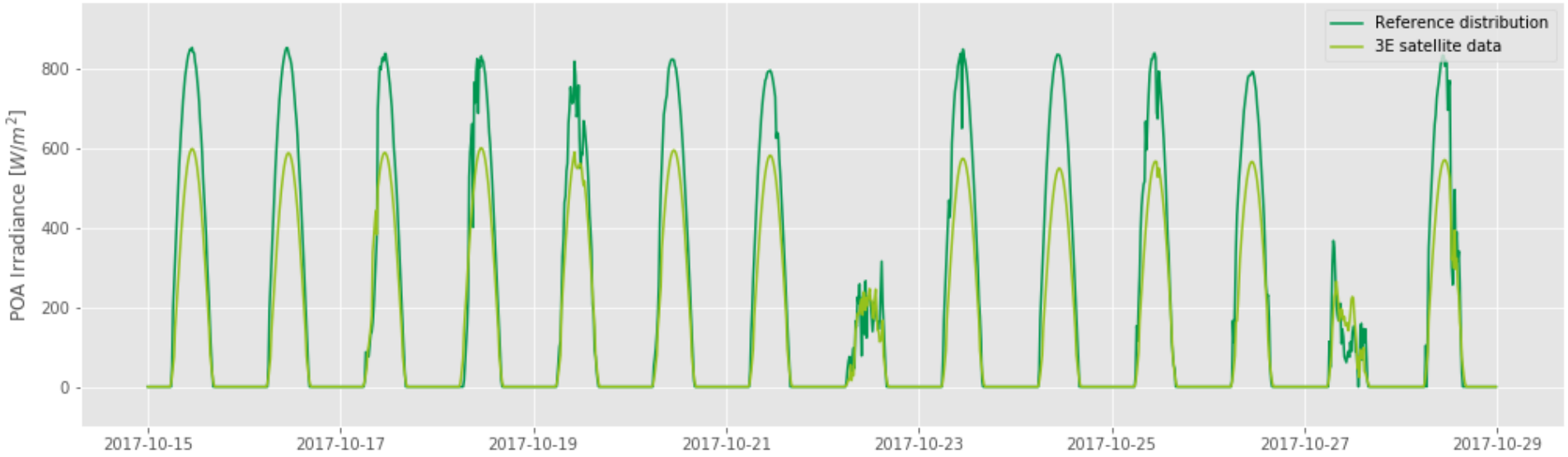

Figure 66. **Synthetic distribution "A": reference distribution vs. Linear Support Vector Regression** (RMSE: 48.68 W/m^2)

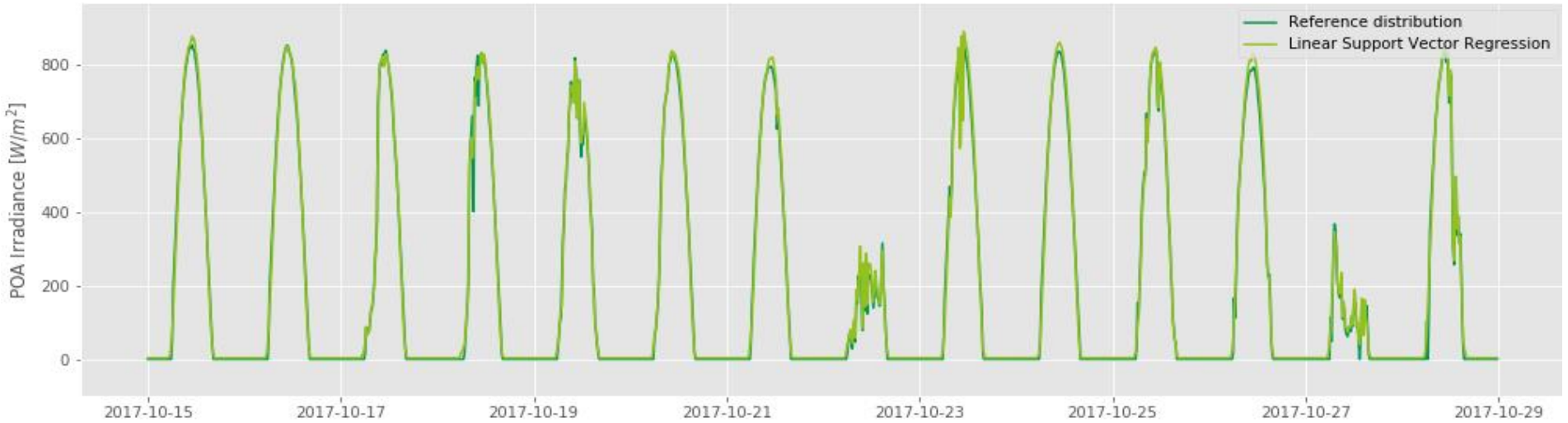

Figure 68. **Synthetic distribution "A": reference distribution vs. Bagging Regressor** (RMSE: 32.77 W/m^2)

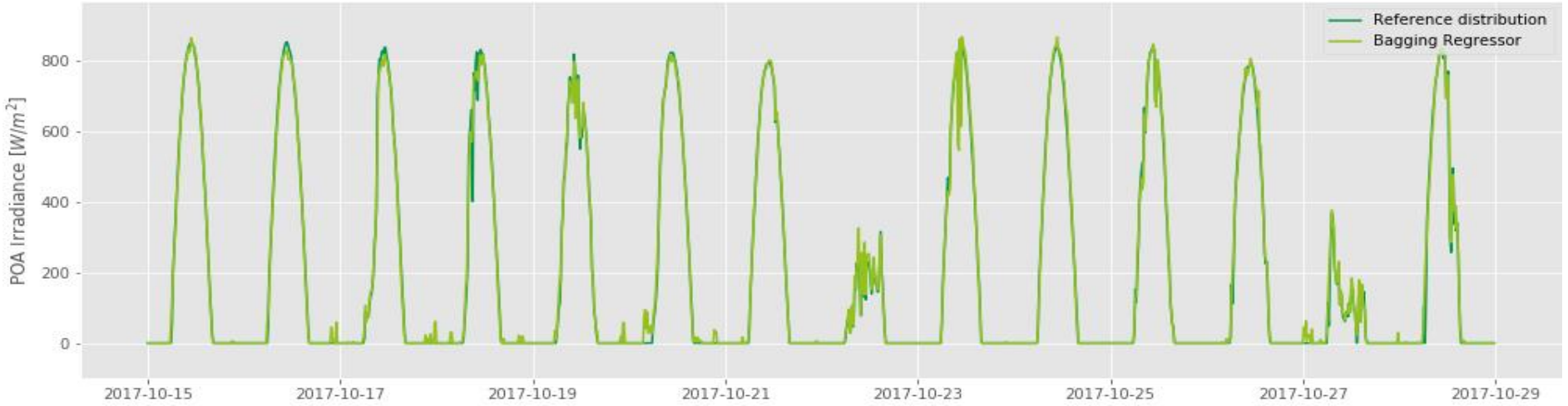

Figure 69. **Synthetic distribution "A": reference distribution vs. Polynomial Regression Degree 2** (MAE: 28.57 W/m^2)

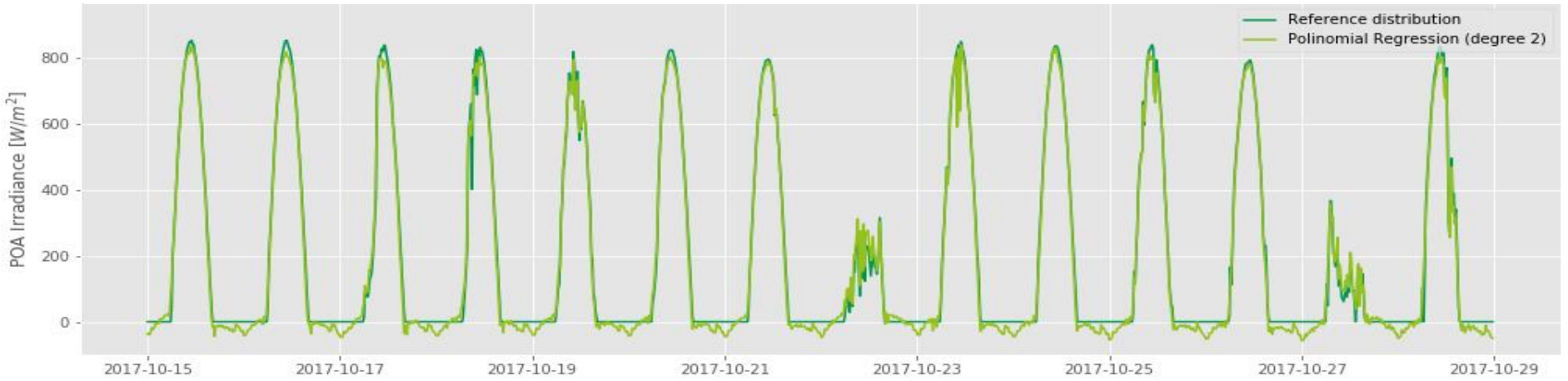

Figure 70. **Synthetic distribution "A": reference distribution vs. Gradient Boosting Regressor** (MAE: 11.84 W/m^2)

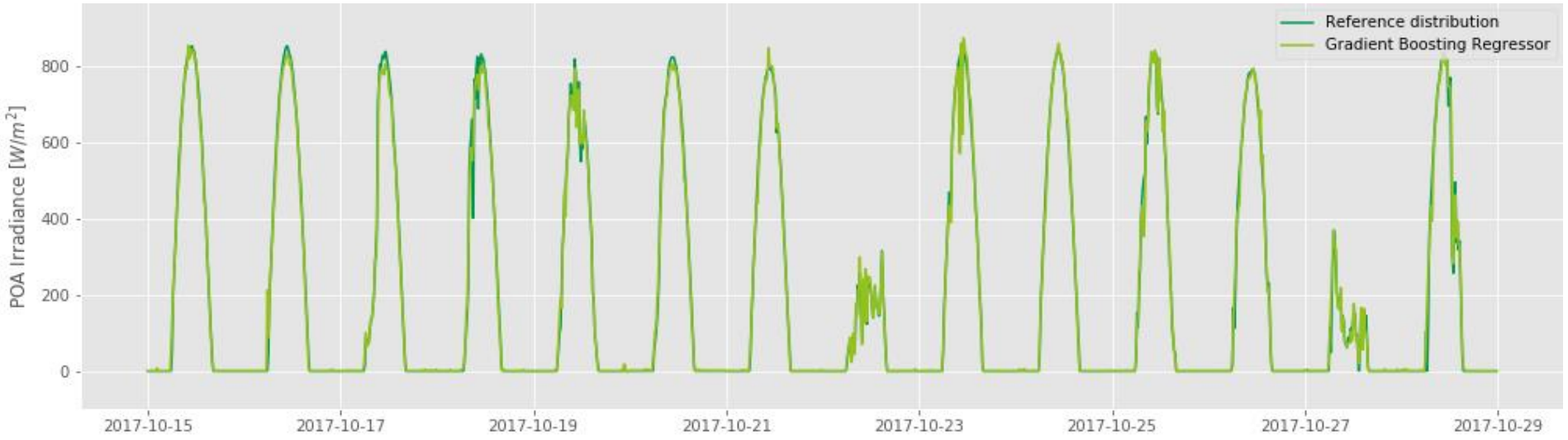

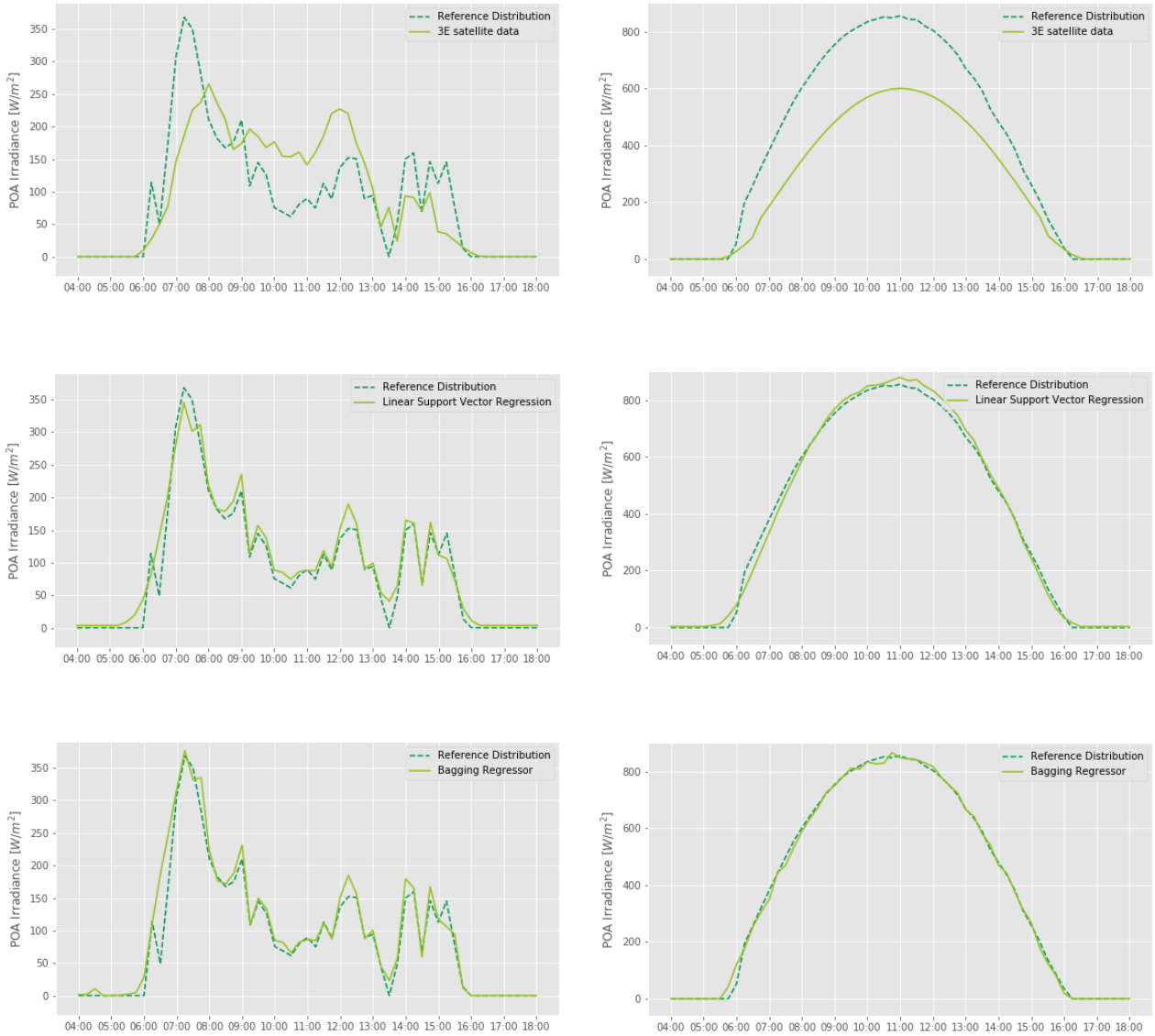

Figure 71. **Comparison between reference distribution**, best (Bagging Regressor) and worst (Linear Support Vector Machine Regression) performing algorithms and 3E satellite-derived irradiance data on a cloudy day (left column) and on a sunny day (right column) – performance metric: RMSE

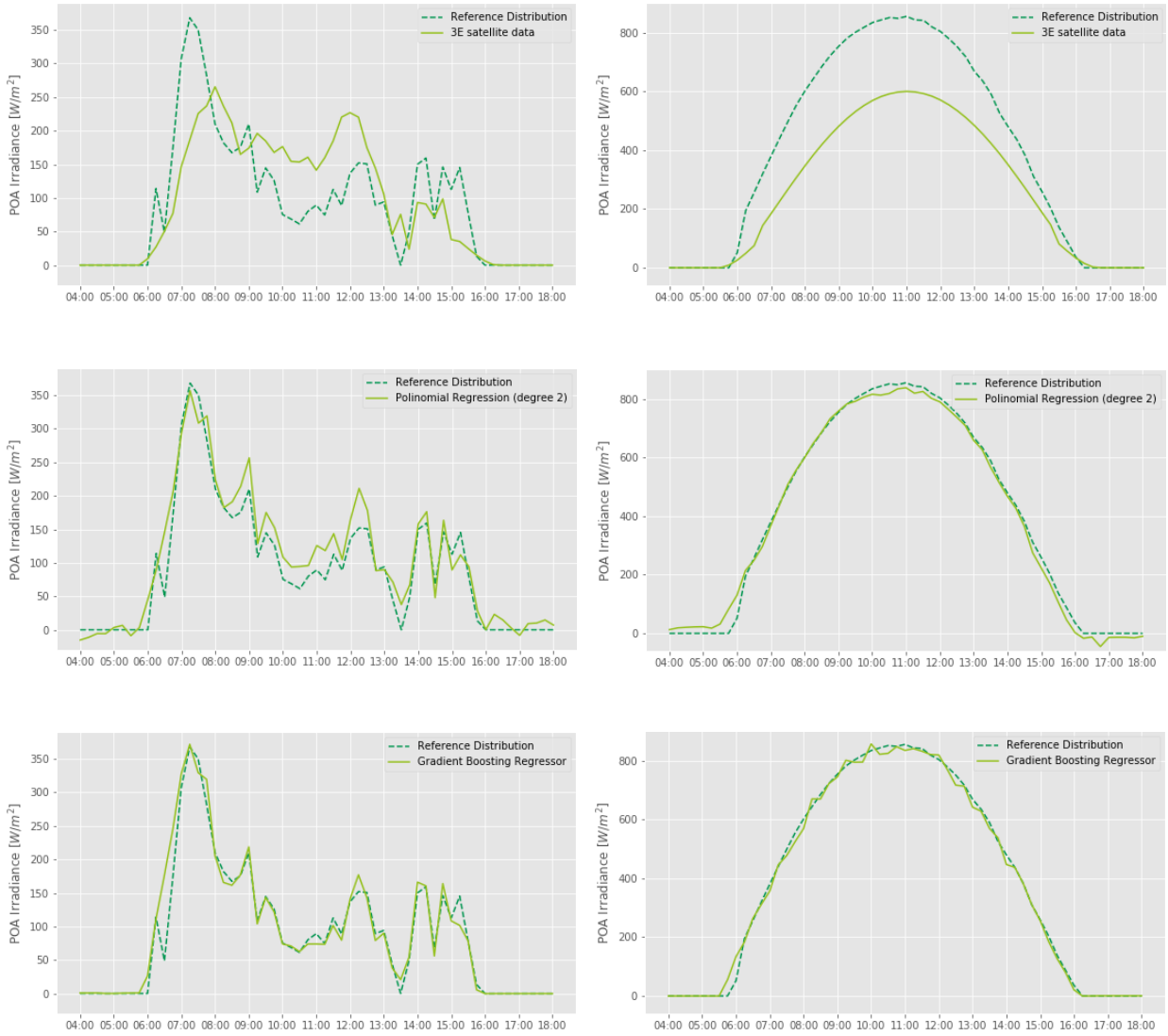

Figure 72. **Comparison between reference distribution**, best (Gradient Boosting Regressor) and worst (Polinomial Regression – degree 2) performing algorithms and 3E satellite-derived irradiance data on a cloudy day (left column) and on a sunny day (right column) – performance metric: MAE

6 Conclusions

In this chapter the most relevant conclusions of this work are presented, organized according to the corresponding chapters.

Chapter 3: Uncertainty evaluation of satellite data

Based on the results of this chapter, the use of a commercial satellite dataset (such as 3E Data Services) is preferred over the free online database (ERA5-Land) because of its high temporal resolution (15 minutes), its high spatial resolution (3x3 km) and because of its documented and validated uncertainties. Furthermore, the use of reference time-series coming from a dedicated calibrated field sensor (research-grade pyranometer) allowed the formulation of precise statements regarding GHI and POA irradiance, limited to one location: Bolzano, Italy

Summary of conclusions (further details in section 3.7 Results and discussion):

- In 95% of the cases (19/20) satellite data overestimated on-site measurements.
- Satellite data deviates the most from ground measurements under cloudy conditions (commercial solutions based their competitive advantage on how well they deal with this issue).
- The uncertainty figures calculated in the present analysis in many cases are twice as big as the reported uncertainties in the literature and in the marketing material of the service providers. This might be mainly due to the fact this analysis was done only for one site for one year (other possible causes might involve the methodology and metrics used).
- Validation should be done more extensively (more sites) to get more precise generic figures, because satellite data is highly sensible to the geographic location and local climates
- The temporal resolution offered by ERA5-Land (1 hour) may be enough for monthly KPIs calculation, but it could be totally insufficient when a higher granularity is needed, for example in case of fault detection. In this case, employing 3E Data Services is the most viable solution (maximum temporal resolution: 15 minutes), despite the well-known uncertainties.

Chapter 4: Data Quality analysis

- The Data Quality analysis proposed in this chapter pointed out the usefulness of evaluating the sensors' health status. The approach is based on a data-driven detection algorithm that in 5 steps deals with the most common anomalies, in compliance with international standards.

- This consistent data cleaning procedure, if combined with expert-knowledge from the field, could lead to targeted preventive or corrective maintenance actions (e.g. sensor cleaning or replacement).
- Furthermore, the usefulness of satellite-derived data was proved (because of its high data integrity and availability, being synthetic) when combined with field measurements to improve the irradiance data integrity (for the detailed discussion see section 4.6 The 'virtual sensor' concept).

Chapter 5: Data imputation with ML techniques

A data imputation procedure with ML techniques was proposed. From an O&M perspective, the Root Mean Square Error (RMSE) was considered the best metric to evaluate the performance of the tested algorithms and ensemble methods (Random Forest, Bagging and Gradient Boosting Regressor) yielded the best results over the set of ML methods employed.

- All machine learning algorithms employed provide an improvement over the satellite-derived data for each of the analysed settings: through ML models it has been possible to obtain lower errors, ranging from 34% to 73% less error than 3E POA irradiance data.
- Among the algorithms applied, ensemble methods[1] provided the best results, with Random Forest, Bagging and Gradient Boosting Regressor yielding very similar scores.
- As expected, the application of dimensionality reduction techniques (PCA) has led to slightly worst performances, while halving the execution time of the algorithms.
- This analysis showed that the use of Principal Components Analysis (PCA) did not bring additional accuracy improvements, even though it could be a viable solution when it is desirable to sacrifice some precision in favour of shortest running time.

In conclusion, based on this analysis, done on almost three years of data (15 minutes time series of electrical variables), it is possible to state that the proposed data imputation technique can avoid the use of a satellite-derived irradiance datasets, due to its higher accuracy. Finally, this work is an example of how an in-house data-driven solution can generate value and save costs to an O&M provider.

For the detailed discussion of results see section 5.6 Results and discussion.

[1] Once a group of predictors, called an *ensemble* (e.g. Decision Tree regressors), has been selected, each one of them can be trained and tested on a random subset of the dataset. The predictions obtained from the individual predictors are then aggregated (e.g. averaged) to form the most efficient predictor. Algorithms that use this strategy are called *ensemble methods*.

Further work

- Review the analysis so to fine-tune the process, avoiding the introduction of additional degrees of uncertainty (e.g. empirical thresholds)
- Experiment more on hyperparameter tuning to fine-tune the employed models (using both Grid Search and Randomized Search)
- Try out additional machine learning algorithms (e.g. Neural Networks) and time -series models
- Experiment with feature engineering
- Use not only meter-level data but also string and inverter-level to determine which level leads to the best predictions
- Restrict the number of electrical parameters to be used as input variables to determine which parameters are fundamental for missing values imputation
- Run again the analysis employing time series coming from a dedicated calibrated pyranometer as reference distribution, thus reducing the uncertainties and obtaining more consistent results
- Experiment on the same dataset both varying the dimension of the test set and using the same dimensions (9% and 20% of the observations) but employing different missing data frequency
- Reduce the quantity of input data so to determine the minimum amount of data (months or years) at a certain granularity necessary to obtain good predictions
- Run the analysis on other plants

7 Annex A: PV performance metrics

This annex provides a comprehensive review of the metrics used to assess PV plant performance. The purposes of a performance monitoring system are diverse and can include the following:

- Identification of performance trends in an individual PV system
- Localization of potential faults in a PV system
- Comparison of PV system performance to design expectations and guarantees
- Comparison of PV systems of different configurations
- Comparison of PV systems at different locations

These diverse purposes give rise to a diverse set of requirements, and different sensor and/or analysis methods may be more or less suited depending on the specific objective.

For example, for comparing performance to design expectations and guarantees, the focus should be on system-level data and consistency between prediction and test methods, while for analysing performance trends and localizing faults, there may be a need for greater resolution at sub-levels of the system and an emphasis on measurement repeatability and correlation metrics rather than absolute accuracy.

7.1 Normative references

Norm/Standard	Title
IEC 61724-1:2017	Photovoltaic system performance - Part 1: Monitoring
IEC TS 61724-2:2016	Photovoltaic system performance - Part 2: Capacity evaluation method
IEC TS 61724-3:2016	Photovoltaic system performance - Part 3: Energy evaluation method
IEC 61853-1:2011	Photovoltaic (PV) module performance testing and energy rating - Part 1: Irradiance and temperature performance measurements and power rating
IEC 61853-2:2016	Photovoltaic (PV) module performance testing and energy rating - Part 2: Spectral responsivity, incidence angle and module operating temperature measurements
IEC 61853-3:2018	Photovoltaic (PV) module performance testing and energy rating - Part 3: Energy rating of PV modules
IEC 61853-4:2018	Photovoltaic (PV) module performance testing and energy rating - Part 4: Standard reference climatic profiles
IEC 62446-1:2016+A1:2018	Photovoltaic (PV) systems - Requirements for testing, documentation and maintenance - Part 1: Grid connected systems - Documentation, commissioning tests and inspection
IEC TS 62446-3:2017	Photovoltaic (PV) systems - Requirements for testing, documentation and maintenance - Part 3: Photovoltaic modules and plants - Outdoor infrared thermography
IEC 61829:2015	Photovoltaic (PV) array - On-site measurement of current-voltage characteristics
IEC 60891:2009	Photovoltaic devices - Procedures for temperature and irradiance corrections to measured I-V characteristics
IEC 60904-1:2006	Photovoltaic devices - Part 1: Measurement of photovoltaic current-voltage characteristics

IEC 60904-5:2011	Photovoltaic devices - Part 5: Determination of the equivalent cell temperature (ECT) of photovoltaic (PV) devices by the open-circuit voltage method
IEC 60904-7:2008	Photovoltaic devices - Part 7: Computation of the spectral mismatch correction for measurements of photovoltaic devices
IEC 60904-10:2009	Photovoltaic devices - Part 10: Methods of linearity measurement

7.2 Terms and definitions

For the purpose of this document, the terms given in IEC 61724-1:2017, as well as their respective nomenclature and symbols are adopted.

Table 32. **Terms and nomenclature**

Term	Symbol	Units	Description
Irradiance	*G*	W/m^2	Generic term that refers to the incident flux of radiant power per unit area. If not specified otherwise, it usually refers to global irradiance.
Global Horizontal Irradiance	*GHI*	W/m^2	The sum of direct, diffuse, and ground-reflected irradiance incident on a horizontal surface. Measured with a suitable irradiance sensor[1] (thermopile pyranometer or reference cell) installed horizontally (parallel to the ground). It can also be estimated from the POA using a decomposition and transposition model.
In-plane or Plane of Array (POA) Irradiance	G_i *or* G_{POA}	W/m^2	Global irradiance incident on an inclined surface parallel to the plane of the PV modules. Measured with a tilted irradiance sensor (thermopile pyranometer or reference cell). It can also be estimated from the GHI using a decomposition and transposition model.
Direct Normal Irradiance	*DNI*	W/m^2	Irradiance emanating from the solar disk and from the circumsolar region of the sky within a subtended full angle of 5° falling on a plane surface normal to the sun's rays. Measured with a pyrheliometer on a two-axis tracking stage which automatically tracks the sun (rarely used for commercial PV plants).
Diffuse Horizontal Irradiance (DHI)	G_d	W/m^2	Global horizontal irradiance excluding the direct portion. It is measured with a horizontally mounted irradiance sensor with a rotating shadow band or tracked ball that blocks the direct normal irradiance.
Irradiation	*H*	kWh/m^2	Irradiance integrated over a specified time interval.
In-plane or Plane of Array (POA) Irradiation	H_i *or* H_{POA}	kWh/m^2	Global irradiation incident on an inclined surface parallel to the plane of the PV modules.
Soiling ratio	*SR*	%	Ratio of the actual power output of the PV array under given soiling conditions to the power that would be expected if the PV array were clean and free of soiling.
Soiling level	*SL*	%	Fractional power loss due to soiling, given by 1 − SR
Sample	--	--	Data acquired from a sensor or measuring device. Samples do not need to be permanently stored.
Sampling interval	--	--	Time between samples.

[1] For irradiance sensors requirements, see IEC 61724-1:2017, table 5, page 21

Record	--	--	Data recorded and stored, based on acquired samples. A record is the average, maximum, minimum, sum, or other function of the samples acquired during the recording interval, as appropriate for the measured quantity. The record can also include supplementary data such as additional statistics of the samples, number of missing data points, error codes, transients, and/or other data of special interest.
Recording interval	τ	min	Time between records. The recording interval should be an integer multiple of the sampling interval, and an integer number of recording intervals should fit within 1 h.
Standard Test Conditions	*STC*	--	Module operation mode: *open circuited* Irradiance on module surface: *1000 W/m²* Cell Temperature: *25 °C* Solar Spectrum: *air mass 1.5 (AM1.5)* Mounting: *open rack*
Nominal Operating Cell Temperature[1]	*NOCT*	--	Defined in IEC 61215:2005 as the equilibrium mean solar cell junction temperature within the following standard reference environment: Module operation mode: *open circuited* Irradiance on module surface: *800 W/m²* Ambient Temperature: *20 °C* Wind Speed: *1 m/s* Mounting: *open rack, tilt angle 45° from the horizontal* It is usually reported in the PV module's datasheet provided by the manufacturer.
Nominal Module Operating Temperature[2]	*NMOT*	--	Defined in IEC 61215-2:2016 as the equilibrium mean solar cell junction temperature within the following standard reference environment: Module operation mode: *Maximum Power Point (MPP)* Irradiance on module surface: *800 W/m²* Ambient Temperature: *20 °C* Mounting: *open rack, tilt angle (37 ± 5)° from the horizontal* NMOT is similar to the former NOCT except that it is measured with the module under maximum power rather than in open circuit. Under maximum power conditions (electric) energy is withdrawn from the module, therefore less thermal energy is dissipated throughout the module than under open-circuit conditions. Therefore, NMOT is typically a few degrees lower than the former NOCT. NMOT can be used by the system designer as a guide to the temperature at which a module will operate in the field, and it is therefore a useful parameter when comparing the performance of different module designs. However, the actual operating temperature at any particular time is affected by the mounting structure, distance from ground, irradiance, wind speed, ambient temperature, sky temperature and reflections and emissions from the ground and nearby objects. For accurate performance predictions, these factors shall be taken into account.

[1] NOCT was replaced by NMOT in the new version of the standard, see IEC 61215-12:2016

[2] See IEC 61853-2:2016 for the methodology for determining coefficients for calculating NMOT

7.3 On-site measured parameters

In this section all the measurements coming from the PV plant via the SCADA system (raw data) are described. For the purposes of this document, the classification given in IEC 61724-1:2017 of monitoring systems based on their accuracy level was adopted.

Table 33. **Monitoring systems classification**

Typical applications	**Class A** High accuracy	**Class B** Medium accuracy	**Class C** Basic accuracy
Basic system performance assessment	●	●	●
Documentation of a performance guarantee	●	●	
System losses analysis	●	●	
Electricity network interaction assessment	●		
Fault localization	●		
PV technology assessment	●		
Precise PV system degradation measurement	●		
Maximum recording interval	1 min	15 min	60 min

The most significant and direct impacts on PV performance are in-plane irradiance, the PV cell temperature, and shading losses (due to soiling, self-shadowing, shadowing from the surroundings or snow). Therefore, their accurate measurement (via the SCADA system) is of vital importance.

In summary, an adequate monitoring system would allow the O&M contractor to perform the following activities:

- Identification of system design and maintenance problems
- Assessment of plant performance (KPIs calculation and other metrics)
- Detection of faults and root-cause analysis
- Quantification of system losses and degradation
- Assess grid interactions
- Energy yield predictions

Table 34 lists the parameters that are measured by monitoring systems of utility-scale PV plants. The three columns on the right specify the requirements by the international standard IEC 61724-1:2017.

The mark ● indicates a required parameter to be measured on site, qualified. The symbol “E” indicates a parameter that may be estimated based on local or regional meteorological data or satellite data, rather than measured on site. Empty cells indicate optional (not required) parameters that may be chosen for specific system requirements or to meet project specifications.

Table 34. **Measured parameters and requirements for each monitoring system class**

Measured variable		Symbol	Units	Monitoring purpose	Required by IEC 61724-1:2017?		
					Class A	Class B	Class C
Irradiance[1]							
In-plane or Plane of Array (POA) Irradiance		G_i	W/m^2	Solar resource assessment, KPIs calculation	●	● or E	● or E
Global Horizontal Irradiance		*GHI*	W/m^2	Solar resource assessment, connection to historical and satellite data	●	● or E	
Direct Normal Irradiance		*DNI*	W/m^2	Solar resource assessment, concentrator (CPV)	● for CPV	● or E for CPV	
Diffuse Irradiance		G_d	W/m^2		● for CPV with <20x concentration	● or E for CPV with <20x concentration	
Environmental factors							
PV module temperature[2]		T_{mod}	°C	Determining temperature-related losses, KPIs calculation	●	● or E	
Ambient air temperature		T_{amb}	°C	Connection to historical data, estimation of PV module temperature	●	● or E	● or E
Wind speed		*WS*	m/s	Estimation of PV module temperature, warranty claims related to wind driven damage	●	● or E	
Wind direction		--	° (clockwise from geographical north)		●		
Rainfall		--	cm	Estimation of soiling losses			
Humidity		*RH*	%	Estimate changes in incident spectrum			
Soiling Ratio		*SR*	%	Determining soiling-related losses	● If soiling losses are expected to be >2%		
Electrical parameters							
DC side	Array Voltage	V_A	V	Diagnostics and fault detection	●		
	Array Current	I_A	A		●		
	Array Power	P_A	kW$_p$		●		
AC side	Output Voltage	V_{out}	V	Energy output., Diagnostics and fault detection	●	●	●
	Output Current	I_{out}	A		●	●	●
	Output Active Power	P_{out}	kW		●	●	●
	Output Energy	E_{out}	kWh	Energy output, KPI calculation	●	●	●
	Output Apparent Power	S_{out}	kVA	Utility request compliance			
	Output Reactive Power	Q_{out}	kVAr				
	Output Power Factor	Φ	°		●	●	

● required E estimated

[1] Thermopile pyranometers may be best for GHI measurement, while reference cells may be best for POA measurement.
Each irradiance sensor type has its benefits:

- Thermopile pyranometers are insensitive to typical spectral variations and therefore measure total solar irradiance. However, this can vary from the PV-usable irradiance by 1 % to 3 % (monthly average) under typical conditions. In addition, thermopile pyranometers have long response times compared to PV devices and photodiodes.
- Matched PV reference devices measure the PV-usable portion of the solar irradiance which correlates with the monitored PV system output. However, this may deviate from historical or meteorological measurements of irradiance, depending on instrumentation used.
- Photodiode sensors have significantly lower cost than the other two types and are appropriate for smaller or lower cost systems but are typically less accurate.

[2] The module temperature measurement may also be performed with the Voc-based method described in section 7.1.1

7.3.1 Soiling ratio

One factor hindering the performance of PV modules is soiling, defined as the accumulation of dust, sand, snow or any other particles on the surface of the modules that reduce irradiation collection. The soiling ratio is the ratio of the actual power output of the PV array under given soiling conditions to the power that would be expected if the PV array were clean and free of soiling.

Measurement devices required

- IV-curve tracer[1] (equipped with irradiance and module temperature sensors)
- Hand-held contact-less temperature sensor (for complementary or more accurate measurements)

Measurement procedure

a) Choose a soiled PV module representative of the general soiling condition of the PV plant.
b) Measure the I-V curve of the soiled PV module following the minimum requirements according to *IEC 61829:2015 On-site measurement of current-voltage characteristics.* (e.g. minimum G_i = 700 W/m^2)
c) Clean the module, following the manufacturer's recommendations.
d) Repeat b) for the cleaned PV module.
e) Calculate SR as described Table *35*.

Table 35. **Calculation of the Soiling Ratio**

Soiling Ratio			**Symbol**	**Units**
			SR	**%**
Symbol	Units	Description		Source
P_{soiled}	W	Power at MPP under STC of soiled PV module		Measured
P_{clean}	W	Power at MPP under STC of clean PV module		Measured
$$SR = \frac{P_{soiled}}{P_{clean}} \times 100$$				

[1] Commercially available I-V curve tracers are usually equipped with a reference cell and a module temperature sensor to be able to automatically translate the measured values into STC. It is advised to measure, additionally, the temperature in several other points of the module and then calculate the average temperature, to be used then for the STC translation.

7.4 Satellite-derived irradiance data

When permitted (see Table *34*), irradiance quantities may be estimated from satellite remote sensing. Such satellite-derived irradiances are extensively used for monitoring the performance of distributed generation systems including non-instrumented class B and class C systems, in order to avoid the cost and maintenance requirements of on-site measurements. Satellite remote sensing is an indirect approach to reliably estimate site- and time-specific irradiance. The approach is indirect because on-board satellite instruments measure the radiance emitted/reflected by the earth's surface through the filter of the atmosphere in a selected number of visible and infrared spectral bands; irradiance is inferred from these on-board satellite measurements via radiative transfer models. In-plane and other irradiance components are further modelled from the radiative transfer model output.

Satellite-derived irradiances, including global horizontal, direct normal, diffuse, and in-plane irradiances are typically available in real time from commercial services. Important considerations when selecting satellite models are as follows:

- Satellite-derived data should be carefully selected after a review of their accuracy, e.g., by reviewing application-pertinent (localized) validations associated with the data source;
- Good satellite models can be trained locally using short-term, regionally/environmentally representative ground measurements.

Satellite-derived irradiances have both advantages and disadvantages compared to on-site measured irradiances:

- The main advantage is their reliability and consistency in terms of calibration and maintenance. With a single set of carefully monitored on-board sensors covering entire continents at once, satellites remove the uncertainty and cost associated with on-site maintenance, instrumentation soiling, calibration drifts and location-to-location mismatches.
- The main disadvantage is their intrinsic accuracy. Unlike ground-based instruments, the accuracy of satellite models is not constant in relative terms over the entire range of irradiances but tends to be constant in absolute terms.

7.4.1 Accuracy

For GHI (the primary product of the radiative transfer models), well-trained satellite models typically have an accuracy of better than 2 % at 1000 W/m^2, but 20 % at 100 W/m^2, i.e., a constant ~20 W/m^2 throughout the 100 - 1000 W/m^2 range. Note that this uncertainty is not defined in absolute terms, but in relation to the ground-based instruments against which satellite models are evaluated.

The best trained satellite models can deliver an accuracy of 1 % at 1000 W/m^2, and 10 % at 100 W/m^2, i.e., a constant ~10 W/m^2 throughout the 100 - 1000 W/m^2 range (relative to the instrumentation used to train them). Quantities derived from GHI, including tilted in-plane irradiance, direct normal irradiance, and diffuse irradiance, have a higher uncertainty due to application of secondary models. Uncertainty for tilted, south-facing (northern hemisphere) or north-facing (southern hemisphere) in-plane irradiances is typically 1.25 times larger than for GHIs, i.e. 2.5 % at 1 000 W/m^2 for an untrained model, and 1.25 % for a trained model, relative to the training instrumentation. Direct normal irradiance uncertainty is of the order of 4 % at full range (1000 W/m^2) for an untrained model and 2 % for a trained model, relative to the training instrumentation.

Table 36. **Relative accuracy of satellite-derived irradiance data compared to on-site measurements**

Type of parameter	Parameter	Accuracy (at 100 - 1000 W/m^2)
Primary output of a radiative transfer model	*GHI*	~2% for an untrained model ~1% for a trained model
Derived from GHI (applying a secondary model)	*POA*	~2.5% for an untrained model ~1.25% for a trained model
	DIN	~4% for an untrained model ~2% for a trained model

If satellite-derived data have not been trained for a local area, variations in the local terrain can introduce substantial error on the order of 10 %. This is especially true in a desert with white sand, which may be difficult to distinguish from white clouds in some situations. Satellite-derived data may be less accurate for short periods but more accurate when averaged over long periods. Therefore, satellite-derived data may be more appropriate, for example, for evaluating system energy production over an extended period as compared to instantaneous power production.

7.5 Calculated parameters

Table 37 presents the parameters calculated from the monitoring measurements already described in section 7.2. All quantities in the table shall be reported with respect to the reporting period (typically daily, monthly, or yearly).

In the formulas given below, involving summation, τ_k denotes the duration of the k^{th} recording interval within a reporting period and the symbol $\sum_k$ denotes summation over all recording intervals in the reporting period. Note also that in formulas involving the product of power quantities with the recording interval τ_k , the power should be expressed in kW and the recording interval in hours, in order to obtain energy in units of kWh.

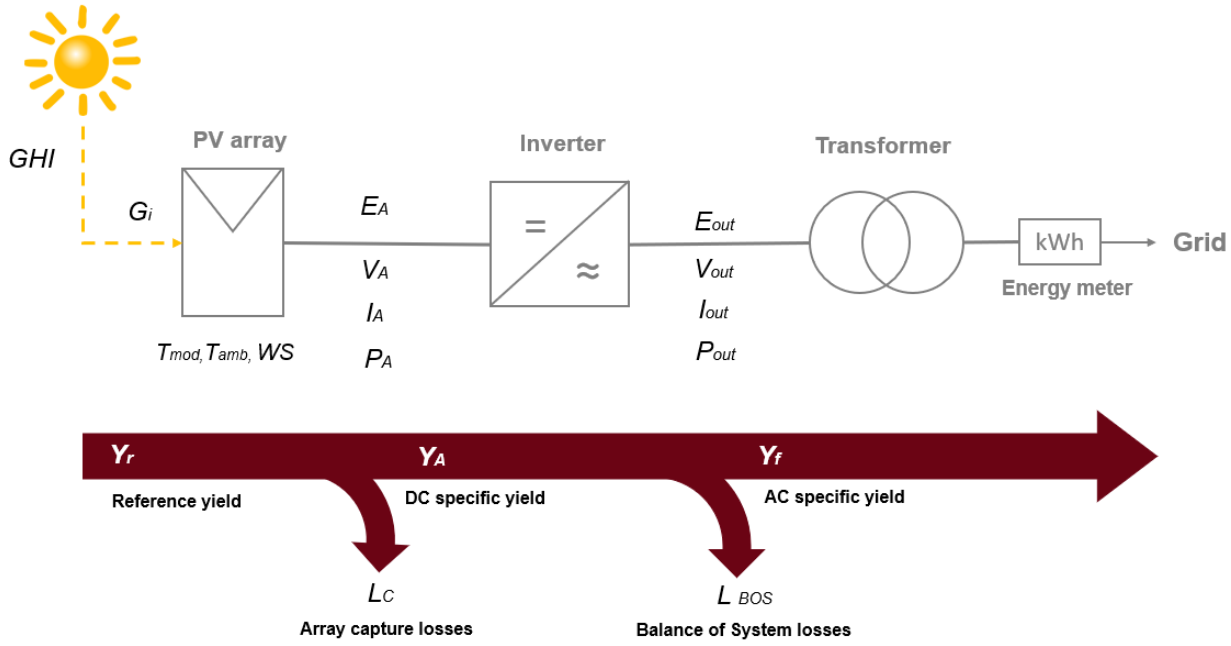

Figure 73. **PV plant parameters and energy flow**. *Source: adapted from SolarPower Europe*

Table 37. **Calculated parameters**

Parameter	Symbol	Units	Comments	Formula
Irradiation				
Global Horizontal Irradiation	H	kWh/m²	Also known as insolation, it is the integral of GHI over a certain period of time.	$H = \sum_k GHI_k \times \tau_k$
In-plane or plane of array (POA) Irradiation	H_i		It is the integral of POA irradiance over a certain period of time.	$H_i = \sum_k G_{i,k} \times \tau_k$
Electrical energy				
DC output energy (module, string or array level)	E_A	kWh	These energy quantities are calculated from the integral of their corresponding measured power parameters over the reporting period.	$E_A = \sum_k P_{A,k} \times \tau_k$

AC output energy (inverter or system level)	E_{out}			$E_{out} = \sum_k P_{out,k} \times \tau_k$
Array power rating				
DC power rating	P_0	kW_p	PV plant nominal power (the total DC power output of all installed PV modules at STC), calculated using the manufacturer's datasheet or module labels or even from alternative power measurements done on-site or by a specialised laboratory.	$P_0 = \sum P_{0,mod}$
AC power rating	$P_{0,AC}$	kW	It is the total rated AC power output of all installed inverters at a specified operating temperature	$P_{0,AC} = \sum P_{0,inv}$
Yields[1]				
DC specific yield (module, string or array level)	Y_A	kWh/kW	It is the measure of the total energy generated per kW_p over a certain period of time. It is calculated for both DC and AC sides. It normalises plant output over a chosen time frame and thus allows the comparison of the production of plants with different nominal power or even different technologies (e.g. PV, wind, biomass etc).	$Y_A = \frac{E_A}{P_0}$
AC specific yield[2] (inverter or system level)	Y_f			$Y_f = \frac{E_{out}}{P_0}$
Reference yield[3]	Y_r	kWh/kW	It represents the energy obtainable under ideal conditions, with no losses, over a certain period of time. Usually $G_{i,ref} = G_{STC} = 1000$ W/m^2	$Y_r = \frac{H_i}{G_{STC}}$
Expected yield	Y_{exp}		It expresses what should have been produced over a certain period of time. PR_{exp} is the Average Expected Performance Ratio of the plant based on the output of a model (simulation), using the actual temperature, irradiation and plant characteristics.	$Y_{exp} = PR_{exp} \cdot Y_r$
Yield losses[4]				
Array capture losses	L_C	kWh/kW	It represents the losses due to array operation, including array temperature effects, soiling, etc.	$L_C = Y_r - Y_A$
Balance of System losses	L_{BOS}		It represents the losses in the BOS components, including the inverter and all wiring and junction boxes	$L_{BOS} = Y_A - Y_f$
Efficiencies				
Array (DC) efficiency	$\eta_{A,0}$	--	A_a is the total module area, corresponding to the sum of the areas of the front surfaces of the PV modules as defined by their outer edges and *PR* is the performance ratio	$\eta_{A,0} = \frac{P_0}{G_{i,ref} \cdot A_a}$
Mean actual array (DC) efficiency	η_A			$\eta_A = \frac{E_A}{H_i \cdot A_a}$
System (AC) efficiency	η_f			$\eta_f = \frac{E_{out}}{H_i \cdot A_a} = \eta_{A,0} \cdot PR$
BOS efficiency	η_{BOS}			$\eta_{BOS} = \frac{E_{out}}{E_A}$

[1] Yields are ratios of an energy quantity to the array power rating P_0. They indicate actual array operation relative to its rated capacity. The ratio of units is equivalent to hours, which indicates the equivalent amount of time during which the array would be required to operate at P_0 to provide the particular energy quantity measured during the reporting period.

[2] Calculating the specific yield on inverter level allows a direct comparison between inverters that may have different AC/DC conversion rates or different nominal powers. Moreover, it is possible to detect whether an inverter is performing better than others.

[3] The reference yield represents the number of hours during which the solar radiation would need to be at reference irradiance levels in order to contribute the same incident solar energy as was monitored during the reporting period while the utility grid and/or local load were available. If the reporting period is equal to one day, then Y_r would be, in effect, the equivalent number of sun hours at the reference irradiance per day, or peak sun-hours if STC values are used.

[4] Yield losses are calculated by subtracting yields. They represent the amount of time the array would be required to operate at its rated power P0 to provide for the respective losses during the reporting period

7.6 Performance metrics

This section describes the metrics used to assess the performance of utility-scale PV plants. Among these, the most used by industry are the so-called Key Performance Indicators (KPIs), which provide the Asset Owner with a quick reference on the performance of the PV power plant. The KPIs are divided into the following categories:

PV plant KPIs, which directly reflect the performance of the PV power plant. PV plant KPIs are quantitative indicators.
O&M Contractor KPIs, which reflect the performance of the service provided by the O&M Contractor. O&M Contractor KPIs are both quantitative and qualitative indicators.

7.6.1 PV plant KPIs

These KPIs can be calculated over different time periods, but often they are computed on an annual basis. When comparing different KPIs or different PV power plants' KPIs, it is important to keep consistency in the time period used in computation.
A number of metrics are defined here for quantifying system performance. These are listed in Table *38* and are further defined in the subsequent sections. The most appropriate metric for a given system depends on the system design, user requirements and contractual agreements.

Table 38. **Summary of PV plant KPIs**

Key Performance Indicator		Symbol	Units	Contractual?
Performance Ratios (rating-based)				
1	Performance ratio	$\boldsymbol{PR}$	%	yes
2	Temperature-corrected performance ratio	PR'_{STC}		no
3	Annual-temperature-equivalent performance ratio	$PR'_{annual-eq}$		no
Performance Indices (model-based)				
4	Power performance index	PPI	%	no
5	Energy performance index	EPI		no
6	Baseline power performance index	$BPPI$		no
7	Baseline energy performance index	$BEPI$		no
Availabilities				
8	Technical Availability	AV_t	%	no
9	Contractual Availability	$\boldsymbol{AV}$		yes
10	Energy-based Availability	AV_e		no
Other				
11	Capacity Factor	CF	%	no

IMPORTANT: Performance ratios are based on the system name-plate rating, while a performance index is based on a more detailed model of system performance. The rating-based performance ratio metrics are relatively simple to calculate but may omit known factors that cause system power output to deviate from expectations based on the name-plate rating alone. For example, systems with high DC-to-AC ratio operate at less than the DC nameplate rating during times of high irradiance, but this is an expected attribute of the system design. Such effects are better treated by a performance index based on a detailed system model.

7.6.1.1 Performance Ratio

The Performance Ratio (*PR*) is a contractual KPI defined as the ratio between the AC specific yield (Y_f) and the reference yield (Y_r). It captures the overall effect of losses of the PV system when converting from nameplate DC rating to AC output. Typically, losses result from factors such as module degradation, temperature, soiling, inverter losses, transformer losses, and system and network downtime. The higher the *PR* is, the more energy efficient the plant is. *PR*, as defined in this section, is usually used to report on long periods of time, such as monthly or yearly (PR_{annual}). Based on it, the O&M contractor can provide recommendations to the plant owners on possible investments or interventions.

Table 39. **PR calculation**

Performance Ratio			**Symbol**	**Units**
			PR	**%**
Symbol	Units	Description		Source
Y_f	kWh/kW	AC specific yield		Calculated, see Table 37
Y_r	kWh/kW	Reference yield		
E_{out}	kWh	AC output energy		
P_0	W_p	PV plant nominal power (installed capacity)		
H_i	kWh/m²	In-plane (POA) irradiation		
G_{STC}	W/m²	STC irradiance (1000 W/m²)		Refence value, see Table 32
P_{out}	kW	AC output power		Measured
$G_{i,k}$	W/m²	In-plane (POA) irradiance		Measured
τ_k	h	Recording interval (granularity)		Monitoring system

$$PR = \frac{Y_f}{Y_r}$$

Expanding the formula:

$$PR = \frac{E_{out}/P_0}{H_i/G_{STC}} = \frac{E_{out} \cdot G_{STC}}{H_i \cdot P_0}$$

If P_o is given in kW and considering that G_{STC} = 1 kW/m², the calculation is simplified as follows:

$$\boldsymbol{PR = \frac{E_{out}}{P_0 \cdot H_i}}$$

Expanding the formula even further:

$$PR = \frac{G_{STC} \cdot \sum_k (P_{out,k} \cdot \tau_k)}{P_0 \cdot \sum_k (G_{i,k} \cdot \tau_k)} = \frac{G_{STC}}{P_0} \sum_k \frac{(P_{out,k} \cdot \tau_k)}{(G_{i,k} \cdot \tau_k)} = \frac{G_{STC}}{P_0} \sum_k \frac{P_{out,k}}{G_{i,k}}$$

Careful attention needs to be paid when interpreting PR, because there are several cases where it can provide misleading information about the status of the PV plant:

a) Seasonal variation of PR ***(lower PR in the hot months, higher in the colder)***

The calculation of PR presented in this section neglects the effect of array temperature, using the fixed value of array power rating, P_0. Therefore, the performance ratio usually decreases with increasing irradiation during a reporting period, even though energy production increases. This is due to an increasing PV module temperature that results in lower efficiency. This gives a seasonal variation, with higher PR values in winter and lower values in summer. It may also give geographic variations between systems installed in different climates.

b) Interpretation of PR for overrated plants ***(misleading lower PR)***

Special attention is needed when assessing the PR of overrated plants (DC/AC ratio higher than 1) where the output of the plant is limited by the inverter maximum AC output ($P_0 > P_{0,AC}$). In such situations, when inverter derating takes place, PR will be lower than normal although there is no technical problem with the plant. Stakeholders should be careful assessing PR values for

overrated plants, although the amount of derating is normally statistically constant or with negligible differences on a yearly basis.

c) Calculation of PR using *GHI* instead of G_i ***(misleading higher PR)***

Calculation of the performance ratio using *GHI* instead of in-plane (POA) irradiance G_i is an alternative in situations where GHI measurements are available, but G*i* measurements are not. In this case, the resulting formula is:

$$PR_{GHI} = \frac{G_{STC}}{P_0} \sum_k \frac{P_{out,k}}{GHI_k}$$

The GHI performance ratio would typically show higher values which may even exceed unity. These values cannot necessarily be used to compare one system to another but can be useful for tracking performance of a system over time and could also be applied to compare a system's measured, expected, and predicted performance using a performance model that is based only on GHI.

d) Soiled irradiance sensors ***(misleading higher PR)***

Special attention is needed when assessing the PR using data from soiled irradiance sensors. In this case, PR will present higher values and will give the false impression that the PV plant is performing better than expected and even some underperformance issues could remain hidden.

7.6.1.2 Temperature-corrected Performance Ratios

The seasonal variation of the performance ratio PR can be significantly reduced by calculating a temperature-corrected performance ratio PR'. While variations in average ambient temperature are the most significant factor causing seasonal variations in measured performance ratio, other factors, such as seasonally dependent shading, spectral effects, and metastabilities can also contribute to the seasonal variation of PR.

There are two different approaches to perform temperature corrections, each with a different scope:

- Temperature-corrected Performance Ratio (see Table 40): to reduce seasonal variations
- Annual-temperature-equivalent Performance Ratio (see Table 41): to compare with a model

Table 40. **Temperature-corrected PR calculation**

Temperature-corrected PR to STC		**Symbol**	**Units**
		PR'_{STC}	**%**
Symbol	Units	Description	Source
Y_f	kWh/kW	AC specific yield	see Calculated, Table 37
Y_r	kWh/kW	Reference yield	
C_k	--	Power rating temperature adjustment factor for interval *k*	Calculated
γ	%/°C	Maximum-power temperature coefficient	Module datasheet
$T_{mod,k}$	°C	Module temperature in recording interval *k*	Measured/Estimated*
E_{out}	kWh	AC output energy	see Calculated, Table 37
P_0	W_p	PV plant nominal power (installed capacity)	
H_i	kWh/m²	In-plane (POA) irradiation	
G_{STC}	kWh/m²	STC irradiance (1000 W/m²)	Refence value, see Table 32
$P_{out,k}$	kW	AC output power in recording interval *k*	Measured
$G_{i,k}$	W/m²	In-plane irradiance in recording interval *k*	Measured
τ_k	h	Recording interval (Monitoring system granularity)	Monitoring system

It is calculated by adjusting the power rating at each recording interval to compensate for differences between the actual PV module temperature and the STC reference temperature of 25 °C. Therefore, an adjustment factor C_k is introduced:

$$PR'_{STC} = \frac{Y_f}{Y_r \cdot \boldsymbol{C_k}}$$

Where C_k defined as the *power rating temperature adjustment factor* given by:

$$\boldsymbol{C_k} = 1 + (\frac{\gamma}{100})(T_{mod,k} - 25°C)$$

Expanding the formula:

$$PR'_{STC} = \frac{Y_f}{Y_r \cdot \boldsymbol{C_k}} = \frac{\frac{E_{out}}{P_0}}{\frac{H_i}{G_{STC}} \cdot \boldsymbol{C_k}} = \frac{E_{out} \cdot G_{STC}}{H_i \cdot (P_0 \cdot \boldsymbol{C_k})}$$

If P_o is given in kW and considering that G_{STC} = 1 kW/m², the calculation is simplified as follows:

$$\boldsymbol{PR'_{STC}} = \frac{\boldsymbol{E_{out}}}{\boldsymbol{H_i} \cdot (\boldsymbol{P_0} \cdot \boldsymbol{C_k})}$$

Expanding the formula even further:

$$PR'_{STC} = \frac{G_{STC} \cdot \sum_k (P_{out,k} \cdot \tau_k)}{\sum_k (P_0 \cdot \boldsymbol{C_k})(G_{i,k} \cdot \tau_k)} = \frac{G_{STC}}{P_0} \sum_k \frac{(P_{out,k} \cdot \tau_k)}{(G_{i,k} \cdot \tau_k) \cdot \boldsymbol{C_k}}$$

And finally, the complete formula is presented:

$$PR'_{STC} = \frac{G_{STC}}{P_0} \sum_k \frac{P_{out,k}}{G_{i,k} \cdot \left[1 + (\frac{\gamma}{100})(T_{mod,k} - 25°C)\right]}$$

Table 41. **Annual-temperature-equivalent PR calculation**

Annual-temperature-equivalent PR		**Symbol**	**Units**
		$\boldsymbol{PR'_{annual-eq}}$	**%**
Symbol	Units	Description	Source
$P_{out,k}$	kW	AC output power in recording interval *k*	Measured
$G_{i,k}$	W/m²	In-plane irradiance in recording interval *k*	Measured
P_0	W_p	PV plant nominal power (installed capacity)	Calculated, see Table 37
G_{STC}	kWh/m²	STC irradiance (1000 W/m²)	Refence value, see Table 32
τ_k	h	Recording interval (Monitoring system granularity)	
γ	%/°C	Maximum-power temperature coefficient	Module datasheet
$T_{mod,k}$	°C	Module temperature in recording interval *k*	Measured/ Estimated*
$T_{mod,avg}$	°C	Annual-average module temperature	Calculated

It calculates the PR during the reporting period with the power rating at each recording interval adjusted to compensate for differences between the actual PV module temperature and an expected annual-average PV module temperature. While this reduces seasonal variation in the metric, it does not remove the effect of annual-average temperature losses and leaves the value of the metric comparable to the value of PR_{annual}.
It is calculated in the same way as PR_{STC} with a slight change in C_k:

$$PR'_{annual-eq} = \frac{G_{STC}}{P_0} \sum_k \frac{(P_{out,k} \cdot \tau_k)}{(G_{i,k} \cdot \tau_k) \cdot \boldsymbol{C_k}}$$

Where C_k is a *power rating temperature adjustment factor* given by:

$$C_k = 1 + (\gamma/100)(T_{mod,k} - T_{mod,avg})$$

$T_{mod,avg}$ is chosen based on historical weather data for the site and an empirical relation for the predicted module temperature as a function of ambient conditions and module construction. It should be calculated by computing an **irradiance-weighted average of the predicted module temperature**.

* The module temperature $T_{mod,k}$ is the most important parameter to perform the above-described calculations of PR. It can be either measured or estimated:

a) Measured: as a best practice, temperature should be registered with a granularity of up to 15 minutes and the average temperature for the reporting period should be weighted according to the Specific Yield:

$$T_{mod,k} = \frac{\sum_k (Y_f \cdot T_{meas,k})}{\sum_k Y_f}$$

b) Estimated: If the monitoring objective is to compare PR'_{STC} to a target value associated with a performance guarantee, $T_{mod,k}$ should instead be estimated from the measured meteorological data with the same heat transfer model used by the simulation that set the performance guarantee value to avoid a bias error. See section 7.8.1 for details.

7.6.1.3 Performance Indices

A detailed performance model may be used to predict electrical output of the PV system as a function of meteorological conditions, known attributes of the system components and materials, and the system design. The performance model attempts to capture as precisely as possible all factors that can affect electrical output. In evaluating the system performance, particularly with respect to a performance guarantee, it is desired to compare the measured output with the predicted and expected outputs, defined as follow:

Measured output is the actual output (power or energy) of the PV plant measured by the monitoring and SCADA system.

Expected output is the output (power or energy) calculated by the performance model when using measured weather data.

Predicted output is the output (power or energy) calculated by the performance model when using historical weather data.

The model is also used to calculate expected energy during times of unavailability. Typically, the model is expected to be the same that was used to describe the plant before construction, but the model may be updated to reflect changes in the plant design, or any model may be used if the goal is to test the accuracy of the model.

A Performance Index (*PI*) is defined as follows:

$$Performance\ Index = \frac{measured\ output}{expected\ \ output}$$

And a Baseline Performance Index (*BPI*) is defined as follows:

$$Baseline\ Performance\ Index = \frac{measured\ output}{predicted\ \ output}$$

These performance indices may be evaluated either on the basis of power or energy, defining therefore the following four different indices:

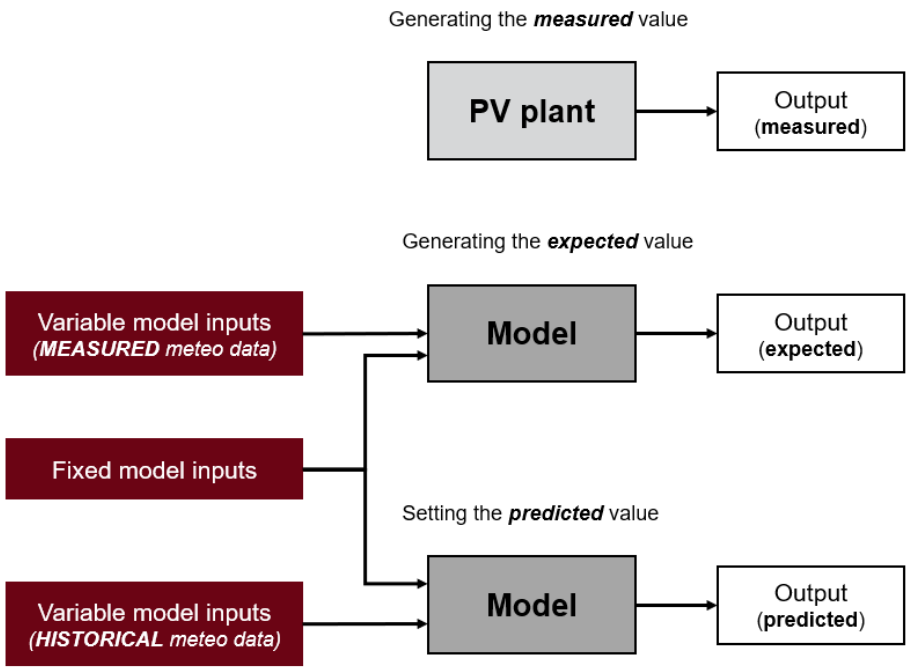

Figure 74. **Predicted, expected and measured outputs**. Adapted from IEC TS 61724-3

Table 42. **Summary of Performance Indices**

	Performance indices	**Baseline performance indices**
Output	*Expected*	*Predicted*
Power	$PPI = \frac{P_{measured}}{P_{expected}}$	$BPPI = \frac{P_{measured}}{P_{predicted}}$
Energy	$\boldsymbol{EPI = \frac{E_{measured}}{E_{expected}}}$	$BEPI = \frac{E_{measured}}{E_{predicted}}$

For evaluation of a performance guarantee, the performance model used for calculation of expected power or energy shall be identical to the performance model used for calculation of predicted power or predicted energy used in the performance guarantee.

The energy performance index (*EPI*) may refer to all times or only times of availability as defined by the all-in energy performance index or the in-service energy performance index, respectively:

- **All-in *EPI***: electricity generation of a PV system relative to the total expected energy over a specified time period, including times when the system is not functioning.
- **In-service *EPI*:** electricity generation of a PV system relative to the expected energy over a specified time period during times when the system is functioning (excluding times when inverters or other components are detected to be offline).

The advantage of using the EPI is that its expected value is 100% at project start-up and is independent of climate or weather. This indicator relies on the accuracy of the expected model. Unfortunately, there are more than one established model for the Expected Yield of PV systems in operation and not all of them are transparent. Therefore, the use of EPIs is recommended mainly for the identification of performance flaws and comparison of plants.

Table 43. **Calculation of the Energy Performance Index**

Energy Performance Index			**Symbol**	**Units**
			EPI	**%**
Symbol	Units	Description		Source
E_{out}	kWh	Actual output energy of the PV plant measured by the monitoring and SCADA system		Measured
E_{exp}	kWh	Expected output energy calculated by the performance model when using measured weather data		Calculated
$$EPI = \frac{E_{out}}{E_{exp}} \times 100$$				

7.6.1.4 Technical Availability or Uptime

Technical Availability (AV_t), or also called Uptime, is the parameter that represents the time during which the plant operates over the total possible time it can (should) operate, without taking any exclusion factors into account. The total possible time is considered the time when the plant is exposed to irradiation levels above the generator's Minimum Irradiance Threshold (MIT). Typical MIT values are 50 or 70 W/m^2. It should be defined according to site and plant characteristics (e.g. type of inverter, DC/AC ratio etc).

Table 44. **Calculation of the Technical Availability**

Technical Availability			**Symbol**	**Units**
			$\boldsymbol{AV_t}$	**%**
Symbol	Units	Description		Source
T_{useful}	h	Period of time with in plane irradiation above MIT		Measured
T_{down}	h	Period of time when the system is down (no production)		Calculated
P_k	kW_p	Installed DC power of the inverter *k*		Nameplate
P_0	kW_p	Total installed DC power of the PV plant		Calculated
$AV_{t,k}$	%	Technical Availability of the inverter *k*		Calculated
$$AV_t = \frac{T_{useful} - T_{down}}{T_{useful}} \times 100$$				

For systems with more than one inverter, it should be measured also at inverter level and it should be weighted according to their respective installed DC power. In this case, the Technical Availability of the total PV power plant can be defined as follows:

$$AV_{t\_total} = 100 \times \sum_{k} (AV_{t,k} \cdot \frac{P_k}{P_0})$$

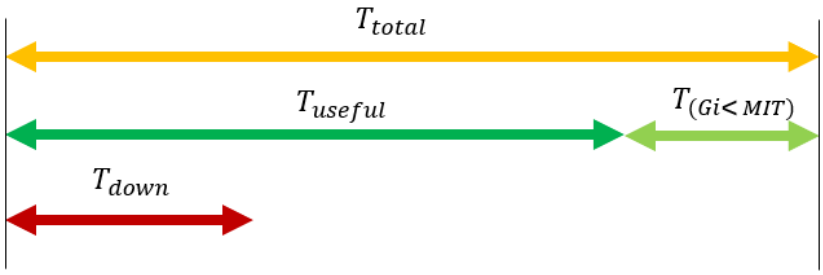

Figure 75. **Periods of time for the Technical Availability calculation**

7.6.1.5 Contractual Availability

Contractual Availability (AV) is a parameter that represents the time in which the plant operates over the total possible time it can (should) operate, taking into account the number of hours the plant is not operating for reasons contractually not attributable to the O&M contractor (exclusion factors). For the European market, where there is no on-site personnel present at all times, a best practice is a minimum guaranteed Contractual Availability of 98% over a year. For contractual KPI reasons, it should be calculated at inverter level, on an annual basis and it can be translated into bonus schemes or liquidated damages.

Table 45. **Calculation of the Contractual Availability**

Contractual Availability		**Symbol**	**Units**
		AV	**%**
Symbol	Units	Description	Source
T_{useful}	h	Period of time with in plane irradiation above MIT	Measured
T_{down}	h	Period of time when the system is down (no production)	Calculated
$T_{excluded}$	h	Period of T_{down} to be excluded because of presence of an exclusion factor	
P_k	kW_p	Installed DC power of the inverter *k*	Nameplate
P_0	kW_p	Total installed DC power of the PV plant	Calculated
AV_k	%	Availability of the inverter *k*	Calculated

$$AV = \frac{T_{useful} - T_{down} + T_{excluded}}{T_{useful}} \times 100$$

For systems with more than one inverter, it should be measured also at inverter level and it should be weighted according to their respective installed DC power. In this case, the Technical Availability of the total PV power plant can be defined as follows:

$$AV_{t\_total} = 100 \times \sum_{k} (AV_k \cdot \frac{P_k}{P_0})$$

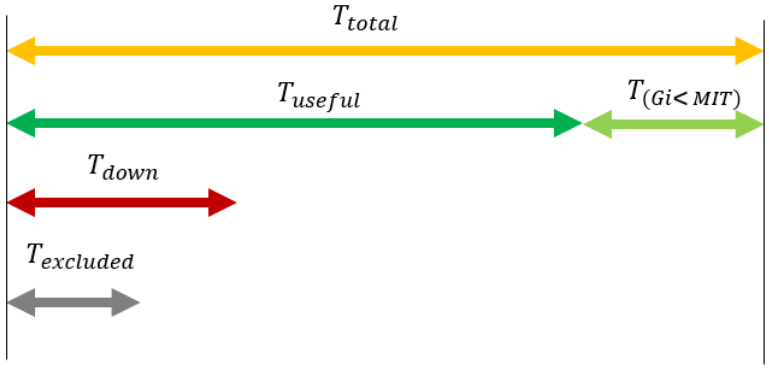

Figure 76. Periods of time for the Technical Availability calculation

The T_{down} represents the whole downtime, before the exclusions are applied. Therefore, $T_{excluded}$ is a part of T_{down} in the diagram. In practice you often first see that a plant is down (= measurement of T_{down}) and only in the course of troubleshooting one gets the information whether you can exclude part of the downtime.

Exclusion factors

The Asset Owner and the O&M Contractor should agree on certain failure situations that are not taken into account in the calculation of Contractual Availability. Some good examples for exclusion factors are:

- Force majeure
- Snow and ice on the PV modules

- Damage to the PV plant (including the cables up to the feed-in point) by the customer or third parties who are not sub-contractors of O&M Contractor, including but not limited to vandalism
- Disconnection or reduction of energy generation by the customer or as a result of an order issued to the customer by a court or public authority
- Operational disruption by grid disconnections or disruptions in the grid of the grid operator
- Disconnections or power regulation by the grid operator or his control devices
- Downtimes resulting from failures of the inverter or MV voltage components (for example, transformer, switchgear), if this requires
  - Technical support of the manufacturer and/or
  - Logistical support (for example supply of spare parts) by the manufacturer
- Outages of the communication system. Any failure time only begins to run when the O&M Contractor receives the error message. If the data connection to the site was not available, failure time shall only begin after reestablishment of the link
- Delays of approval by the customer to conduct necessary works
- Downtimes for implementation of measures to improve the PV plant, if this is agreed between the parties
- Downtimes caused by the fact that the customer has commissioned third parties with the implementation of technical work on the PV plant
- Downtimes caused Serial Defects on Plant components

Bonus Schemes and Liquidated Damages

The availability guarantee provided by the O&M contractor can be translated into bonus schemes and liquidated damages. These ensure that the asset owner is compensated for losses due to lower-than-guaranteed availability and that the O&M contractor is motivated to improve its service in order to achieve higher availability. Higher availability usually leads to higher energy generation and an increase of revenues for the benefit of the plant owner. Hence the bonus scheme agreements lead to a win-win situation for both parties and ensures that the O&M contractor is highly motivated.

The following are examples of bonus schemes and liquidated damages:

- Bonus Schemes: if the Minimum Guaranteed Availability is overachieved, the additional revenue based on the base case scenario expected annual revenue will be equally divided (50/50) between the asset owner and the O&M contractor.
- Liquidated Damages: if the Minimum Guaranteed Availability is underachieved, 100% of the lost revenue due to the availability shortfall based on the base case scenario expected

annual revenue will be compensated by the O&M contractor. This is usually translated into a reduction of the O&M annual fee.

- The amount of liquidated damages is capped at 100% of the O&M annual fee on a period of 12 months. Reaching this cap usually results in contract termination rights.

7.6.1.6 Energy-based Availability

Energy-based Availability (AV_e) takes into consideration that an hour in a period with high irradiance is more valuable than in a period with low irradiance. Therefore, its calculation uses energy instead of time. The exclusion factors defined for the Contractual Availability should be also applied here.

Table 46. **Calculation of the Energy-based Availability**

Energy-based Availability		**Symbol**	**Units**
		AV_e	%
Symbol	Units	Description	Source
E_{out}	kWh	Plant energy AC production	Measured
E_{loss}	kWh	Calculated lost energy after applying exclusion factors	Calculated

$$AV_e = \frac{E_{out}}{E_{out} - E_{loss}} \times 100$$

7.6.1.7 Capacity factor

The capacity factor (*CF*) is a metric commonly applied to power plants for comparison purposes. It can be used, for example, to compare PV plants with conventional gas-fired power plants. Its calculation is based on the AC rating of the plant (the sum of the inverter ratings in the system) and defines the fraction of electrical energy that was generated compared with what the plant would have generated if it operated at the AC rated power 100 % of the time.

Table 47. **Calculation of the Capacity factor**

Capacity Factor			Symbol	Units
			CF	%
Symbol	Units	Description		Source
E_{out}	kWh	Power at MPP under STC of soiled PV module		Measured
$P_{0,AC}$	kW	It is the total rated AC power output of all installed inverters at a specified operating temperature		Calculated
$days$	--	the number of days of the period of interest, typically 365		--
$$CF = \frac{E_{out}}{P_{0,AC} \cdot (24 \cdot days)} \times 100$$				

7.6.2 O&M contractor KPIs

As opposed to power plant KPIs described in the previous section, which provide the Asset Owner with information about the performance of their asset, O&M Contractor KPIs assess the performance of the O&M service. Four KPIs are then defined:

Table 48. **Definition of the O&M contractor KPIs**

O&M contractor KPI		Units	Description	Contractual ?
1	Acknowledgement time (Reaction time)	h	It is the time between detecting the problem (receipt of the alarm or noticing a fault) and the acknowledgement of the fault by the O&M Contractor by dispatching a technician. The Acknowledgement time reflects the O&M Contractor's operational ability.	no
2	Intervention time		Time to reach the plant by a service technician or a subcontractor from the moment of acknowledgement. In certain cases, remote repair is possible. The Intervention time assesses the capacity of the O&M Contractor to mobilise field personnel to the plant.	no
3	Response time		It is the Acknowledgement time plus the Intervention time. Used for contractual purposes, minimum Response times are guaranteed based on fault classes that consider the unavailable power, the consequent energy loss and their relevance in terms of safety.	yes
4	Resolution time (Repair time)		It is the time to resolve the fault starting from the moment of reaching the PV plant. It is generally not guaranteed, because resolution often does not depend totally on the O&M Contractor	not always

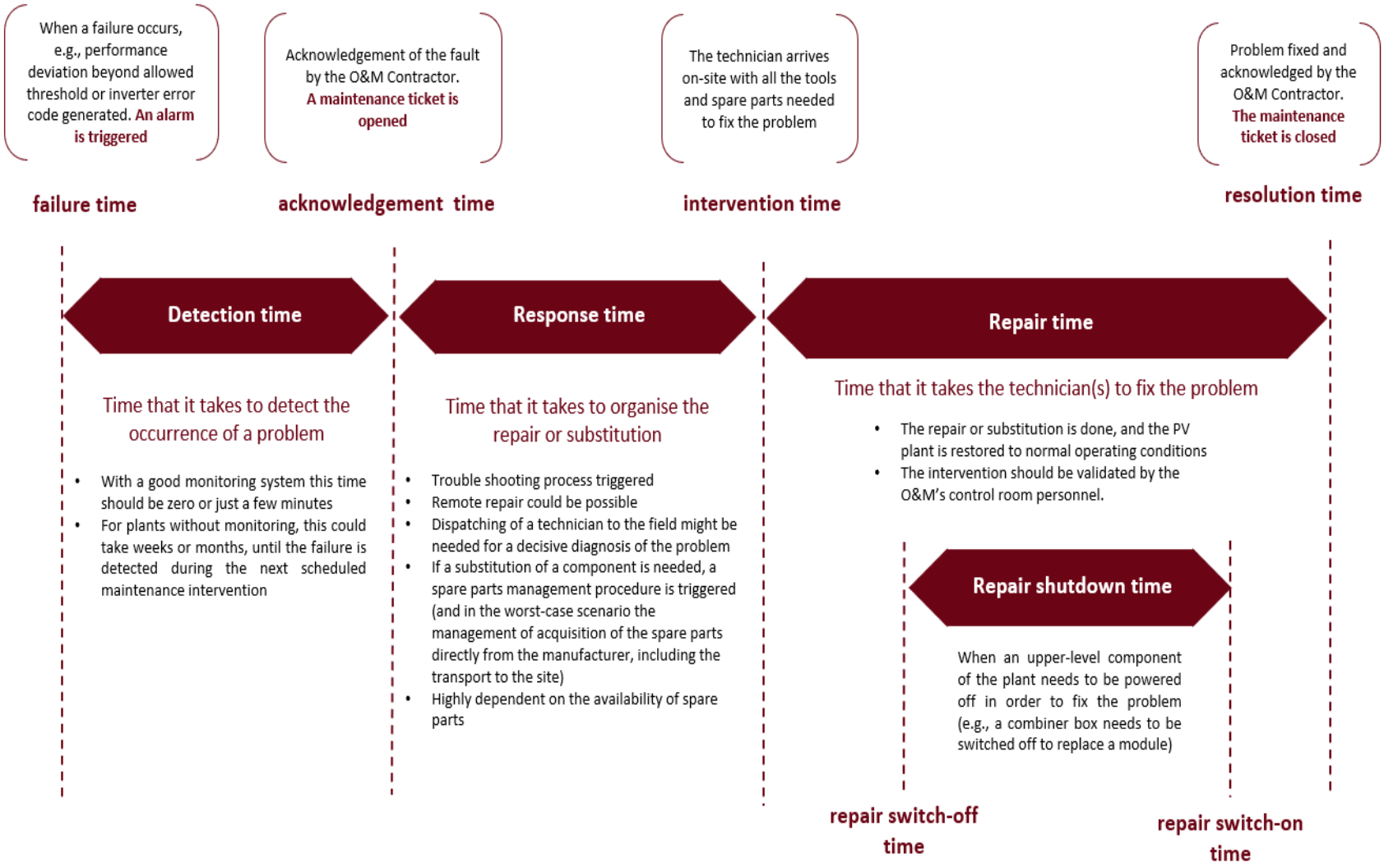

Figure 77. **O&M contractor KPIs**. *Source: own design*

7.6.2.1 Response Time guarantee

The O&M contractor should guarantee to react on alarms received from the plant through the monitoring and supervision system within a certain period of time, 7 days a week. This translates in a minimum guaranteed Response Time. When setting it, it is recommended to differentiate between hours and periods with high and low irradiance levels as well as fault classes, based on the (potential) loss of energy or relevance in terms of safety impact of the failure.
In the following table an example is provided:

Table 49. **Example of Response time guarantees**

Fault Class	Description	Response time guaranteed
Fault Class 1	The entire plant is off, 100% power loss	4 daytime hours
Fault Class 2	More than 30% power loss or more than 300 kW_p down	24 hours
Fault Class 3	0%-30% power loss	36 hours

In case the replacement of equipment is needed, the O&M contractor should commit to make it available on-site and replace it within 8 business hours from the end of the Response Time if the spare part is included in the portfolio of minimum spare parts list. If the spare part is not included in the minimum spare parts list, the O&M contractor should commit to order the spare part within 8 business hours from the end of the Response Time and to replace it in the fastest possible way after receiving the related spare part from the equipment supplier.

In case the fault cannot be fixed by the O&M contractor and the equipment supplier's intervention is required, the following actions are necessary:

- If the intervention requires spare parts up to the limit under the O&M cost responsibility, the O&M contractor may proceed without separate approval (insurance aspects to be considered);
- If the costs exceed the above budget limit, the O&M contractor should communicate the issue in writing to the Asset Owner within 8 business hours from the end of the Response Time.

Force Majeure events are excluded from Response Time obligations.

7.6.2.2 Resolution Time guarantee

Resolution Time can also be guaranteed in certain restricted situations. The O&M contractor is able to guarantee the Resolution Time in situations where the problem has been assessed and approved to be due to a faulty spare part that needs to be replaced and the spare part is available in the warehouse or has just been delivered. Such a Resolution Time guarantee can incentivise the O&M contractor to replace spare parts rapidly. Events beyond the O&M Contractor's control, such as a delay in spare part delivery, as well as Force Majeure events are excluded from Resolution Time guarantees.

7.7 System Performance Evaluation

The performance of a PV system is dependent on the weather, seasonal effects, and other intermittent issues, so demonstrating that a PV system is performing as predicted requires determining that the system functions correctly under the full range of conditions relevant to the deployment site.

The following table presents the existing standards that deal with system performance evaluation, each with its specific scope and limitations:

Table 50. **Current standards on System Performance Evaluation**

Norm/Standard	Title	Scope	Limitations
IEC 62446-1:2018	Photovoltaic (PV) systems - Requirements for testing, documentation and maintenance - Part 1: Grid connected systems - Documentation, commissioning tests and inspection	Describes a procedure for ensuring that the plant is constructed correctly and powered on properly by verification through incremental tests	Does not attempt to verify that the output of the plant meets the design specification
IEC 61724-1:2017	Photovoltaic system performance - Part 1: Monitoring	Defines the data that shall be measured and collected to calculate performance metrics (PR and Performance indices)	Does not define how to analyse that data in comparison to predicted performance
IEC TS 61724-2:2016*	Photovoltaic system performance - Part 2: Capacity evaluation method	Describe methods for determining the power output of a photovoltaic system and are intended to document completion and system turn on and report a short-term power capacity measurement of a PV system	Are not intended for quantifying performance over all ranges of weather or times of year, just for a short period of time (some days)
ASTM E2848-11**	Standard Test Method for Reporting Photovoltaic Non-Concentrator System Performance		
IEC TS 61724-3:2016	Photovoltaic system performance - Part 3: Energy evaluation method	Describes a method for determining the energy output of a photovoltaic system for long-term evaluation (1 year)	Does not attempt to describe the method for predicting the electrical energy production (the prediction method and assumptions are left to the user)
IEC 62670-2:2015	Photovoltaic concentrators (CPV) - Performance testing - Part 2: Energy measurement	Describes how to measure the energy from a CPV plant.	Does not describe how to compare the measured energy with a model

* non-regression-based method for determining power output
** regression-based method for determining power output

As already explain in section 7.6.1.3, in evaluating the system performance, particularly with respect to a performance guarantee, it is desired to compare the measured output with the predicted and expected outputs, defined as follow:

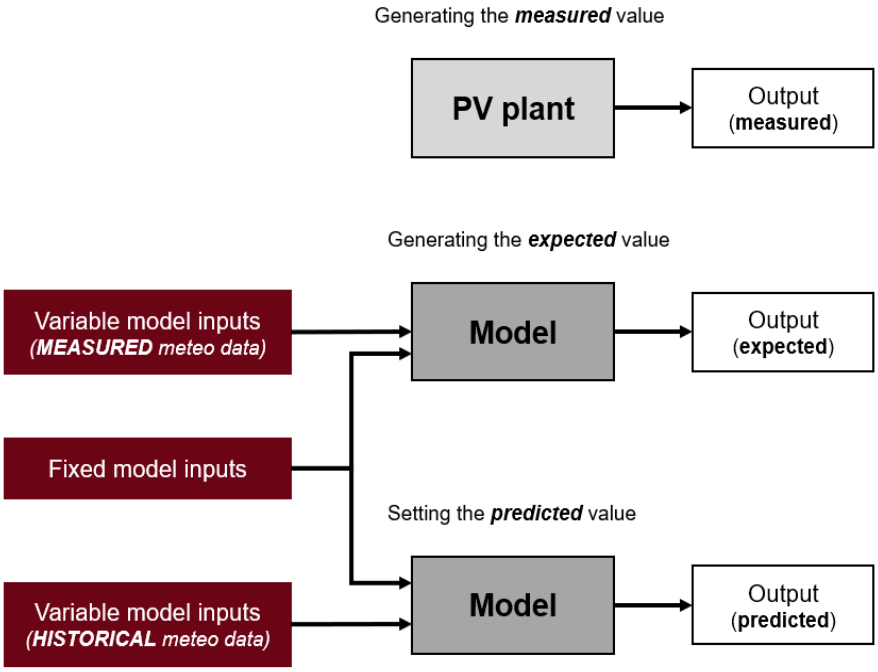

Figure 78. **Predicted, expected and measured outputs**. Adapted from *IEC TS 61724-3*

The model is also used to calculate expected energy during times of unavailability. Typically, the model is expected to be the same that was used to describe the plant before construction, but the model may be updated to reflect changes in the plant design, or any model may be used if the goal is to test the accuracy of the model.

In the following sections, two evaluation methods to assess system performance are described:

a) **Energy method**: defined in *IEC TS 61724-3:2016*, describes a one-year test that evaluates performance over the full range of operating conditions and is the preferred method for evaluating system performance.

b) **Capacity method**: defined in *IEC TS 61724-2:2016*, describes a short-term method that evaluates the power output of a photovoltaic system, usually before/after its completion, commissioning, revamping or hand-over. As a capacity test, it measures power (not energy) at a specified set of reference conditions (which can differ from standard test conditions that have been designed to facilitate indoor measurements). This method is a non-regression-based method for determining power output.

7.7.1 Energy evaluation method

Scope

This method (based on *IEC TS 61724-3*), defines a procedure for measuring and analysing the energy production of a specific photovoltaic system relative to the expected electrical energy production for the same system from actual weather conditions. It is intended to address the full range of relevant operating conditions and for a sustained time (generally a complete year) to verify long-term expectations of energy production to capture all types of performance issues, including outages or instances of reduced performance of the plant.

Multiple aspects of PV system performance are dependent on both the weather and the system quality, so it is essential to have a clear understanding of the system being tested. For example, the module temperature is primarily a function of irradiance, ambient temperature, and wind speed; all of which are weather effects. However, the module-mounting configuration also affects the module temperature, and the mounting is an aspect of the system design.

The performance of the system is characterized both by quantifying the energy lost when the plant is not functioning (unavailable) and the extent to which the performance meets expectations when it is functioning.

Inverter operation and other status indicators of the system are first analysed to find out whether the system is operating. Times when inverters (or other components) are not operating are characterized as times of unavailability and the associated energy loss is quantified according to the expected energy production during those times. For times when the system is operating, actual photovoltaic system energy produced is measured and compared to the expected energy production for the observed environmental conditions, quantifying the energy performance index (EPI), as defined in section 7.6.1.3:

$$EPI = \frac{E_{out}}{E_{exp}} \times 100$$

As a basis for this evaluation, expectations of energy production are developed using a model of the PV system under test that will serve as the guarantee or basis for the evaluation. Typically, the model is complex and includes effects of shading and variable efficiency of the array.

This procedure evaluates the quality of the PV system performance with the assumption and expectation that the model used to predict performance accurately describes the system. If the initial model is found to be inaccurate, the design of the system is changed, or it is desired to test the accuracy of an unknown model, the model may be revised relative to one that was applied earlier, but the model should be fixed throughout the completion of this procedure.

Energy unavailability: metric that quantifies the energy lost when the system is not operating (as judged by an automatic indication of functionality such as the inverter status flag indicating that the inverter is actively converting DC to AC electricity or not). The energy unavailability is the ratio of the expected energy (as calculated from the original model and the measured weather data) that cannot be delivered because of inverters or other components being offline divided by the total expected energy for the year.

$$Energy\ unavailability = \frac{E_{not\ delivered}}{E_{total\ expected}} \times 100$$

Some possible reasons of energy unavailability are:

- Hardware failure
- Plant degradation
- Planned outage (maintenance interventions)
- Not expected weather conditions
- Grid requirements limiting the energy uptake (curtailment)
- Grid support events (e.g. deviation from unity power factor)
- Operational set points (inverter clipping[1])
- Poor maintenance procedures
- Force majeure

Energy availability: metric of energy throughput capability that quantifies the expected energy when the system is operating relative to the total expected energy. It is calculated from the energy unavailability and may be expressed as a percentage or a fraction.

$$Energy\ availability = 100 - Energy\ unavailability = \frac{E_{delivered}}{E_{total\ expected}} \times 100$$

In summary, this test procedure was created to:

a) Facilitate the documentation of a performance guarantee
b) Verify accuracy of a model
c) Track performance (e.g., degradation) of a system over the course of multiple years

[1] When the inverter output is limited by the capability of the inverter rather than by the input power from the PV array

d) Document system quality for any other purpose

Test applicability and duration

This test may be applied at one of several levels of granularity of a PV plant. The smallest level to which the test may be applied is the smallest AC power generating assembly capable of independent on-grid operation.

Some PV modules show measurable performance changes within hours or days of being installed in the field, others do not. The start of the test should be negotiated between the stakeholders using the manufacturer's guidance for the number of days or the irradiance exposure needed for the plant to reach the modelled performance along with the details of the actual installation and interconnection dates. Any degradation assumptions should be agreed to by all stakeholders and documented as part of the model description.

It is recommended that the test lasts 365 days. If the test is not continued for a full year, seasonal variations (including shading, spectrum, temperature, and wind) may cause the performance to deviate from what would be obtained over a full year.

The performance metric, in-service energy performance index, is reported only for times when the inverters and other components are online. Expected energy for times when the inverters or other components are offline is quantified in the energy unavailability metric. The energy unavailability metric may be further divided into situations with internal and external causes, as agreed to by the stakeholders.

Notes about data collection:

- Verification of accurate positioning of the sensors is accomplished through comparison of data from a clear day with modelled irradiance for a clear day and the results included in the documentation of the uncertainty of the application of the test.
- When irradiance sensors are deployed in the plane of the array, the ground albedo should be measured to demonstrate consistency with that assumed in the model and the results included in the documentation of the uncertainty of the application of the test.
- For Class A tests, because the irradiance measurement is so crucial to the test, the calibrations should be independently verified either by using sensors calibrated at different test locations or at different times so as to prevent a systematic bias to the calibration.

Procedure

In the following table and diagram, a step-by-step description of the procedure is provided.

Step		Description
1	Calculation of **predicted** energy[1] and documentation of method that will be used to calculate the expected energy	Calculation of the predicted energy (using historical weather data) and the method that will be used to calculate the expected energy. Definition of test boundaries, meteorological inputs format, PV system inputs and assumptions regarding soiling, shading, snow coverage, outages, etc. The predicted energy may assume 100 % availability or may be reduced to account for expected times of unavailability. The uncertainty defining the pass/fail criteria of the test results should be agreed at this stage.
2	Collection of **measured** data	Collect recorded data at the specified frequency and in the specified format with every effort made to avoid gaps in data, to maintain sensor function and calibration through early detection of failures, and to strictly adhere to agreed-upon procedures.
3	Identification of data associated with **unavailability**	The data should be screened for times when any inverter is offline (not converting DC to AC electricity) or some other component is off line. The expected energy production associated with the unavailability is tabulated and aggregated to provide the expected energy for the times during the year when the plant is unavailable.
4	Data quality check	Identification of erroneous data and replacement or adjustment of such data and preparation of model input dataset: filtering, cleaning, time interval consistency check, time stamp alignment, etc.
5	Calculation of **expected** energy	The expected energy generated by the facility is calculated by inputting the measured variable input data during the test period into the performance model, paying attention to the acceptability of data, Time interval consistency, Time stamp alignment
Calculate expected energy during times of **unavailability**		Input measured meteorological data into the performance model to calculate the expected energy for times of unavailability during the test period. Document all times of unavailability and the associated expected energy that was not realized during the test period, and, if desired, separate these into energy associated with internally and externally caused unavailability, commenting on any identified causes for unavailability.
Calculate expected energy during times of **availability**		Input measured meteorological data into the performance model to calculate the expected energy for times of availability during the test period. Both real and apparent expected energy should be calculated.
Calculate total expected energy		The total expected energy is calculated as the sum of the expected energies during the times of unavailability and availability. Both real and apparent expected energy should be calculated.
Analyse discrepancies		If the measured energy deviates from the expected energy significantly (by more than 10 %), then a root cause diagnosis should be completed. For example, such a diagnosis might be that the weather for the year was unexpected, the simulation model is different than the as-built plant, or there was unusual missing data. The test report should comment on whether the test should still be considered valid.
6	Calculation of **measured** energy	The measured energy is the result of all energy generated by the facility as measured at the metering location during the test period after subtracting out energy associated with parasitic power losses. If substitutions were made for missing data, care should be taken that the measured energy production is estimated in a way that is consistent with how the expected energy for that period was defined.
7	Calculation of **performance metrics** from **measured** data	Calculation of KPIs as defined in section 7.6.1 (PR, availability, energy performance indices and capacity factor). The all-in energy performance index is calculated using the total expected energy. The in-service energy performance index is calculated using the expected energy during times of availability. The external-cause-excluded energy availability is calculated excluding the expected energy during times of unavailability that were caused by circumstances outside of the control of the plant. The comparison of measured and expected energy includes a consideration of the uncertainties.
8	Uncertainty analysis	The uncertainty should be determined for the test result, not for the original prediction. Both systematic (bias) and random (precision) uncertainties are included in the analysis. The contributions to the uncertainty depend on the model that is used, but generally include uncertainty in the measurements of the irradiance, temperature, and electricity generated. The uncertainties associated with each sensor are taken from the manufacturer's specification and/or from the calibration report provided by the calibration laboratory.

[1] Although the final comparison of expected and measured energy does not use the predicted energy directly, the predicted energy is usually required for project planning.

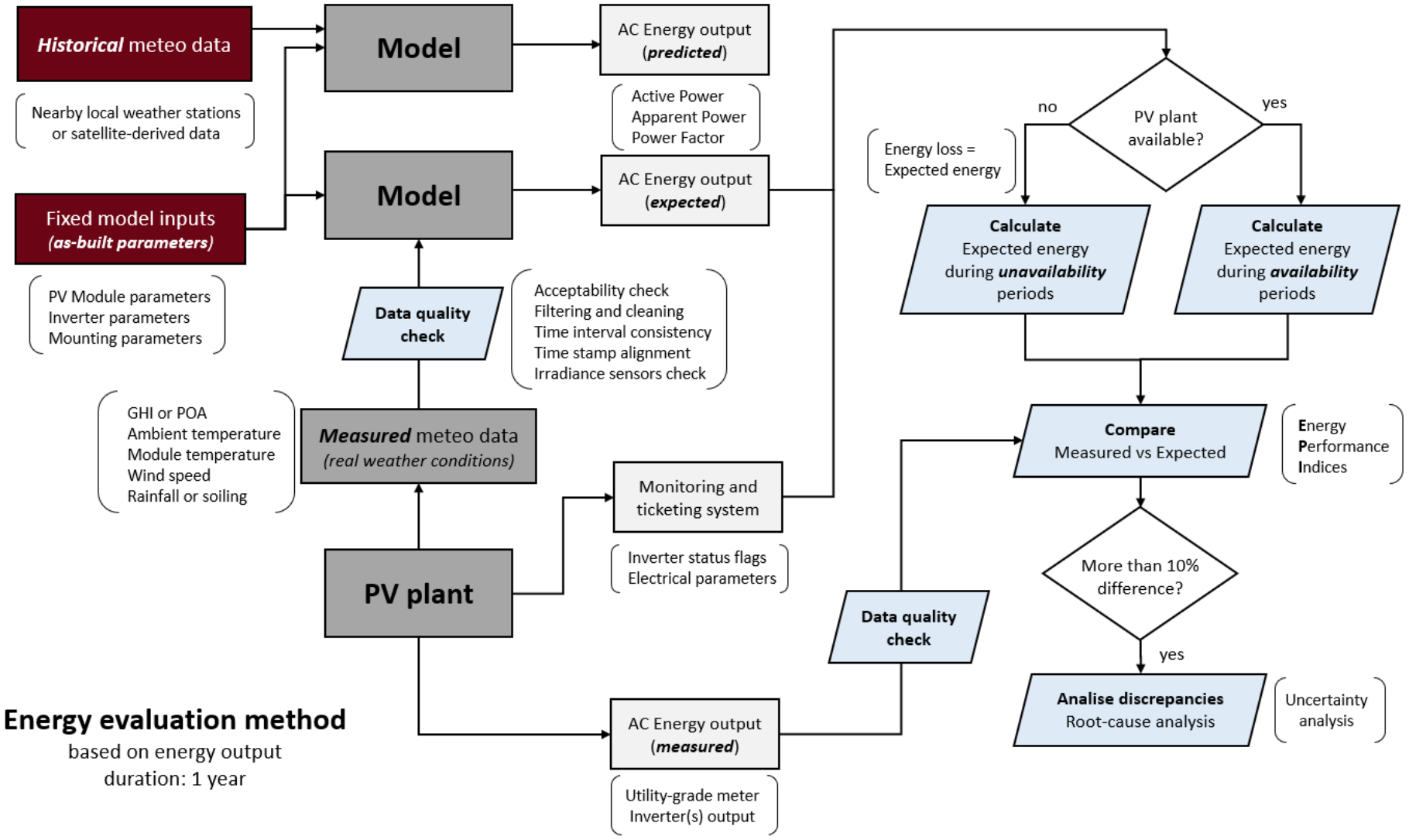

Figure 79.**Energy Evaluation Method** – procedure flow diagram. Source: own design

Data quality check: filtering and flagging criteria

Each data stream should be checked for data out of range, missing data, or unreasonable trends as described in IEC 61724-1. An example procedure is given in more detail in *Table 51*. Depending on the local conditions, the details of the plant design, and the addition of other data streams, the filtering criteria may be modified, but all four types of filters (range, missing data, dead value, and abrupt change) shall be applied and documented as part of the final report. Flagged data are examined to determine the underlying cause and whether the flag should be retained.

Table 51. **Example of data filtering criteria, to be adjusted according to local conditions**. Source: IEC TS 61724-3:2016

		Suggested criteria for flag (15 min data)			
Flag type	**Description**	**Irradiance** W/m^2	**Temperature** °C	**Wind speed** m/s	**Power (AC power rating)**
Range	Value outside of reasonable bounds	< –6 or > 1 500	> 50 or < –30	>32 or < 0	> 1,02 × rating or < –0,01 × rating
Missing	Values are missing or duplicates	n/a	n/a	n/a	n/a
Dead	Values stuck at a single value over time. Detected using derivative.	< 0,0001 while value is > 5	< 0,0001	?	?
Abrupt change	Values change unreasonably between data points. Detected using derivative.	> 800	> 4	> 10	> 80 % rating
May be adjusted depending on the tilt of the system and the season of data acquisition.					

As part of the data filtering, the data should be binned into times when inverters (or other system parts if desired) were on line and off line. In the case where a single inverter is off line, but the system output is measured at a single point for the entire system, the expected energy is partitioned to reflect the expected energy from the functioning inverters (or other system parts, if desired) and the expected energy from the offline inverters and aggregated separately. The energy aggregated for times when the system was off line may be separated into two categories: problems caused by internal and external reasons.

Irradiance sensors check

Because of the sensitivity of the test to the irradiance data, special attention should be given to the irradiance data. Specifically, irradiance data that may result from accidental shading of a sensor or sensor malfunction should be removed before taking the average of the data from the remaining sensors. Accurate calibrations are needed for all sensors to provide a test result with low uncertainty. In addition to confirming that the calibrations were completed as planned, the

night-time data should be checked to confirm accurate zero-point calibration, noting that it is common for a pyranometer to show a negative signal of 1 W/m^2 to 3 W/m^2
A recommended procedure for identifying such data in the case where multiple sensors are being used is:

Step 1: Identify a clear day.
Step 2: Compute the average irradiance value for each sensor during each time interval and compare each individual value with the average value for all sensors. If this difference is greater than the uncertainty of the sensors, inspect the data to identify a probable cause. (Note that if the data are taken more frequently than once per minute, the data should be averaged over a time period of at least 1 min.)
Step 3: Look for drifts of the calibrations of the sensors.
Step 4: Discard data that can be traced to malfunctioning of the sensor or data acquisition system. Discard data from sensors that are out of calibration (this action should be done only with mutual consent of the stakeholders).
Step 5: Discard individual data points that are compromised by sensor maintenance or cleaning.
Step 6: If all data for some time periods are removed, this time period is treated as missing data. The missing data, cause for removal of the data, and the impact of the removal of the data are presented in the report (this action should be done only with mutual consent of the stakeholders).

Using data from multiple sensors

The ambient temperature and irradiance used as input to the model should be the average of the available measurements, except where a measurement is determined to be erroneous, in which case the input to the model should be the average or median of the remaining measurements. Temperature and irradiance data from nearby meteorological stations, from numerical weather models, or from satellite data may be used when it is expected to improve the accuracy of the test and with mutual consent of the stakeholders. The type of sensor, its mounting, maintenance, accuracy, resolution and calibration status shall be consistent with the initial model definition.

Missing weather data

Missing or invalid data may be treated in one of the following ways according to *IEC 61724-1:2017*:

- The invalid or missing data may be replaced by values estimated from the valid data recorded before and/or after the invalid or missing data

- The invalid or missing data may be replaced with an average value for the analysed interval

Three scenarios may occur where no data is identified to replace missing weather data:

A. If the inverter was not functioning during that period, the expected energy for the period is modelled from the historical weather data and is aggregated with the expected energy for the times of unavailability.

B. If the inverter is functioning, then the expected energy is taken to equal the measured energy during that period.

C. If both the measured energy output and the weather data are missing, but the plant was known to be functioning during that period, the predicted energy (calculated from the model using the historical weather data) is used for both the expected and measured energy during that period.

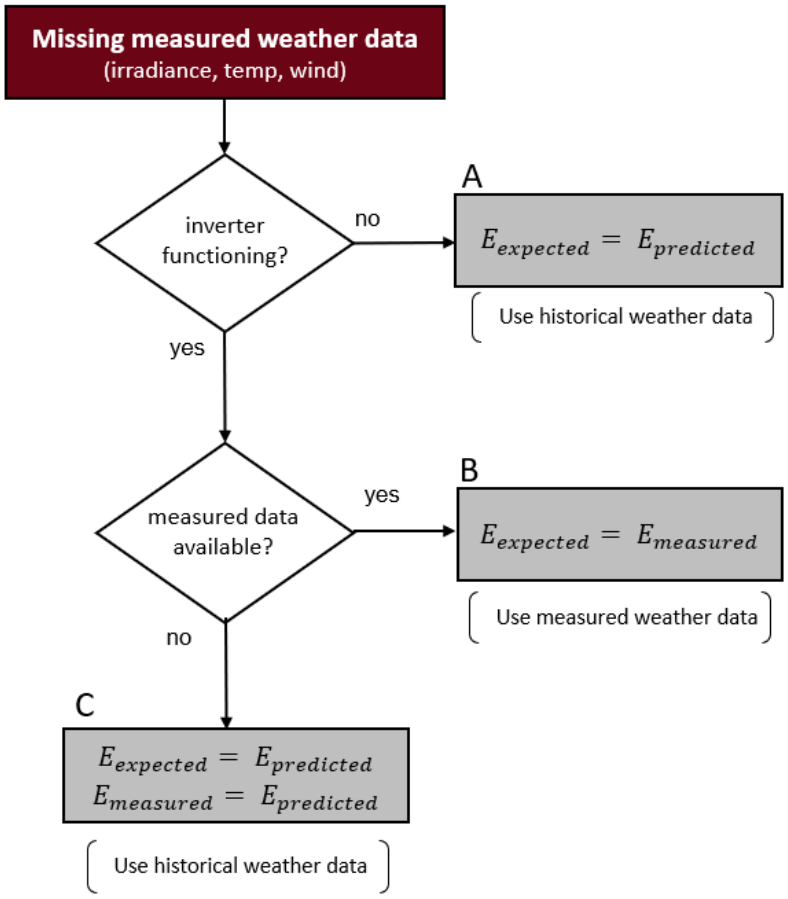

If the missing data affect more than a week of performance out of a year, the bias introduced by the above approach may become unacceptable and the parties to the test shall agree upon the best way to handle the missing data, including the possibility that the test may be considered invalid if too many data are missing.

Partially missing data or partial unavailability

When data is available for part of a period (e.g., if the model is using hourly averages and the data are available only for part of the hour) if < 10 % of the electricity or irradiance data are missing, the average of the available data for that time period may be used. For temperature and wind data, this requirement is < 20 % and < 50 %, respectively. When the fraction of missing data is small enough to use the data for that hour, the existing data are averaged for that hour. If the fraction of missing data exceeds these guidelines, the data should be treated as missing data. In any case, data for the same period are handled consistently between both the irradiance and PV performance data.

Specifically, if data is substituted because of anomalies associated with inverter start up or shut down, reliable data will be retained for the fraction of the hour when data are available in order to reflect the state of the system as accurately as possible during these hours because the energy generated during these hours typically differs significantly from the expected energy.

Table 52. **Missing data tolerances**

Parameter	Maximum missing data tolerable
Energy output	10 %
Irradiance	10 %
Temperature	20%
Wind	50%

7.7.2 Capacity evaluation method

Scope

This method (based on *IEC TS 61724-2*), measures power (not energy) at a specified set of reference conditions (which can differ from standard test conditions that have been designed to facilitate indoor measurements). It is a non-regression-based method for determining power output. It uses the design parameters of the plant to quantify a correction factor for comparing the plant's measured performance to the performance targeted under reference conditions. In other

words, the measured performance, adjusted by the correction factor, is then compared with the target plant performance to identify whether the plant operates above or below expectations at the target reference conditions.

This test procedure was designed with the primary goal of facilitating the documentation of a performance target, but it can also be used to verify a model, track performance (e.g., degradation) of a system over the course of multiple years, or to document system quality for any other purpose. The intent of this document is to specify a framework procedure for comparing the measured power produced against the expected power from a PV system on relatively sunny days.
In this procedure, actual photovoltaic system power produced is measured and compared to the power expected for the observed weather based on the design parameters of the system. The expected power under reference and measured conditions are typically derived from the design parameters that were used to derive the performance target for the plant as agreed to prior to the commencement of the test. For cases when a power model was not developed during the plant design, a simple model that increases transparency is presented in section 7.7.2.1 as a possible approach.

It is to be noted that when the output of a PV system exceeds the capability of the inverter, the output of the system is defined more by the inverter operation than by the PV modules. In this case, the measurement of the capacity of the plant to generate electricity is complicated by the need to differentiate situations in which the inverter is saturated (“constrained operation”) and when the output of the PV system reflects the module performance (“unconstrained operation”). For PV plants with high DC-to-AC power ratios, the operation of the plant can reflect the capability of the inverters for most of the day, with the capability of the DC array only being measurable for a short time in the morning and in the evening. In this case, it can be necessary to disconnect parts of the DC array to reduce the DC-to-AC power ratio during the measurement period.

Test duration

It is recommended that the test include data from at least two days if enough stable data are acquired. The test may be extended to seven or more days if desired to assess repeatability or if weather is volatile. The filtering criteria for selecting relatively stable times are described later in this section. The test may be completed at any time of year, though the deviation from reference conditions and the effects of variable angle of incidence should be minimized.

Terms and definitions

Constrained operation: condition when all inverters are limited by their capability (also referred to as inverter saturation) rather than by the output from the PV array, as it is observed for a system with high DC rating relative to the AC rating and when the irradiance is high.

Curtailed operation: when the output of the inverter(s) is limited due to external reasons such as inability of the local grid to receive the power or contractual agreement.

Unconstrained operation: outputs of all inverters freely following the DC array's capability to respond to the solar insolation rather than being limited by the capability of the inverters or curtailing influences.

Expected power: power of a PV system that is expected for actual weather data collected at the site during operation of the system based on the design parameters of the system

Target reference conditions (TRC): reference conditions at which the expected power is the target power, which include irradiance, ambient temperature, wind, and any other parameter used to define the target performance.

Procedure

In the following table and flow diagram, a step-by-step description of the procedure is provided.

Step		Description
1	Definition of the performance target under "unconstrained" and "constrained" operation	The targeted system output is defined for unconstrained operation under the TRC and by a model that defines how the power varies with irradiance, temperature, and wind using the design parameters of the plant. The performance target under constrained operation is typically defined by the capability of the inverter.
Definition of the target reference conditions (TRC) for "unconstrained" operation		TRC should be chosen to result in unconstrained operation (i.e. within the inverter's capability). Preferably, they should be chosen to reflect an ambient temperature and wind speed that are frequently observed at the site and the highest irradiance that is unlikely to cause constrained operation for the lowest temperature expected. The optimal choice of TRC may depend on the weather during the test.
Definition of the temperature dependence of the plant output under "unconstrained" operation		If a temperature model has not been defined, a possible model is provided in *section 7.8.1*. It is preferable to use a temperature model based on ambient temperature and wind speed rather than measuring the back-of-module temperature because the assessment then includes some aspects of the module mounting that could cause the modules to run hot and because it avoids the challenges of characterizing the module temperature, which may be highly variable across the field.
2	Collect measurement data	The power output, irradiance, temperature, wind speed, state of cleanliness of both the sensors and PV systems are collected over several days.
3	Data checks for each data stream	Each data stream shall be checked for data out of range or unreasonable trends. Then it shall be checked whether the number of valid data points is enough for a reasonable uncertainty value of the test.
4	Calculation of correction factor	The correction factor is calculated to adjust the measured power to the conditions used for the performance target.
5	Comparison of measured power with the performance target	Finally, the average measured corrected power and performance target are compared either as a simple difference, percent difference, or ratio calculation.
6	Uncertainty analysis	As part of the performance target or test plan, the agreement shall state how the uncertainty of the measurement is considered. Thus, it can be essential to quantify the uncertainty of the measurement as part of determining whether the measured performance meets expectations. Regardless of whether the uncertainty is used as part of determining the test result, uncertainty analysis should be part of the assessment.

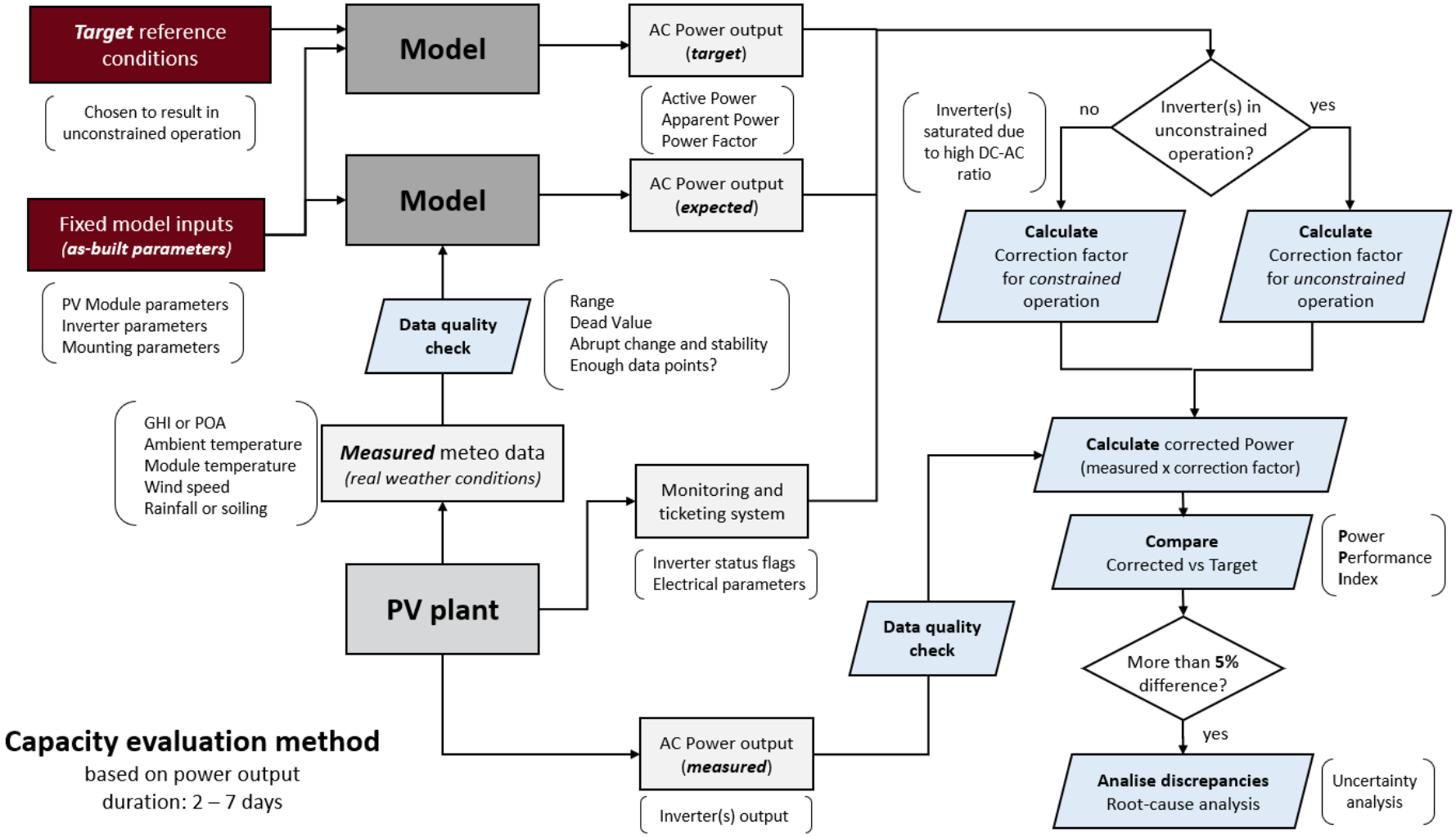

Figure 80. Capacity Evaluation Method – procedure flow diagram. Source: own design

Data checks for each data stream

A recommendation for application of this procedure for this application is given in more detail in *Table 53* . Depending on the local conditions, the details of the plant design, the addition of other data streams and the frequency of data collection, the filtering criteria may be modified, but all four types of filters (range, dead value, abrupt change/stability and inverter status) shall be applied and documented as part of the final report.

Table 53. Capacity method: data validation and filtering criteria. Source: *IEC TS 61724-2:2016*

		Suggested criteria for flagging rejected data (15-min data)			
Flag type	**Description**	**Irradiance** (W/m^2)	**Ambient temperature** (°C)	**Wind speed** (m/s)	**Power (AC power rating)**
Range	Value outside of acceptable bounds	< 0,5·TRC irradiance or > 1,2·TRC [b]	> 50 or < −10 [a]	>15 or < 0,5	> 1,02·rating or < −0,01·rating
Dead value	Values stuck at a single value over time. Detected using derivative.	Derivative < 0,000 1 while value is > 5	< 0,000 1 and > −0,000 1	< sensitivity of sensor	< 0,1 % change in 3 readings
Abrupt change and stability	Values change unacceptably between data points. Detected using derivative for temperature and wind speed.	Assuming 15 min data derived from at least 1 min data, standard deviation > 5 % of average	> 4	> 10	Assuming 15 min data derived from at least 1 min data, standard deviation > 5 % of average
Inverter status	The states of the inverters are inconsistent (not all are constrained – see text)	Not applicable	Not applicable	Not applicable	Not applicable

NOTE 1 The irradiance filtering may be adjusted to align with the range of linear system performance with irradiance. Flagged data are considered for exclusion and documented in the test report regarding the rationale for exclusion.

NOTE 2 Potential-induced degradation (PID) effects may start to reduce the power output at low irradiance conditions remarkably, without a measurable effect at high irradiance. Early detection of evidence of PID is outside the scope of this test.

[a] May be adjusted depending on the season of data acquisition.

[b] The maximum irradiance included in the analysis may be adjusted to account for the possibility of cloud edge effects, whereby light is scattered by a nearby cloud and can cause irradiance readings up to approximately 1 500 W/m^2. For most systems, these conditions will cause saturation of the inverter, and will typically be excluded from the evaluated data by the stability filter.

The inverter's self-reported output power or inverter's self-reported status flags are used to identify when the inverter operation is constrained. If the status flags are not available, the data may be screened for reporting values near the maximum capability of the inverter. Records are categorized according to whether:

a) zero inverters are constrained: data records can be treated as unconstrained
b) all inverters are constrained: data records can be treated as constrained

c) some, but not all, are constrained: data records cannot be used for evaluating system performance

The stability filter recommended here calculates the average of at least 15 data points (measured at least every minute during 15 min) and confirms that the standard deviation for those data points is less than 5 % of the average of the same data points. Applying the stability filter to both the irradiance and power data is recommended.

The number of data points identified as meeting the criteria in *Table 53* will affect the uncertainty of the test. As a guide to determining an adequate, yet reasonable, number of data points, the following table may be used:

a

Table 54. Example guide for seasonal minimum stable irradiance requirements for flat-plate application. Source: *IEC TS 61724-2:2016*

Season (northern hemisphere)	Dates	Minimum POA irradiance (W/m^2)	Required number of 15-min average data points
Winter	22/11 to 21/1	450	20
Spring	22/1 to 23/3	550	30
Summer	24/3 to 21/9	650	60
Autumn	22/9 to 22/11	550	40

The larger number of data points during the summer reflects the ease of collecting more data on longer days and is expected to result in a higher accuracy measurement, depending on the local weather. Locations that seldom experience clear, sunny days may require longer data collection times or reduction of the targeted number of data points, resulting in higher test uncertainty. For CPV applications, *Table 54* is not directly relevant. For CPV, after filtering for stable conditions, the data collected should include at least 30 data points (assuming 15 min averages) or at least 7.5 h of filtered data if averages for a different time period are used.

Calculation of the correction factor

The correction factor is calculated to adjust the measured power to the conditions used for the performance target in four steps:

a) Calculation of correction factor for each data point

Input measured meteorological data into the system's model and calculate the correction factor needed to translate the measured data to the temperature, wind and irradiance conditions specified by the TRC for all points measured during "unconstrained" stable operation.

Calculate the correction factor for each point using the power model:

$$C_{factor} = \frac{P_{target}}{P_{expected}}$$

C_{factor}	is the correction factor
P_{target}	is the model's output power at the target reference conditions (TRC)
$P_{expected}$	is the model's output power at the measured conditions

The correction factor could be corrected for the operating temperature as follows:

$$C'_{factor} = 1 + \gamma(T_{cell} - T_{TRC})$$

C'_{factor}	is the operating temperature cell correction factor
γ	is the temperature coefficient for power (taken from the module's datasheet)
T_{cell}	is the calculated cell temperature as described in *section 7.8.1*
T_{TRC}	is the cell temperature associated with the Target Reference Conditions (TRC)

b) Correct measured power output for all points measured

Correct the measured power by the correction factor for all points measured during "unconstrained" stable operation:

$$P_{corr} = P_{measured} \cdot C_{factor}$$

c) Average all values of corrected power

Taking care to consider only the data that were included after data filtering, average all corrected power output values taken under "unconstrained" operating conditions, and separately average all power values measured during constrained operation.

$$P_{corr_{avg}} = \frac{1}{n}\sum_{i=1}^{n} P_{corr_i}$$

d) Analyse discrepancies

If an individual corrected power deviates from the average by more than 5 %, then a root-cause diagnosis should be completed for the data point to see if any outlier situation was in effect and not caught by the data filtering

Comparison of measured power with the performance target

The average measured corrected power and performance target can be compared either as a simple difference, percent difference, or ratio calculation:

Difference calculation [kW]:

$$\Delta_{power} = P_{corr} - P_{target}$$

Percent difference calculation [%]:

$$\Delta_{power} = \frac{P_{corr} - P_{target}}{P_{target}} \times 100$$

Ratio (power performance index) [%]:

$$PPI = \frac{measured\ output}{expected\ \ output} \times 100 = \frac{P_{corr}}{P_{target}} \times 100$$

Uncertainty analysis

The uncertainty is determined for P_{corr}, not for the performance target. Uncertainties associated with the model are neglected. However, uncertainties associated with the measured weather data will introduce uncertainty in P_{corr}.

Both systematic (bias) and random (precision) uncertainties should be included in the analysis. The contributions to the uncertainty depend on the model that is used, but generally include uncertainty in the measurements of the irradiance, temperature, wind speed, and electricity generated as well as uncertainties in corrections of these.

All measurements and associated uncertainties are tabulated and combined using standard propagation of errors as described in:

- ASME Performance Test Code 19.1
- ISO 5725
- ISO/IEC Guide 98-1

The uncertainties associated with each sensor are taken from the manufacturer's specification and/or from the calibration report provided by the calibration laboratory. The uncertainty analysis should also include systematic errors that may arise from misplacement or inappropriate installation of the sensors including:

- Irradiance sensor placement (tilt, azimuth, and height)
- Positioning of temperature sensors relative to power model
- Positioning of wind sensor relative to power model
- Soiling that has not been addressed

- Spatial variation when a subset of point measurements may not capture the true array bulk values (e.g. wind speed).

Data acquisition device uncertainties should also be considered.

7.7.2.1 Simple model for system power

The model for the electrical power output of a system can be fairly simple or complex. A simple example is given here:

Table 55. **Model for system power.** Source: IEC TS 61724-12:2016

System power model			
Symbol	Units	Description	Source
P_{pred}	W	Predicted power	Calculated
P_{target}	W	Predicted power at targeted conditions	Calculated
G_i	W/m²	POA irradiance	Measured
G_{TRC}	W/m²	Rating irradiance used to specify the target power	Defined by user
P_{zero}	W	(negative) intercept often observed when plotting the output power as a function of irradiance when inverters require a minimum power input to function.	Calculated
P'_{pred}	W	Temperature-corrected predicted power	Calculated
γ	%/°C	Power temperature coefficient of the module	Module's datasheet
T_{cell}	°C	Cell temperature calculated for each measurement point	Calculated (see section 7.8.1)
T_{TRC}	°C	Cell temperature calculated by the thermal model at the Target Reference Conditions (TRC) conditions	Calculated (see section 7.8.1)

As an example of implementation of a linear assumption, the plant power can be defined as follows:

$$P_{pred} = P_{target}\left(\frac{G_i}{G_{TRC}}\right) + P_{zero}\left(1 - \frac{G_i}{G_{TRC}}\right)$$

Adding a temperature correction and neglecting the P_{zero} term, results in the following relationship to predict power from measured irradiance and cell temperatures:

$$P'_{pred} = P_{target}\left(\frac{G_i}{G_{TRC}}\right)\left[1 + \left(\frac{\gamma}{100}\right)(T_{cell} - T_{TRC})\right]$$

7.8 Complementary calculations

7.8.1 Module and cell temperature calculations

Generally, there are two parts to defining the temperature dependence of the power output of a PV system:

1) relating the weather conditions to the module temperature and
2) the power output as a function of module temperature

The module temperature can be measured directly using a sensor on the back of the module as described in IEC 61829 or in Annex B of IEC 61724-1:2016, or an infrared camera that has been carefully calibrated for the emissivity of the module, but the module temperature reflects both the weather conditions and the quality of the installation or design, since improper installation of modules or a poor mounting design may cause modules to operate at elevated temperatures when compared to design expectations. To include module operating temperature within the test, the ambient temperature and wind speed may be used to calculate an expected average module temperature.

7.8.1.1 Heat transfer model to calculate expected cell operating temperature

This section presents a heat transfer model that has demonstrated good results. However, other models exist, and practitioners should choose the model that best fits their situation. Of great importance is using identical heat transfer models for setting the capacity performance target as well as the target reference conditions.

Table 56. **Model for module temperature**

Thermal model for module and cell temperature			
Symbol	Units	Description	Source
T_{mod}	°C	Module temperature (at the back surface)	Calculated
G_i	W/m^2	POA irradiance	Measured
T_{amb}	°C	Ambient temperature	Measured
WS	m/s	Wind speed corrected to a 10 m height or to the height that is relevant to the power model	Calculated
a	--	Module glazing coefficient	Defined empirically (see Table A.1)
b	--	Forced convection glazing coefficient	Defined empirically (see Table A.1)
WS_{meas}	m/s	Wind speed	Measured

h_{ref}	m	height used by performance model (for this model 10 m)	Defined by user
h_{meas}	m	height of the anemometer	Site characteristic
α	--	Resistance coefficient for ground cover or the Hellmann exponent	Defined empirically (see Table A.2)
T_{cell}	°C	Cell temperature	Calculated
dT_{cond}	°C	Conduction temperature coefficient to determine the difference between module surface and cell centre	Defined empirically (see Table A.1)

The module temperature (at the back surface) can be calculated as follows:

$$\boldsymbol{T_{mod} = G_i \cdot e^{(a+b \cdot WS)} + T_{amb}}$$

If the measured and reference heights are different, the wind speed needs to be corrected as follows:

$$WS = WS_{meas} \cdot \frac{h_{ref}}{h_{meas}} \cdot \alpha$$

The temperature difference (T_{mod} - T_{amb}) is largely independent of the ambient temperature and is essentially linearly proportional to the irradiance at levels above 400 W/m^2.

The cell temperature can be calculated as follows:

$$\boldsymbol{T_{cell} = T_{mod} + \frac{G_i}{1000} \cdot dT_{cond}}$$

and therefore, the conductive temperature drop between the module's back surface and the PV cells can be determined.

It is also possible to use IEC 60904-5 to determine the junction temperature (*see 7.8.1*), but this is usually difficult when evaluating the performance of a continuously operating system because IEC 60904-5 uses the measured open circuit voltage. It should be noted that junction temperature calculated from measured open circuit voltage will reflect the rapid fluctuation of the cell temperature during rapid changes of irradiance due to high wind and cloud speed in the sky that is not in accordance with the directly measured temperature of the rear surface. Therefore, the electrical output power evaluation of the system should be performed when the irradiation is stable as required by the filtering described in *Table 53.*

Table 57. **Empirical coefficients for module temperature modelling**. Source: IEC TS 61724-2:2016

Table A.1 – Empirically determined coefficients used to predict module temperature

Module type	Mount	a	b (s/m)	dT_{cond} (°C)
Glass/cell/glass	Open rack	−3,47	−0,0594	3
Glass/cell/glass	Close roof mount	−2,98	−0,0471	1
Glass/cell/polymer sheet	Open rack	−3,56	−0,0750	3
Glass/cell/polymer sheet	Insulated back	−2,81	−0,0455	0
Polymer/thin-film/steel	Open rack	−3,58	−0,113	3
22× linear concentrator	Tracker	−3,23	−0,130	13
NOTE Wind speed was measured at the standard meteorological height of 10 m.				

Table A.2 – Hellmann coefficient, α, for correction of wind speed according to measured height, if values in Table A.1 are used

Location or situation	α
Unstable air above flat open coast	0,11
Neutral air above flat open coast	0,16
Unstable air above human inhabited areas	0,27
Neutral air above human inhabited areas	0,34
Stable air above flat open coast	0,40
Stable air above human inhabited areas	0,60

7.8.1.2 Equivalent Cell Temperature (ECT)

Here is described the preferred method (IEC 60904-5:2011) for determining the equivalent cell temperature (ECT) of PV devices (cells, modules and arrays of one type of module), for the purposes of comparing their thermal characteristics, determining NOCT (nominal operating cell temperature) and translating measured I-V characteristics to other temperatures.

When temperature sensors, such as thermocouples, are used to determine the cell temperature of PV devices under natural or simulated steady-state irradiance, some problems arise:

a) A considerable spread of temperature can be observed over the area of the module.
b) As the solar cells are usually not accessible, sensors are attached to the back of the module and the measured temperature thus is influenced by the thermal conductivity of the encapsulant and back materials.

c) Problems when determining the equivalent cell temperature for on-site measurements of array performance where all cells have slightly different temperatures and one cannot easily determine the average cell temperature.

The equivalent cell temperature (ECT) is the average temperature at the electronic junctions of the device (cells, modules, arrays of one type of module) which equates to the current operating temperature if the entire device were operating uniformly at this junction temperature.

In summary, ECT can be used for:

- Calculating PV module temperature (T_{mod})
- Comparing the thermal characteristics of different PV modules
- Determining NOCT (nominal operating cell temperature)
- Translating measured I-V characteristics to other temperatures

Measurement devices required

- Reference PV module
- IV-curve tracer
- Thermometer

Measurement procedure

This method is based on the fact that the open-circuit voltage (V_{OC}) of a solar cell changes with temperature in a predictable fashion. If the V_{OC} of the device at standard test conditions (STC) is known, together with its temperature coefficient (β), the equivalent temperature of all the cells in the device can be determined.

> NOTE: The V_{OC} is also slightly affected by the irradiance, so an additional correction may be required as outlined in IEC 60891. Experience shows that the equivalent cell temperature can be determined more precisely by the method described here than by any alternative technique. However, as the temperature coefficient β drops rapidly at irradiances below **200 W/m²**, this method should only be used at irradiances above this threshold.

a) Take simultaneous readings of the open-circuit voltage V_{OC2}, short-circuit current I_{SC2} and the incident irradiance G_2.
b) Carry out a correction of V_{OC2} to an irradiance equal to G_1.
c) Calculate the ECT as described in *Table 58*.

Table 58. **Calculation of the Equivalent Cell Temperature**

Equivalent Cell Temperature			**Symbol**	**Units**
			ECT	**°C**
Symbol	Units	Description		Source
β	%/°C	Temperature coefficient of the open-circuit voltage		Measured / Datasheet
G_1, T_1	W/m², °C	Irradiance and module temperature of reference condition 1		Measured / Datasheet
G_2, T_2	W/m², °C	Irradiance and module temperature of reference condition 2		Measured
V_{OC1}	V	Open-circuit voltage at a reference condition 1 (G_1, T_1)		Measured / Datasheet
V_{OC2}	V	Open-circuit voltage at a reference condition 2 (G_2, T_2)		Measured
I_{SC2}	A	Short-circuit current at a reference condition 2 (G_2, T_2)		Measured
V_{STC}	V	Open-circuit voltage at STC (G_{STC}=1000 W/m², T_{STC}=25°C)		Datasheet
I_{STC}	A	Short-circuit current at STC (G_{STC}=1000 W/m², T_{STC}=25°C)		Datasheet
a	--	Irradiance correction factor for open circuit voltage which is linked with the diode thermal voltage D of the pn junction and the number of cells *ns* serially connected in the module D as defined in IEC 60891. A typical value is 0.06		IEC 60891:2010

General formula:

$$ETC = T_1 + \frac{1}{\beta}\left[\frac{V_{OC2}}{V_{OC1}} - 1 - a\ ln\left(\frac{G_2}{G_1}\right)\right]$$

Variation 1

If the STC values are used as reference condition (G_{STC}=1000 W/m², T_{STC}=25°C) and considering a = 0.06, then

$$ETC = 25°C + \frac{1}{\beta}\left[\frac{V_{OC2}}{V_{STC}} - 1 - 0.06\ ln\left(\frac{G_2}{1000\frac{W}{m^2}}\right)\right]$$

Variation 2

Instead of the irradiances G_1 and G_2, one can also use the ratio of short-circuit currents, which then is called self-reference. This requires short circuit current to be linear according to IEC 60904-10. This simplifies the measurements to be taken significantly as one essentially eliminates the requirement for measuring the irradiance and the dependence on the spectrally matched devices.

$$ETC = 25°C + \frac{1}{\beta}\left[\frac{V_{OC2}}{V_{STC}} - 1 - 0.06\ ln\left(\frac{I_{SC2}}{I_{STC}}\right)\right]$$

8 Annex B: Hyperparameters tuning

8.1 Models applied on the full dataset

Model	Hyperparameters tested	Values	Best combination
Linear Regression	-	-	-
Polynomial Regression – Degree 2	-	-	-
Stochastic Gradient Descent Regressor	'penalty'	'l1', 'l2', 'elasticnet', 'none'	'l1'
	'alpha'	0.01, 1, 5, 100	1
	'l1_ratio'	0.01, 0.15, 0.5, 0.9	0.5
Linear Support Vector Regression	'C'	0.9, 1, 10	10
	'fit_intercept'	True, False	True
	'intercept_scaling'	1, 5, 10	10
Decision Tree Regressor	'min_samples_split'	2, 5, 6, 7, 10	5
	'min_samples_leaf'	5, 7, 8, 10, 20	10
	'max_depth'	20, 50, 70, 75, 100	50
	'max_features'	'auto', 'sqrt', 'log2', 0.5, 0.9	'auto'
Random Forest Regressor	'n_estimators'	100, 150, 175, 200, 300	200
	'max_features'	'auto', 'sqrt', 0.9	0.9
	'max_depth'	20, 50, 100	50
Bagging Regressor	'n_estimators'	100, 300, 500, 1000	1000
	'max_samples'	0.25, 0.5, 0.7, 0.9, 1	0.9
	'max_features'	0.25, 0.5, 0.7, 0.9, 1	0.9
Gradient Boosting Regressor	'max_depth'	10, 20, 100	10
	'n_estimators'	10, 70, 100, 200	100
	'learning_rate'	0.1, 0.2, 1.0	0.1

Table 8.1. **Hyperparameters tuning**: synthetic distribution “A” – performance metric: MAE

Model	Hyperparameters tested	Values	Best combination
Linear Regression	-	-	-
Polynomial Regression – Degree 2	-	-	-
Stochastic Gradient Descent Regressor	'penalty'	'l1', 'l2', 'elasticnet', 'none'	'l1'
	'alpha'	0.01, 1, 5, 100	1
	'l1_ratio'	0.01, 0.15, 0.5, 0.9	0.5
Linear Support Vector Regression	'C'	0.9, 0.95, 1, 10	10
	'fit_intercept'	True, False	True
	'intercept_scaling'	1, 10, 50	50
Decision Tree Regressor	'min_samples_split'	2, 5, 6, 7, 10	5
	'min_samples_leaf'	5, 7, 8, 10, 20	10
	'max_depth'	20, 50, 70, 75, 100	50
	'max_features'	'auto', 'sqrt', 'log2', 0.5, 0.9	'auto'
Random Forest Regressor	'n_estimators'	100, 150, 175, 200, 300	150
	'max_features'	'auto', 'sqrt', 0.9	0.9
	'max_depth'	20, 50, 100	20
Bagging Regressor	'n_estimators'	100, 300, 500, 1000	300
	'max_samples'	0.25, 0.5, 0.7, 0.9, 1	0.7
	'max_features'	0.25, 0.5, 0.7, 0.9, 1	0.7
Gradient Boosting Regressor	'max_depth'	10, 20, 100	10
	'n_estimators'	10, 70, 100, 200	100
	'learning_rate'	0.1, 0.2, 1.0	0.1

Table 8.2. **Hyperparameters tuning**: synthetic distribution “A” – performance metric: RMSE

Model	Hyperparameters tested	Values	Best combination
Linear Regression	-	-	-
Polynomial Regression – Degree 2	-	-	-
Stochastic Gradient Descent Regressor	'penalty'	'l1', 'l2', 'elasticnet', 'none'	'elasticnet'
	'alpha'	0.01, 1, 5, 100	0.01
	'l1_ratio'	0.01, 0.15, 0.5, 0.9	0.9
Linear Support Vector Regression	'C'	0.9, 0.95, 1, 10	10
	'fit_intercept'	True, False	True
	'intercept_scaling'	1, 10, 50	50
Decision Tree Regressor	'min_samples_split'	2, 5, 6, 7, 10	5
	'min_samples_leaf'	5, 7, 8, 10, 20	10
	'max_depth'	20, 50, 70, 75, 100	50
	'max_features'	'auto', 'sqrt', 'log2', 0.5, 0.9	'auto'
Random Forest Regressor	'n_estimators'	100, 150, 175, 200, 300	200
	'max_features'	'auto', 'sqrt', 0.9	0.9
	'max_depth'	20, 50, 100	50
Bagging Regressor	'n_estimators'	100, 300, 500, 1000	300
	'max_samples'	0.25, 0.5, 0.7, 0.9, 1	0.7
	'max_features'	0.25, 0.5, 0.7, 0.9, 1	0.7
Gradient Boosting Regressor	'max_depth'	10, 20, 100	10
	'n_estimators'	10, 70, 100, 200	100
	'learning_rate'	0.1, 0.2, 1.0	0.1

Table 8.3. **Hyperparameters tuning**: synthetic distribution “B” – performance metric: MAE

Model	Hyperparameters tested	Values	Best combination
Linear Regression	-	-	-
Polynomial Regression – Degree 2	-	-	-
Stochastic Gradient Descent Regressor	'penalty'	'l1', 'l2', 'elasticnet', 'none'	'l1'
	'alpha'	0.01, 1, 5, 100	1
	'l1_ratio'	0.01, 0.15, 0.5, 0.9	0.5
Linear Support Vector Regression	'C'	0.9, 0.95, 1, 10	10
	'fit_intercept'	True, False	True
	'intercept_scaling'	1, 10, 50	50
Decision Tree Regressor	'min_samples_split'	2, 5, 6, 7, 10	5
	'min_samples_leaf'	5, 7, 8, 10, 20	10
	'max_depth'	20, 50, 70, 75, 100	50
	'max_features'	'auto', 'sqrt', 'log2', 0.5, 0.9	'auto'
Random Forest Regressor	'n_estimators'	100, 150, 175, 200, 300	175
	'max_features'	'auto', 'sqrt', 0.9	0.9
	'max_depth'	20, 50, 100	50
Bagging Regressor	'n_estimators'	100, 300, 500, 1000	300
	'max_samples'	0.25, 0.5, 0.7, 0.9, 1	0.7
	'max_features'	0.25, 0.5, 0.7, 0.9, 1	0.7
Gradient Boosting Regressor	'max_depth'	10, 20, 100	10
	'n_estimators'	10, 70, 100, 200	100
	'learning_rate'	0.1, 0.2, 1.0	0.1

Table 8.4. **Hyperparameters tuning:** synthetic distribution “B” – performance metric: RMSE

8.2 Models applied on the dataset pre-processed through PCA

Model	Hyperparameters tested	Values	Best combination
Linear Regression	-	-	-
Polynomial Regression – Degree 2	-	-	-
Stochastic Gradient Descent Regressor	'penalty'	'l1', 'l2', 'elasticnet', 'none'	'l1'
	'alpha'	0.01, 0.1, 1, 5, 100	1
	'l1_ratio'	0.01, 0.15, 0.5, 0.9	0.01
Linear Support Vector Regression	'C'	0.5, 0.9, 1, 10	1
	'fit_intercept'	True, False	True
	'intercept_scaling'	1, 5, 8, 10	1
Decision Tree Regressor	'min_samples_split'	2, 5, 6, 7, 10	2
	'min_samples_leaf'	5, 7, 8, 10, 20, 40	40
	'max_depth'	20, 50, 70, 75, 100	20
	'max_features'	'auto', 'sqrt', 'log2', 0.5, 0.9	'auto'
Random Forest Regressor	'n_estimators'	100, 200, 300, 400	400
	'max_features'	'auto', 'sqrt', 0.5, 0.9	0.5
	'max_depth'	20, 50, 100	50
Bagging Regressor	'n_estimators'	90, 100, 300, 500	300
	'max_samples'	0.25, 0.5, 0.85, 1	0.85
	'max_features'	0.25, 0.5, 0.85, 1	0.85
Gradient Boosting Regressor	'max_depth'	10, 50, 100	10
	'n_estimators'	10, 70, 100, 200	100
	'learning_rate'	0.1, 0.5, 1.0	0.1

Table 8.5. **Hyperparameters tuning**: synthetic distribution “A” – performance metric: MAE

Model	Hyperparameters tested	Values	Best combination
Linear Regression	-	-	-
Polynomial Regression – Degree 2	-	-	-
Stochastic Gradient Descent Regressor	'penalty'	'l1', 'l2', 'elasticnet', 'none'	'l1'
	'alpha'	0.01, 0.1, 1, 5, 100	0.01
	'l1_ratio'	0.01, 0.15, 0.5, 0.9	0.15
Linear Support Vector Regression	'C'	0.5, 0.8, 0.9, 1	0.9
	'fit_intercept'	True, False	True
	'intercept_scaling'	1, 8, 10, 50	10
Decision Tree Regressor	'min_samples_split'	2, 5, 6, 7, 10	2
	'min_samples_leaf'	5, 7, 8, 10, 20, 40	40
	'max_depth'	20, 50, 70, 75, 100	20
	'max_features'	'auto', 'sqrt', 'log2', 0.5, 0.9	'auto'
Random Forest Regressor	'n_estimators'	100, 200, 300, 400	400
	'max_features'	'auto', 'sqrt', 0.5, 0.9	0.5
	'max_depth'	20, 50, 100	50
Bagging Regressor	'n_estimators'	90, 100, 300, 500	90
	'max_samples'	0.25, 0.5, 0.85, 1	0.85
	'max_features'	0.25, 0.5, 0.85, 1	0.85
Gradient Boosting Regressor	'max_depth'	10, 50, 100	10
	'n_estimators'	10, 70, 100, 200	100
	'learning_rate'	0.1, 0.5, 1.0	0.1

Table 8.6. **Hyperparameters tuning**: synthetic distribution “A” – performance metric: RMSE

Model	Hyperparameters tested	Values	Best combination
Linear Regression	-	-	-
Polynomial Regression – Degree 2	-	-	-
Stochastic Gradient Descent Regressor	'penalty'	'l1', 'l2', 'elasticnet', 'none'	'l1'
	'alpha'	0.01, 0.1, 1, 5, 100	0.01
	'l1_ratio'	0.01, 0.15, 0.5, 0.9	0.15
Linear Support Vector Regression	'C'	0.5, 0.8, 0.9, 1	0.8
	'fit_intercept'	True, False	True
	'intercept_scaling'	1, 8, 10, 50	50
Decision Tree Regressor	'min_samples_split'	2, 5, 6, 7, 10	2
	'min_samples_leaf'	5, 7, 8, 10, 20, 40	40
	'max_depth'	20, 50, 70, 75, 100	20
	'max_features'	'auto', 'sqrt', 'log2', 0.5, 0.9	'auto'
Random Forest Regressor	'n_estimators'	100, 200, 300, 400	400
	'max_features'	'auto', 'sqrt', 0.5, 0.9	0.5
	'max_depth'	20, 50, 100	50
Bagging Regressor	'n_estimators'	90, 100, 300, 500	300
	'max_samples'	0.25, 0.5, 0.85, 1	0.85
	'max_features'	0.25, 0.5, 0.85, 1	0.85
Gradient Boosting Regressor	'max_depth'	10, 50, 100	10
	'n_estimators'	10, 70, 100, 200	70
	'learning_rate'	0.1, 0.5, 1.0	0.1

Table 8.7. **Hyperparameters tuning**: synthetic distribution “B” – performance metric: MAE

Model	Hyperparameters tested	Values	Best combination
Linear Regression	-	-	-
Polynomial Regression – Degree 2	-	-	-
Stochastic Gradient Descent Regressor	'penalty'	'l1', 'l2', 'elasticnet', 'none'	'l1'
	'alpha'	0.01, 1, 5, 100	0.01
	'l1_ratio'	0.01, 0.15, 0.5, 0.9	0.15
Linear Support Vector Regression	'C'	0.9, 0.95, 1, 10	0.9
	'fit_intercept'	True, False	True
	'intercept_scaling'	1, 10, 50	10
Decision Tree Regressor	'min_samples_split'	2, 5, 6, 7, 10	2
	'min_samples_leaf'	5, 7, 8, 10, 20, 40	40
	'max_depth'	20, 50, 70, 75, 100	20
	'max_features'	'auto', 'sqrt', 'log2', 0.5, 0.9	'auto'
Random Forest Regressor	'n_estimators'	100, 150, 175, 200, 300, 400	400
	'max_features'	'auto', 'sqrt', 0.9	'sqrt'
	'max_depth'	20, 50, 100	50
Bagging Regressor	'n_estimators'	90, 100, 300, 500	300
	'max_samples'	0.25, 0.5, 0.85, 1	0.85
	'max_features'	0.25, 0.5, 0.85, 1	0.85
Gradient Boosting Regressor	'max_depth'	10, 50, 100	10
	'n_estimators'	10, 70, 100, 200	70
	'learning_rate'	0.1, 0.5, 1.0	0.1

Table 8.8. **Hyperparameters tuning**: synthetic distribution “B” – performance metric: RMSE

9 References

[1] United Nations Framework Convention on Climate Change, *Paris Agreement - status of ratification,* 2016.

[2] A. Jäger-Waldau, *PV Status Report 2019,* Luxembourg: Publications Office of the European Union, 2019.

[3] International Energy Agency (IEA), *World Energy Outlook 2020*, www.iea.org

[4] International Energy Agency (IEA), Photovoltaic Power Systems Programme, *Trends in Photovoltaic Applications 2020*

[5] SolarPower Europe, *Global Market Outlook for Solar Power 2021-2025, July* 2021.

[6] G. Oviedo Hernandez, S. Lindig, D. Moser and P.V. Chiantore, *Optimization of the Cost Priority Number (CPN) Methodology to the Needs of a Large O&M Operator*, 36th European Photovoltaic Solar Energy Conference and Exhibition (2019) 1613 – 1617

[7] D. Moser, M. Del Buono, M. Jahn, M. Herz, M. Richter and K. De Brabandere, I*dentification of Technical Risks in the PV Value Chain and Quantification of the Economic Impact on the Business Model,* Progress in Photovoltaics: Research and Applications, vol. 25, no. 7, pp. 592-604, 2017.

[8] Solar Bankability project, www.solarbankability.org

[9] SolarPower Europe, *EU Market Outlook for Solar Power 2020-2024, December* 2020.

[10] SolarPower Europe, O*peration & Maintenance Best Practices Guidelines v4.0*, , December 2019

[11] International Electrotechnical Commission, *IEC 61724-1:2017 Photovoltaic system performance - Part 1: Monitoring*

[12] M. Kanellos and S. Hanawalt, "*Solar's hidden secret: the data*," 27 November 2019. [Online]. Available: https://www.renewableenergyworld.com/2019/11/27/solars-hidden-secret-the-data/. [Accessed August 2021].

[13] A. Géron, *Hands-On Machine Learning with Scikit-Learn, Keras, and TensorFlow*, O'Reilly Media, Inc., 2019.

[14] William F. Holmgren, Clifford W. Hansen, and Mark A. Mikofski. "pvlib python: a python package for modeling solar energy systems." Journal of Open Source Software, 3(29), 884, (2018). https://doi.org/10.21105/joss.00884

[15] E. Capra, *Consistent data quality control and Machine Learning imputation techniques for Irradiance measurements and Performance KPIs of Photovoltaic plants*, Master in Big Data in Business, Università degli Studi di Roma "Tor Vergata", January 2020.

[16] A. Driesse and J. Stein, *In pursuit of accurate irradiance measurements Part 2: Sensors and beyond*, vol. X, 2017

[17] Kipp & Zonen, *Instruction manual - Pyranometers - CMP series*, 2016.

[18] World Meteorological Organization, *Guide to meteorological instruments and methods of observation*, 2018.

[19] M. Richter, K. De Brabandere, J. Kalisch, T. Schmidt, Lorenz and E., *Best Practice Guide on Uncertainty in PV Modelling*, 2015.

[20] Eppley, *Global Precision Pyranometer Datasheet*

[21] Kipp & Zonen, 6 *Key Influences that determine PV Performance Ratios* (White Paper)

[22] A. Woyte, K. De Brabandere, B. Sarr and M. Richter, *The Quality of Satellite-Based Irradiation Data for Operations and Asset Management*, Munich, 2016, p. 1470–1474.

[23] Copernicus Climate Change Service, Copernicus Climate Change Service (C3S) (2019*): C3S ERA5-Land reanalysis*, 2019.

[24] Copernicus Climate Change Service Climate Data Store (CDS), Copernicus Climate Change Service (C3S) (2017): ERA5: *Fifth generation of ECMWF atmospheric reanalyses of the global climate*, 2017.

[25] H. Hersbach and D. Dee, *ERA5 reanalysis is in production*, 2016, p. 7.

[26] T. Cebecauer, M. Šúri and C. Gueymard, *Uncertainty sources in satellite-derived direct normal irradiance: how can prediction accuracy be improved globally?*, Granada, 2011, pp. 20-23.

[27] International Electrotechnical Commission, I*EC 61724-1:2017 Photovoltaic system performance - Part 3: Energy evaluation method*

[28] P. A. G. M. Amarasinghe e S. K. Abeygunawardane, *Application of Machine Learning Algorithms for Solar Power Forecasting in Sri Lanka, Colombo*, 2018, pp. 87-92.

[29] S. Theocharides, G. Makrides, A. Kyprianou e G. Georghiou, *Machine Learning Algorithms for Photovoltaic System Power Output Prediction*, Limassol, 2018.

[30] E. Isaksson and M. Karpe Conde, *Solar Power Forecasting with Machine Learning Techniques*, 2018.

[31] G. van Rossum and F. Drake, *Python Reference Manual*, Virginia, 2001.

[32] Anaconda Software Distribution, Anaconda Vers. 2-2.4.0., 2016.

[33] W. F. Holmgren, C. W. Hansen and M. A. Mikofski, *pvlib python: a python package for modeling solar energy systems,* 2018.

[34] T. Cebecauer, M. Šúri and C. Gueymard, *Uncertainty sources in satellite-derived direct normal irradiance: how can prediction accuracy be improved globally?,* Granada, 2011, pp. 20-23.

[35] ISO/IEC Guide 98-3, *Uncertainty of measurement – Part 3: Guide to the expression of uncertainty in measurement* (GUM:1995), 2008.

[36] M. Lave, W. Hayes, A. Pohl e C. W. Hansen, *Evaluation of Global Horizontal Irradiance to Plane-of-Array Irradiance Models at Locations Across the United States*, vol. V, 2015, pp. 597-606.

[37] Sandia National Laboratories, "*Global Horizontal Irradiance,"* 2018. [Online]

[38] G. James, D. Witten, T. Hastie e R. Tibshirani, *An Introduction to Statistical Learning: With Applications in R*, Springer, 2017.

List of tables

List of figures